Natural Resources Canada | Ressources naturelles Canada

GEOLOGICAL SURVEY OF CANADA
OPEN FILE 8074

Evaluating the Impact of Earth Transfer Function on the Geoelectric Field for GIC Modelling

M. Tinel, D. Boteler, L. Trichtchenko

2016

Canada

GEOLOGICAL SURVEY OF CANADA
OPEN FILE 8074

Evaluating the Impact of Earth Transfer Function on the Geoelectric Field for GIC Modelling

M. Tinel[1], D. Boteler[2], L. Trichtchenko[2]

[1] University of Waterloo, Waterloo, Ontario

[2] Natural Resources Canada, Ottawa, Ontario

2016

doi:10.4095/298818

This publication is available for free download through GEOSCAN (http://geoscan.nrcan.gc.ca/).

Recommended citation
Tinel, M., Boteler, D., Trichtchenko, L., 2016. Evaluating the Impact of Earth Transfer Function on the Geoelectric Field for GIC Modelling; Geological Survey of Canada, Open File 8074, 76 p. doi:10.4095/298818

Publications in this series have not been edited; they are released as submitted by the author.

Summary

Geomagnetic disturbances that occur as a result of solar activity create electric fields that affect power systems on the surface of the Earth. The effect on the power system depends on the size of the surface electric field, which depends on the conductivity structure of the Earth in the area of the power system. To assess the geomagnetic hazard to power systems Earth conductivity models have been produced for different geological regions across Canada. This study examines how uncertainties in the Earth model affect the calculated electric fields.

All of the Earth conductivity models tested in this report are related to a one-dimensional Earth model composed of several layers of different characteristics. The conductivity models tested are variations where each layer property is always within a range of possible values. The purpose of this was to determine the effect of conductive and resistive Earth layer combinations on the surface impedance, which is used to calculate the surface electric field.

In general, a more resistive Earth creates a higher surface Earth response. It was found in a basic test Earth model that, within two uniform Earth models with different conductivities which produce a specific Earth transfer function response; there are some conductivity combinations that can produce even greater Earth transfer function amplitudes. This idea was applied to an artificial geomagnetic field, in order to determine a theoretical electric field. It was found that it is possible to find an Earth structure model to maximize the Earth transfer function amplitude at different frequencies, and consequently the electric field amplitudes in the frequency and time domain.

The same procedure of changing the conductivities of individual layers was applied to the Quebec Earth model. Using geomagnetic field measured during different days at the Ottawa Magnetic Observatory, it was again possible to determine the earth model that gave the highest electric field amplitude in the time domain. It was discovered that the particular maximum Earth model is specific to the frequency content of the geomagnetic field, which is different for each geomagnetic storm. In some cases the difference between the maximized electric field amplitude and highest amplitude of the electric field due to the highest resistivity model would be significant. This would mean that the combinations within an Earth model with some uncertainties cannot be neglected, even if determining the absolute highest electric field for a particular geomagnetic storm is not straight forward. However, more analysis of the electric field amplitudes shows that in the general case, the highest electric field values can be estimated by the Earth model with the highest resistivities.

Table of Contents

List of Figures

List of Tables

1.0 Introduction

Earth's geomagnetic field is constantly changing due to internal and external factors. Solar activity and ejection of charged particles from the sun is the primary cause for major geomagnetic disturbances. These geomagnetic storms and their interaction with Earth's magnetic field are what cause changes in the surface electric field. For geomagnetic storms like the one that occurred on March 13, 1989, electric field accumulation can be excessive and damaging. Accumulation of Geomagnetically Induced Currents (GIC) in long conductors on the surface of the Earth, such as power lines, can cause effects like: saturation of transformers, overload of equipment, burnt out transformers and collapse of the power system. Such events have been previously observed, for example in Quebec during the geomagnetic storm in 1989. More effects can be observed on other conductors, such as pipelines, where accumulation of GIC's increases corrosion, which decreases the lifespan of the pipeline.

Impedance of the Earth and the geomagnetic field are used to calculate electric field at surface of the Earth, which drives GIC's. While geomagnetic field measurements are readily available through NRCan's geomagnetic observatory network (www.spaceweather.gc.ca), surface impedances are derived based on the Earth conductivity model in the local area. Across Canada, the Earth's structure varies greatly from the surface to the core. Local Earth models are composed of conductive layers of sedimentary basin rock, and resistive layers of igneous and metamorphic rock like the Canadian Shield. It has been shown for the size of GIC, that the best case scenario is for a conductive Earth model at low magnetic latitudes, and the worst case scenario is for a resistive Earth model at high magnetic latitudes (Zheng, 2013). Clearly, electric fields are dependent on two factors: level of geomagnetic activity, and the Earth conductivity model.

The simplest Earth conductivity model is the so-called "layered Earth" model, which is a one dimensional model with a set of horizontal layers representing changes of conductivity with depth. The identification of the conductivity of each layer is usually done based on magnetotelluric measurements (Simpson, 2005). However, these conductivities cannot be defined exactly for many reasons, for example, due to the non-uniqueness of the inversion methods, due to the fact that the original three dimensional structures within the Earth are replaced by the one dimensional model. Thus, there are uncertainties in the Earth conductivity model.

The purpose of this study is to examine how uncertainty in the conductivity of the layered Earth model affects surface impedance, and consequently the electric fields produced during geomagnetic disturbances. Then, using these relationships we can determine upper and lower limit bounds for the calculated electric fields. First, the report outlines the possible variation in Earth's structure for a simple general test Earth model. Next, the transfer functions of all possible Earth variations are applied to a test case geomagnetic field, and the differences in the electric fields are studied in the time domain. The second step of this study involves applying the same analysis technique to a real Earth model and actual geomagnetic records. The particular Earth model is the Quebec Earth Model, of which the electric field and its limit bounds have been preliminarily studied by D. H. Boteler in

(Boteler, 2015). The electric fields in the second part of this study are analysed in the time and the frequency domain.

2.0 Theory

The surface impedance of the Earth is a frequency dependant function. It can be calculated by modelling the Earth using multiple layers of different conductivity as shown in Figure 2.1. Each layer contains different physical properties, which determine the relationship between electric and geomagnetic fields at the surface of the Earth and at depth, moving through the mediums and interfaces. Figure 2.1 also shows the dependency of variables in the recursive calculation of the surface impedance.

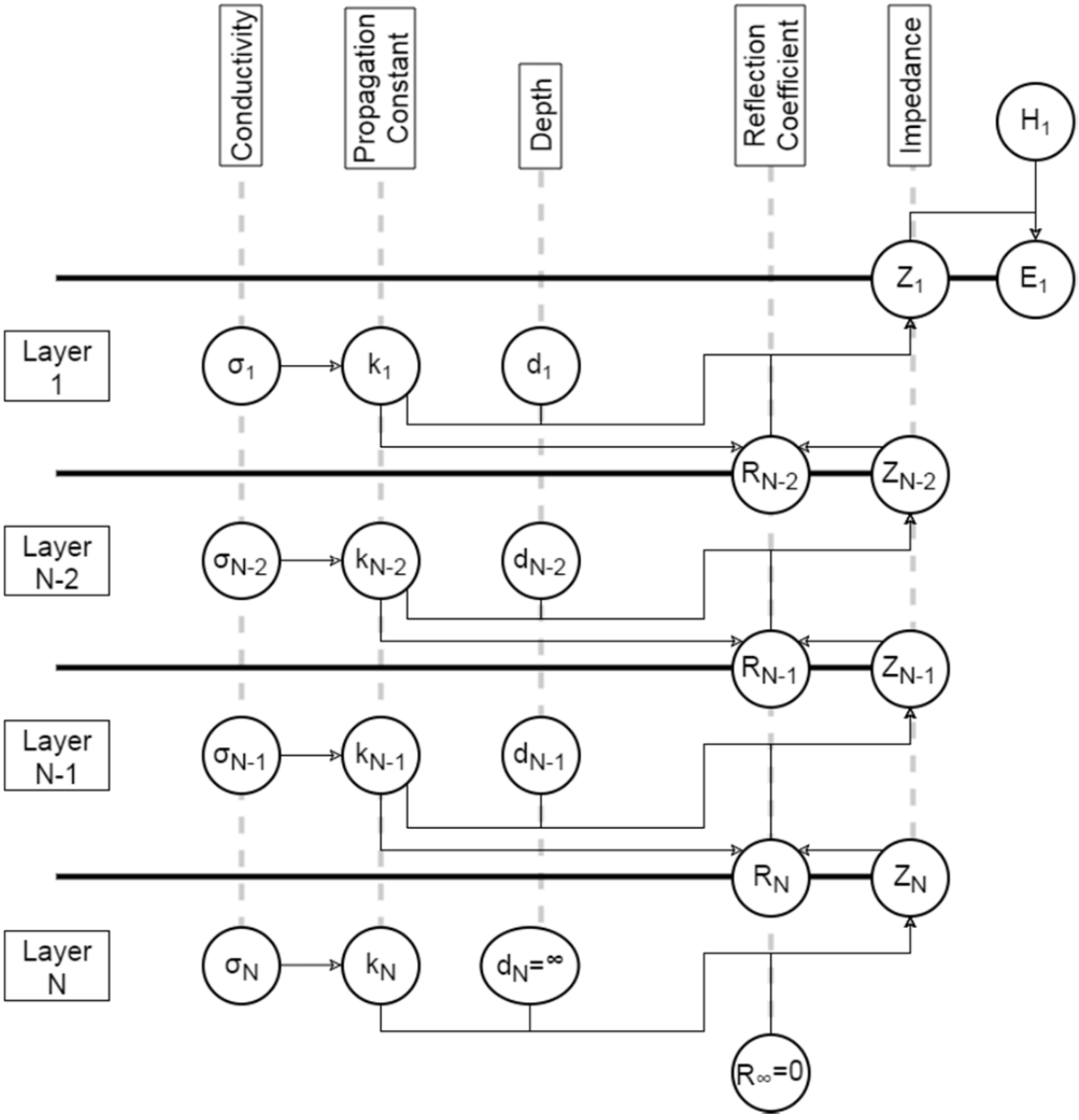

Figure 2.1 - N Layer Earth Model and its Properties and Dependencies

Resistivity, Propagation Constant and Layer thickness are properties of each layer. Reflection Coefficient and Impedance occur at the interface between layers. The N^{th} layer is a half space with infinite thickness and a reflection coefficient of 0. The electric field at the surface is related to surface impedance Z and geomagnetic field H.

In this approach the electric and magnetic field defined by Maxwell's equations, are related in the frequency domain. Displacement currents are small in comparison with the conductivity currents for frequencies of natural geomagnetic variation produced by space weather events. Therefore, both electric field (E) and geomagnetic field (H) in the frequency domain can be given by the diffusion equations (Kaufman, 1989),

$$\frac{d^2E}{dz^2} = i\omega\mu_0\sigma E \tag{1}$$

$$\frac{d^2H}{dz^2} = i\omega\mu_0\sigma H \tag{2}$$

where ω is the angular frequency, μ_0 is the permeability of free space, σ is the conductivity, and i is the square root of -1. The solutions to the differential equations have the form,

$$E = A(e^{-kz} + re^{kz}) \tag{3}$$

$$H = A\left(\frac{e^{-kz}}{Z_0} - \frac{re^{kz}}{Z_0}\right) \tag{4}$$

where A is the amplitude, k is the propagation constant, r is the reflection coefficient, Z_0 is the characteristic impedance of a uniform media, and z is the depth. Here Z_0 is given by,

$$Z_0 = \frac{i\omega\mu_0}{k} \tag{5}$$

In our case of a layer Earth, the electric field at the surface (E_s) is given by,

$$E_s = H_s Z_1 \tag{6}$$

where H_s is the geomagnetic field at the surface and Z_1 is the impedance on the top of the surface layer. Alternatively, given the measured geomagnetic flux density on the surface (B_s), E_s can be written as,

$$E_s = B_s T_1 \tag{7}$$

where T_1 is the Earth transfer function at the top of the surface layer. B_s is measured, but can be calculated from H_s by,

$$B_s = H_s\mu_0 \tag{8}$$

and T1 is calculated by,

$$T_1 = \frac{Z_1}{\mu_0} \tag{9}$$

The determination of impedance at the surface requires a recursive calculation using the properties of each layer for a 1-D layered Earth (Weaver, 1994, p.293). For each layer n from N-1 to 1, the impedance (Z_n) at the surface of the layer n is given by,

$$Z_n = \frac{i\omega\mu_0}{k_n}\left(\frac{1+r_{n+1}e^{-2k_n d_n}}{1-r_{n+1}e^{-2k_n d_n}}\right) \tag{10}$$

where k_n is the propagation constant of the layer, d_n is the thickness, and r_{n+1} is the reflection coefficient at the interface between layer n and n+1. k_n is given by,

$$k_n = \sqrt{i\omega\mu_0\sigma_n} \tag{11}$$

where it is related to σ_n, the conductivity of the layer n. r_{n+1} on interface between layer n and n+1 is determined using,

$$r_{n+1} = \frac{Z_{n+1} - \frac{i\omega\mu_0}{k_n}}{Z_{n+1} + \frac{i\omega\mu_0}{k_n}} \tag{12}$$

where Z_{n+1} is the impedance at the bottom of layer n (top of layer n+1). For the half space N, since the thickness is infinite and reflection coefficient is equal to 0, the impedance (Z_N) is given by,

$$Z_N = \sqrt{\frac{i\omega\mu_0}{\sigma_N}} \tag{13}$$

In all cases, ω is calculated for a single frequency (f) as,

$$\omega = 2\pi f \tag{14}$$

Finally, the transfer function (T_n) of any layer n is related to the impedance Z_n and permeability of free space μ_0 by,

$$T_n = \frac{Z_n}{\mu_0} \tag{15}$$

The geomagnetic flux density is always measured in three components: the Northward, x direction; Eastward, y direction; and vertically down, z direction. Since it is assumed that the geomagnetic field arrives as a horizontal plane wave, there is no vertical electric field. The Eastward electric field (E_y) is related to the Northward geomagnetic flux density component (B_x), and the Northward electric field (E_x) is related to the negative Eastward geomagnetic flux density component (B_y):

$$E_x = B_y T \tag{16}$$

$$E_y = -B_x T \tag{17}$$

The magnitude of the total a field |E| is calculated from the Northward (E_x) and Eastward (E_y) components:

$$|E| = \sqrt{E_x^2 + E_y^2} \tag{18}$$

It is also possible to calculate the electric fields at any depth. Figure 2.2 shows a diagram of the n^{th} layer in the Earth, and the relationship between fields for a given depth and at interfaces.

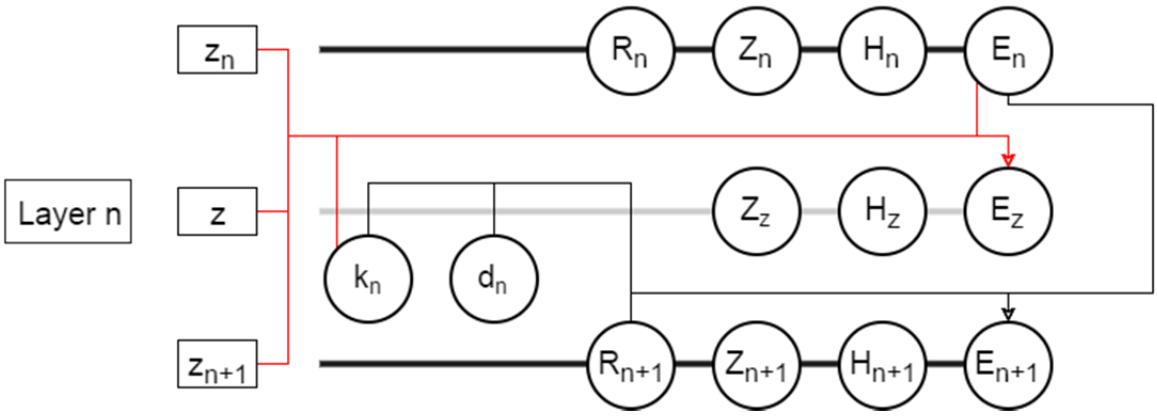

Figure 2.2 - n^{th} Layer of the Earth Model

This represents the n^{th} layer of the Earth Model. The top and bottom interfaces have fields and impedances, which occur at depth z_n and z_{n+1}, respectively. For the intermediate depth z, there is a related impedance, electric field and geomagnetic field. For reference, the depth at the surface is 0.

At any interface n+1, the electric field (E_{n+1}) is,

$$E_{n+1} = E_n \frac{(1+r_{n+1})e^{-k_n d_n}}{1+r_{n+1}e^{-2k_n d_n}} \tag{19}$$

related to the electric field E_n, reflection coefficient r_{n+1}, propagation constant k_n and layer thickness d_n. Similarly, the geomagnetic field (H_{n+1}) at any interface n+1 is calculated through,

$$H_{n+1} = H_n \frac{(1-r_{n+1})e^{-k_n d_n}}{1-r_{n+1}e^{-2k_n d_n}} \tag{20}$$

using the geomagnetic field H_n, reflection coefficient r_{n+1}, propagation constant k_n, and layer thickness d_n. Finally, for any intermediate depth z between z_n and z_{n+1}, the electric field (E(z)) is calculated using,

$$E(z) = E_n \frac{e^{-k_n(z-z_n)}+r_{n+1}e^{-2k_n(z_{n+1}-z_n)}e^{k_n(z-z_n)}}{1+r_{n+1}e^{-2k_n(z_{n+1}-z_n)}} \tag{21}$$

With the electric field E_n, propagation constant k_n, reflection coefficient r_{n+1}, and depths z_n, z and z_{n+1}. Similarly, the geomagnetic field (H(z)) is calculated using,

$$H(z) = H_n \frac{e^{-k_n(z-z_n)}-r_{n+1}e^{-2k_n(z_{n+1}-z_n)}e^{k_n(z-z_n)}}{1-r_{n+1}e^{-2k_n(z_{n+1}-z_n)}} \tag{22}$$

from the geomagnetic field H_n, propagation constant k_n, reflection coefficient r_{n+1}, and depths z_n, z and z_{n+1}. Lastly, the impedance (Z(n)) is related to reflection coefficient r_{n+1}, propagation constant k_n, and depths z and z_{n+1} using,

$$Z(z) = \left(\frac{1+r_{n+1}e^{-2k_n(z_{n+1}-z)}}{1-r_{n+1}e^{-2k_n(z_{n+1}-z)}}\right)\frac{i\omega\mu_0}{k_n} \tag{23}$$

Geomagnetic flux density is measured in the time domain. In order to calculate electric field, the measured geomagnetic field record needs to be converted into the frequency domain, where it is used to calculate the electric field, which is then converted back to the time domain (Kaufman, 1989). The conversion is completed using the Fourier Transform, which extracts the amplitude and phase for different frequencies and composes the time series record as a sum of sinusoidal functions.

For a discrete dataset having N elements of equal time step, the forward (F_n) and inverse (f_k) Fourier transforms are calculated as N summations of N elements,

$$F_n = \sum_{k=0}^{N-1} f_k e^{-\frac{2\pi i k n}{N}} \tag{24}$$

$$f_k = \frac{1}{N} \sum_{n=0}^{N-1} F_n e^{\frac{2\pi i k n}{N}} \tag{25}$$

where f_k represents the k^{th} data point in the time domain and F_n represents n^{th} data point in the frequency domain. The frequencies that result from the Fourier transform range between the maximum frequency (f_{max}) called the Nyquist frequency, and the minimum frequency (f_{min}),

$$f_{max} = \frac{1}{2\Delta t} \tag{26}$$

$$f_{min} = \frac{N}{\Delta t} \tag{27}$$

which are determined by the time step Δt. If N is even there are (N/2)-1 frequencies, and if it is odd there are (N-1)/2 frequencies. Each frequency is used in the recursion to calculate the transfer function amplitudes.

3.0 Test Layered Earth Models

The sensitivity of the transfer function to variations in the Earth conductivity model was tested for six different cases, which are built on models of a uniform Earth. Tested cases include adding a conductive or resistive layer of varying thickness at different depths, of one order of magnitude increased or one order of magnitude decreased resistivity than the parent uniform Earth. Tests are aimed at determining how a change in targeted layer resistivity affects the amplitude and phase of the resultant Earth transfer function. The frequencies considered for this study are between 10^{-5} Hz and 1 Hz, which covers periods between 27.7 hours and 1 second.

3.1 Uniform Earth Models

The first test was to compare five different uniform Earth models, with resistivity values between 10 Ωm and 100,000 Ωm, varying by single orders of magnitude. The resulting transfer function amplitudes are equally spaced and linear in the log – log domain, and all phases are constant at 45˚. Figure 3.1 shows the amplitude and phase of each Earth transfer functions. Figures later in text, focus on two uniform Earth models: the 100 Ωm and 1,000 Ωm resistivity models.

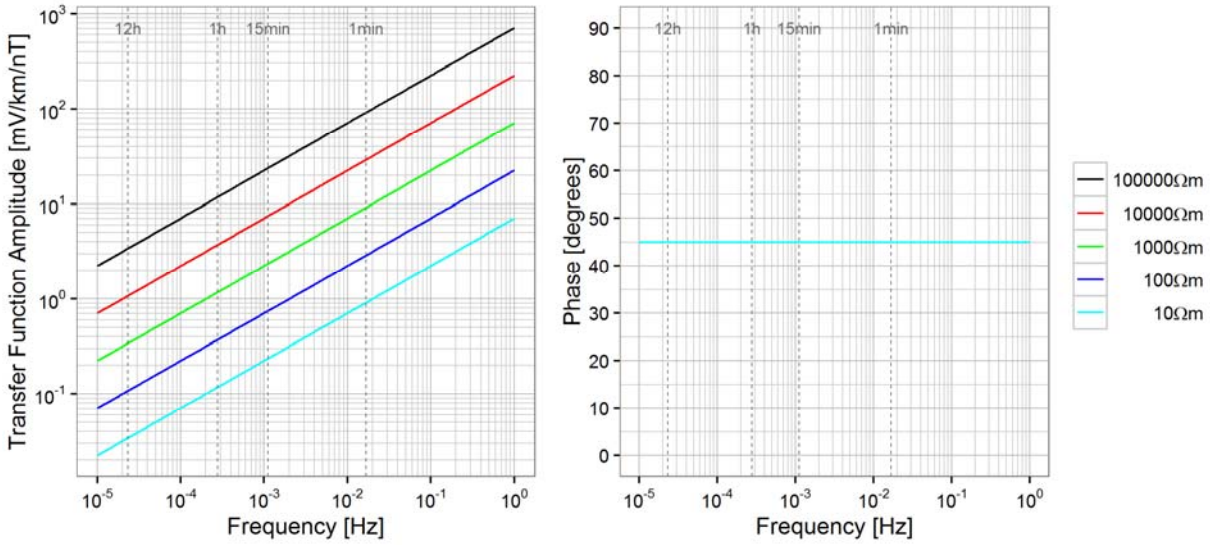

Figure 3.1 - Transfer Function Amplitude and Phase for Uniform Earth Models

Five uniform Earth models show linear relationship between transfer function amplitude and frequency, and a constant 45˚ phase. Vertical dotted lines show corresponding periods for 12h, 1h, 15 min and 1 min. The legend indicates resistivity of the uniform Earth in Ωm.

3.2 Varying Thickness of the Surface Layer

The second test introduces a surface layer to the basic uniform Earth model. This Earth model considers one surface layer above a uniform half space, and tests the effect of altering the thickness of the surface layer on the transfer function. In the resistive case, the top layer has a resistivity of 1,000 Ωm and the half space has a resistivity of 100 Ωm. The conductive case considers a top layer of resistivity 100 Ωm over a half space of resistivity 1,000 Ωm. The thickness of the surface layer is between 10 km and 100 km. Table 3.1 presents the layer thicknesses and resistivities for both test

cases. Results for the transfer function in both cases (Figure 3.2 and 3.3) are plotted along with the transfer function of uniform half spaces at 100 Ωm and 1000 Ωm.

Table 3.1 - Varying Thickness of Surface Layer Earth Model

Layer	Thickness [km]	Resistive [Ωm]	Conductive [Ωm]
Surface	10 – 100	1,000	100
Half Space	-	100	1,000

3.2.1 Resistive Surface Layer

Figure 3.2 shows the transfer function amplitude and phase of the Earth model with a resistive surface layer varying in thickness. For any thickness of the surface layer, for higher frequency the transfer function amplitude approaches the transfer function amplitude for the uniform Earth model of resistivity 1,000 Ωm. Whereas at the lower frequencies, it approaches the transfer function amplitude for the uniform Earth model of resistivity 100 Ωm. The transfer function phase for all cases has the same shape, but is shifted to lower frequency for increased depth of the change of resistivity. This means that the change due to an increase in resistivity in the Earth is equal, positive, and dependant on the depth of the change.

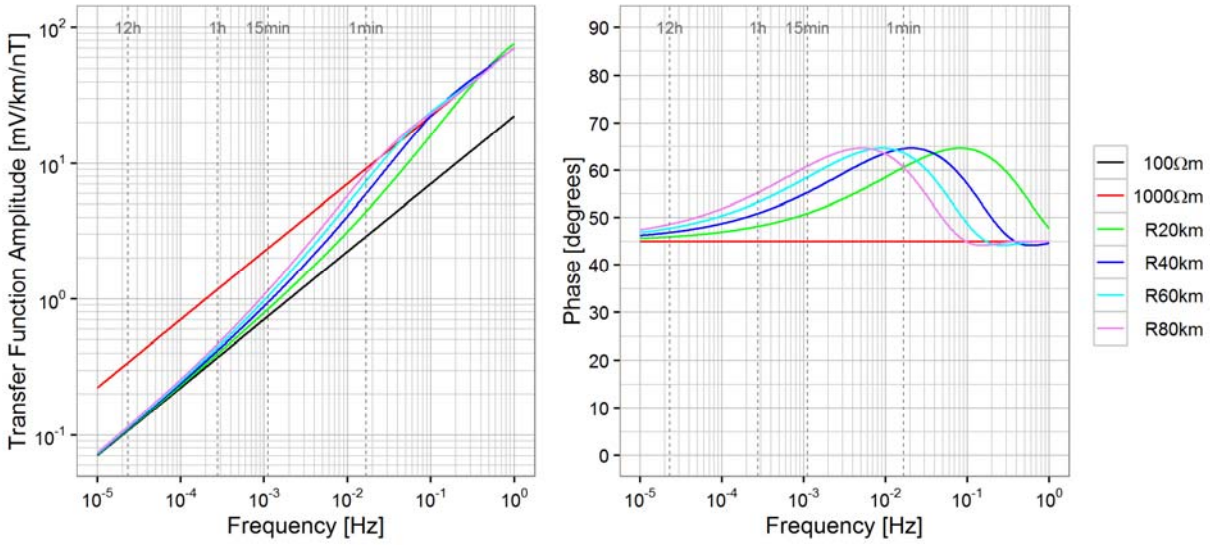

Figure 3.2 - Amplitude and Phase of Resistive Surface Layer Varying in Thickness
Two uniform Earth models of resistivity 100 Ωm and 1,000 Ωm, and four cases of a resistive surface layer 20km, 40km, 60km and 80km thick, show the relationship between amplitude and frequency, and phase and frequency of the Earth transfer function. Dotted lines indicate particular periods of 12h, 1h, 15 min and 1min.

3.2.2 Conductive Surface Layer

Figure 3.3 presents the transfer amplitude and phase for Earth models with a conductive surface layer of varying thickness. For low frequencies the transfer function amplitude approaches the amplitude of transfer function for a uniform Earth model of 1,000 Ωm. Whereas for high frequencies it approaches the amplitude of transfer function for a uniform Earth model of resistivity 100 Ωm. The shape of the phase change of the transfer function is also equivalent, and shifted to lower frequencies for increased depth of the change, just like in the previous case. However, for a conductive layer over a resistive half

space the change is negative, meaning increasing frequency causes a decrease in transfer function amplitude and phase.

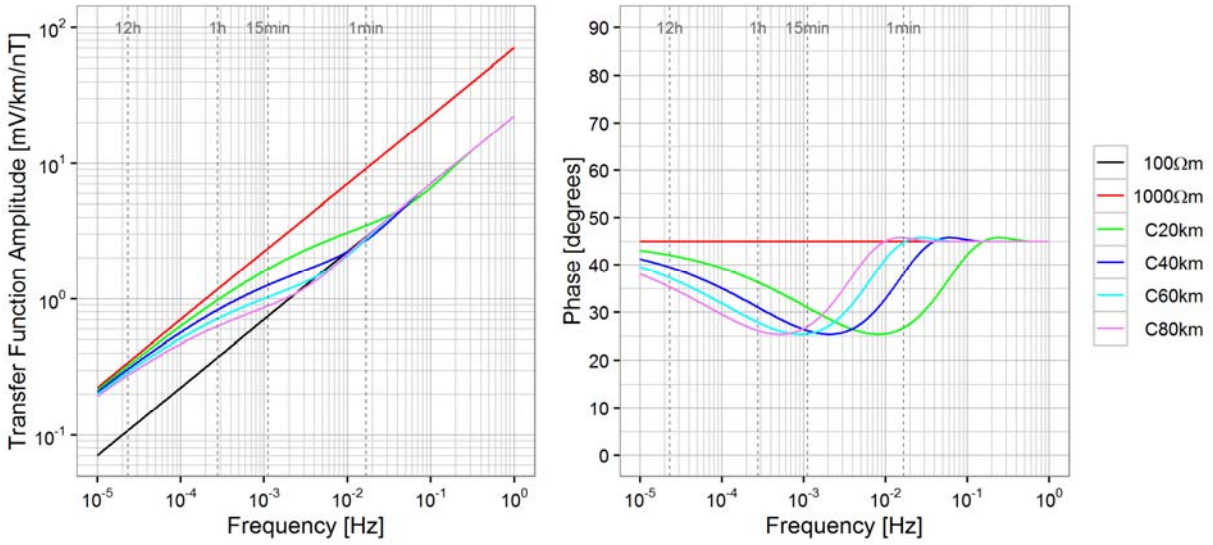

Figure 3.3 - Amplitude and Phase of Conductive Surface Layer of Varying Thickness
Two uniform Earth models of 100 Ωm and 1,000 Ωm, and four cases of conductive surface layer 20km, 40km, 60km and 80km thick, show the relationship between the frequency and amplitude, and frequency and phase of the Earth transfer function. Particular periods of 12h, 1h, 15 min and 1 min are represented as dotted lines.

3.3 Varying Thickness of Intermediate Layer

The third test introduces a third intermediate layer to the previous uniform Earth model. The intermediate layer will be resistive or conductive, and will have a varying thickness. The surface and half space have the same resistivity. In the resistive layer Earth model, the surface and half space both have a resistivity value of 100 Ωm, and the intermediate layer a value of 1,000 Ωm. In the conductive case, the surface and half space have a value of 1,000 Ωm and intermediate layer has a value of 100 Ωm. The surface layer has a constant thickness of 10 km and the intermediate layer ranges between 10 km and 90 km, for both cases. Table 3.2 presents the layer thickness and resistivity for the conductive and resistive layer Earth models. Results (in Figure 3.4 and 3.5) are plotted along with the transfer function of a uniform Earth of resistivity 100 Ωm and 1,000 Ωm.

Table 3.2 - Varying Thickness of Intermediate Layer Earth Model

Layer	Thickness [km]	Resistive [Ωm]	Conductive [Ωm]
Surface	10	100	1000
Intermediate	10 – 90	1000	100
Half Space	-	100	1000

3.3.1 Resistive Intermediate Layer

Figure 3.4 presents the transfer function amplitude and phase for the Earth model with a resistive intermediate layer of varying thickness. For higher and low frequencies, the amplitude of the transfer function approaches the amplitude of the transfer function for a uniform Earth model of resistivity 100 Ωm. For any particular frequency in the range, the amplitude increases for models with a thicker intermediate layer. The phase for this Earth model has a general increase and then decrease in angle as

the layered Earth structure changes from conductive to resistive, and back to conductive. The change in phase is greater for the Earth model with the thickest intermediate layer. Also, for the high end frequency range, in all the cases of the intermediate layer the phase change is the same.

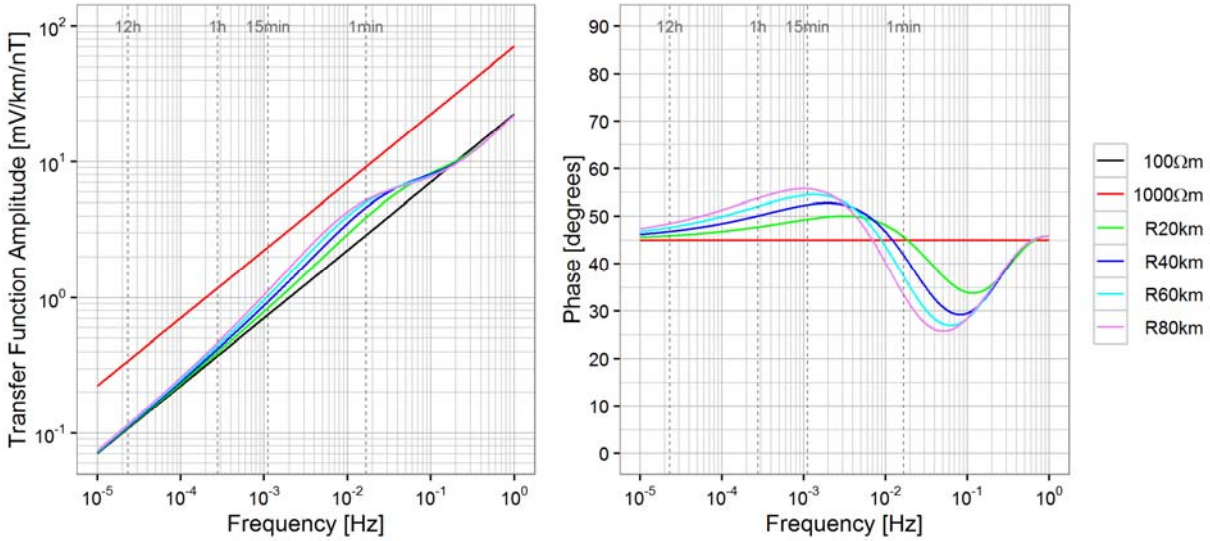

Figure 3.4 - Phase and Amplitude of Resistive Intermediate Layer of Varying Thickness
Two uniform Earth models of 100 Ωm and 1,000 Ωm, and four cases of resistive intermediate layer of thickness 20km, 40km, 60km, and 80km, show the relationship between frequency and amplitude and frequency and phase of the Earth transfer function. Dotted lines indicate particular periods of 12h, 1h, 15 min and 1min.

3.3.2 Conductive Intermediate Layer

Figure 3.5 shows the amplitude and phase of the Earth model with a conductive intermediate layer of varying thickness. For the high and low frequencies, the amplitude of the transfer function approaches the amplitude of the transfer function for a uniform Earth model of resistivity 1,000 Ωm. At any particular frequency, the amplitude is lower for a thicker intermediate conductive layer. The phase is a general decrease and then increase in angle, the same effect as in the previous test but inverted. The angle difference is biggest for the thickest intermediate layer. Also, at the high end of the frequency range, all cases of the resistive intermediate layer give the same phase change. As well, there is a short frequency range for which the change in phase is almost linear in the log – the frequency domain. This range extends to lower frequencies for increasing thickness of the intermediate layer.

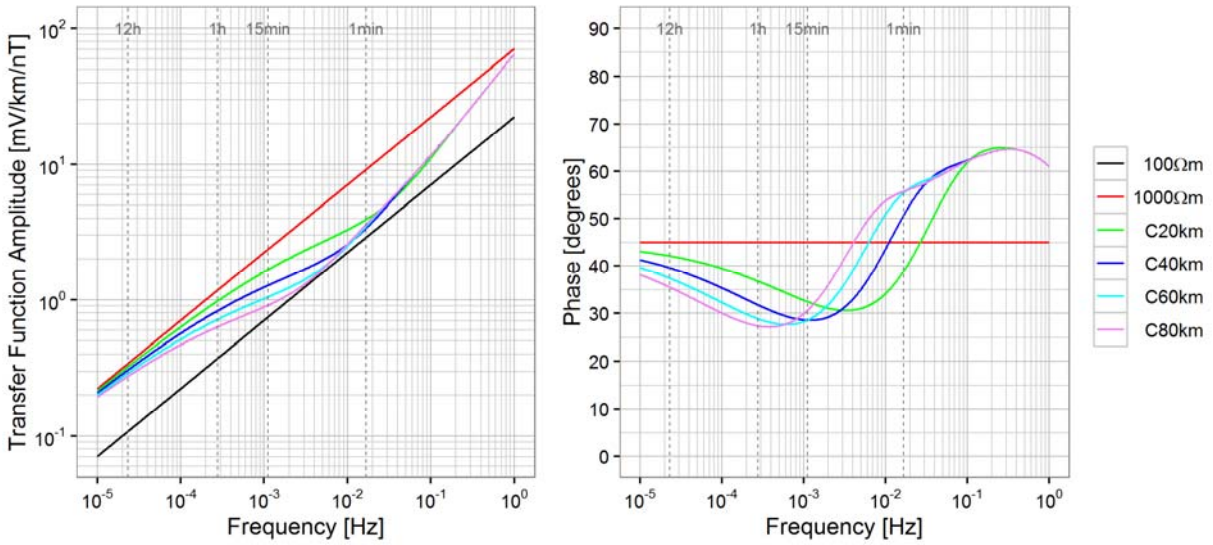

Figure 3.5 - Phase and Amplitude of Conductive Intermediate Layer of Varying Thickness
Two uniform Earth models of 100 Ωm and 1,000 Ωm, and four cases of conductive intermediate layer 20km, 40km, 60km and 80km thick, show the relationship between the frequency and amplitude, and frequency and phase of the Earth transfer function. Particular periods of 12h, 1h, 15 min and 1 min are represented as dotted lines.

3.4 Varying Depth of Intermediate Layer

The fourth test considers a three layer Earth model: surface and intermediate layers over a half space layer. The change in the transfer function due to varying thickness of the surface layer (i.e. depth of the intermediate layer) is tested. The surface layer and half space are uniform, and the intermediate layer is either resistive or conductive. In the resistive case the uniform Earth layers have a resistivity of 100 Ωm and the intermediate layer a resistivity of 1,000 Ωm. In the conductive case the uniform Earth is 1,000 Ωm and the intermediate layer is 100 Ωm. The thickness of the intermediate layer is a constant 10 km and the surface ranges between 0 km and 90 km. For the case of a 0 km thick surface layer, the intermediate conductive or resistive layer is exposed and equivalent to a two Earth layer model. Table 3.3 presents the thickness and resistivity of both Earth models tested. The resultant transfer functions (Figures 3.6 and 3.7) are plotted along with uniform Earth models of 100 Ωm and 1,000 Ωm.

Table 3.3 - Varying Depth of Intermediate Layer Earth Model

Layer	Thickness [km]	Resistive [Ωm]	Conductive [Ωm]
Surface	0 – 90	100	1000
Intermediate	10	1000	100
Half Space	-	100	1000

3.4.1 Resistive Intermediate Layer

Figure 3.6 presents the amplitude and phase of the transfer function of the Earth model with a varying depth of the resistive layer. In all cases, the low and high frequency amplitude approaches the amplitude of the transfer function for a uniform Earth of resistivity value of the half space and surface layer. In the case of a 0 km depth, the surface is 1,000 Ωm and 100 Ωm otherwise. For increasing depth of the intermediate layer, the amplitude change is positive but becomes smaller and less

significant. The shape of the phase change is a general increase followed by a decrease. With increasing depth of the resistive layer, the phase change becomes smaller and moves to lower frequencies. In the case of an exposed resistive layer the phase change is large and positive, and there is no observed decrease in the phase for studied frequencies. For any case of depth, the increase in phase and amplitude does not exceed the increase due to the same resistive layer at a shallower depth.

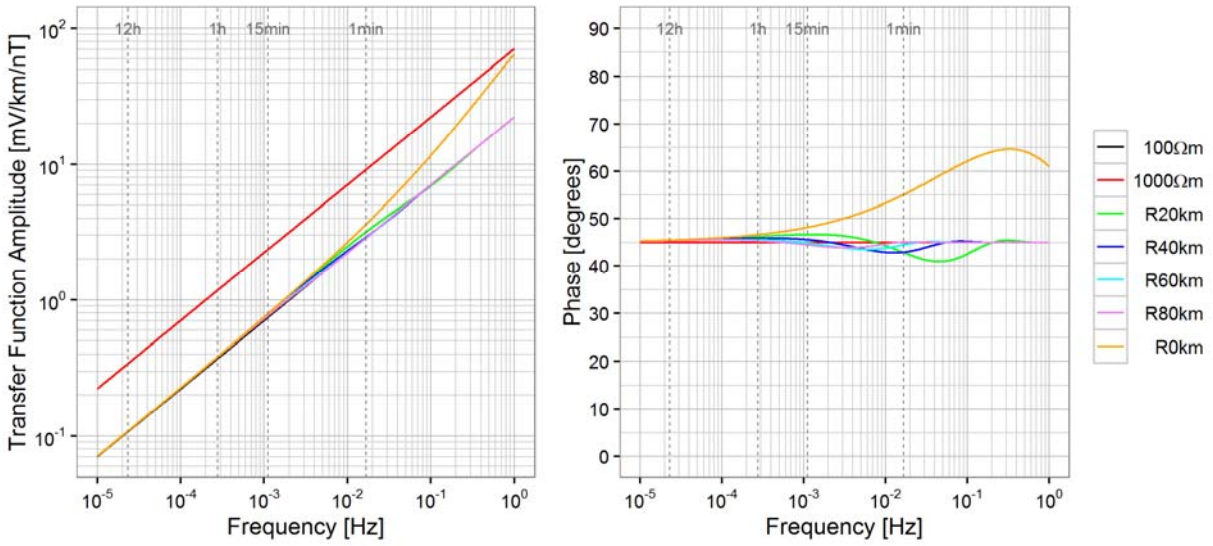

Figure 3.6 - Phase and Amplitude of Resistive Intermediate Layer of Varying Depth
Two uniform Earth models of 100 Ωm and 1,000 Ωm, and five cases of resistive layers at depths 0km, 20km, 40km 60km and 80km. The relationship between frequency and amplitude, and phase and amplitude, if the resistive layer is exposed (0km), is related to 3.2.1 – Resistive Surface Layer. Particular periods of 12h, 1h, 15 min and 1 min are represented as dotted lines.

3.4.2 Conductive Intermediate Layer

Figure 3.7 shows the transfer function amplitude and phase for models with a conductive intermediate layer at various depths in the Earth. In all cases, the low and high frequency amplitude approaches the amplitude of the transfer function for a uniform Earth model of resistivity of the surface layer and half space layer. For increasing depth of the intermediate layer, the amplitude change is generally negative but becomes smaller and insignificant. The shape of the phase change is in general a decrease followed by an increase. With increaing depth to the conductive layer, the phase change becomes smaller and moves to lower frequencies. If the conductive layer is exposed, the phase change is large and negative, and there is no observed positive change within the frequency range studied. In any case, the decrease in phase and amplitude does not exceed the increase due to the same conductive layer at a shallower depth.

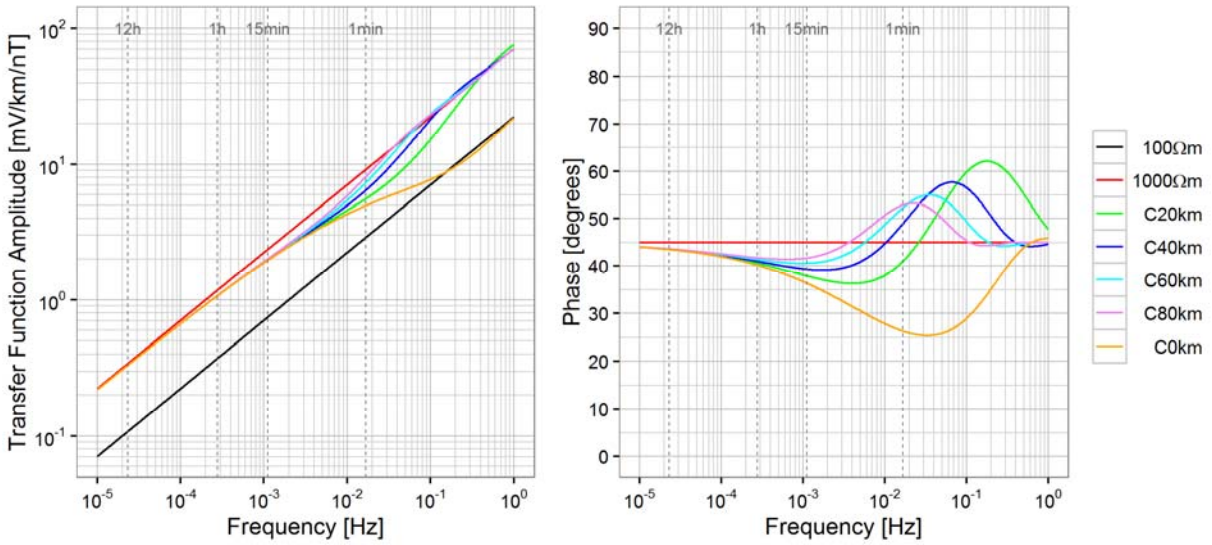

Figure 3.7 - Phase and Amplitude of Conductive Intermediate Layer of Varying Depth
Two uniform Earth models of 100 Ωm and 1,000 Ωm, and five cases of conductive layers at depths 0km, 20km, 40km 60km and 80km. The relationship between frequency and amplitude, and phase and amplitude, if the conductive layer is exposed (0km), is the related to 3.2.2 – Conductive Surface Layer. Particular periods of 12h, 1h, 15 min and 1 min are represented as dotted lines.

3.5 Varying Order of Increased Resistivity

This Earth model tests the effect of increasing the resistivity of the intermediate layer by several orders of magnitude from one to three. This is repeated for three different uniform Earth resistivity values. In each Earth model, the surface layer of thickness 10 km and the uniform half space have the same resistivity, 0.1 Ωm, 1 Ωm or 10 Ωm. The intermediate layer between the surface layer and half space is 10 km thick as well, and has resistivity multiplied by 10^1, 10^2, and 10^3 for each order of increase. Table 3.4 lists all the Earth models tested, with the thickness and resistivity of each layer.

Table 3.4 - Varying Order of Increased Resistivity of Intermediate Layered Earth Model

Layer	Thickness [km]	Order 1 [Ωm]	Order 2 [Ωm]	Order 3 [Ωm]
Uniform Earth of 0.1 Ωm				
Surface	10	0.1	0.1	0.1
Intermediate	10	1	10	100
Half Space	-	0.1	0.1	0.1
Uniform Earth of 1 Ωm				
Surface	10	1	1	1
Intermediate	10	10	100	1000
Half Space	-	1	1	1
Uniform Earth of 10 Ωm				
Surface	10	10	10	10
Intermediate	10	100	1000	10000
Half Space	-	10	10	10

Figure 3.8 shows the transfer function amplitude and phase for all the three Earth models, and the corresponding intermediate layer variability. It is seen that the shape of the transfer function as well as the phase is the same for any of the three Earth model cases. For amplitude, the resistivity of the Earth model is related to the relative amplitude and frequency at which Earth variation causes a difference in transfer function. That is, for increasing resistivity of the surface and half space, the relative amplitude increases, and the frequency at which the difference occurs also increases. For example in [1] it occurs at 10^{-4} Hz, in [2] at 10^{-3} Hz, and in [3] at 10^{-2} Hz. For phase, the resistivity of the Earth model is related to the frequency at which the phase change occurs. That is, for increasing resistivity of the Earth model, the frequency at which the phase changes increases.

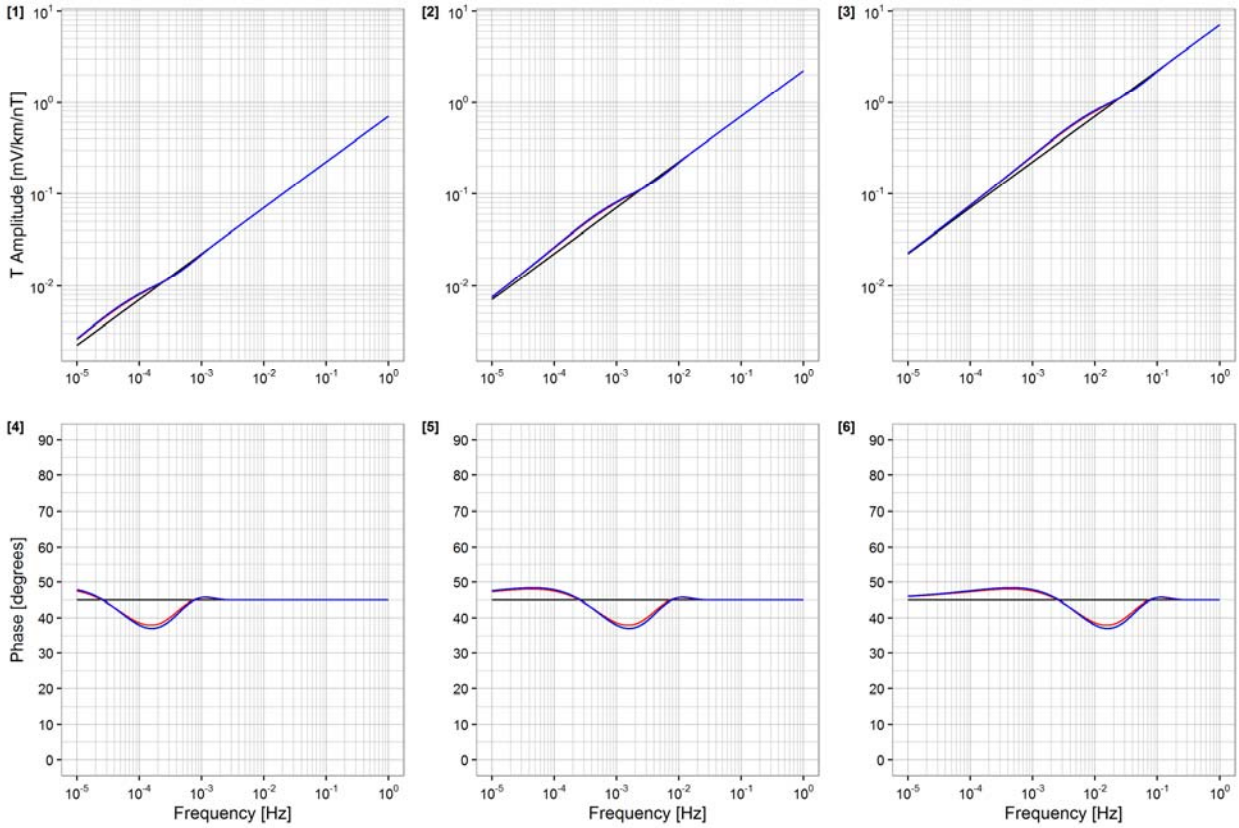

Figure 3.8 - Earth Model with Increased Resistivity

Row one shows the amplitudes of each Earth model with increased resistivity on intermediate layer by several orders of magnitude for uniform Earth models of [1] 0.1 Ωm, [2] 1 Ωm and [3] 10 Ωm. Row two shows the phases of each Earth model with increased resistivity of intermediate layer by several orders of magnitude for uniform Earth models of [4] 0.1 Ωm, [5] 1 Ωm, and [6] 10 Ωm. [black] represents uniform Earth, and [red], [blue], and [green] represent a 1, 2, and 3 order of magnitude increase of resistivity.

Furthermore, it is noticed that the order of increased resistivity does not have a greater effect on the transfer function amplitude and phase, meaning that the amount of increase in resistivity is not related to the amount of increase in the transfer function amplitude or phase. This is given by the fact that for a single plot the transfer function amplitude and phase for the model variety is almost identical.

3.6 Varying Order of Increased Conductivity

This Earth model tests the effect of increasing the conductivity of the intermediate layer by several orders of magnitude from one to three. This is repeated for three different uniform Earth resistivity values. In each Earth model, the surface of thickness 10 km and uniform half space have the same resistivity, 10,000 Ωm, 1,000 Ωm or 100 Ωm. The intermediate layer between the surface and half space is 10 km thick as well, and has resistivity divided by 10^1, 10^2, and 10^3 for each order of increased conductivity. Table 3.4 lists all the Earth models tested, with thickness and resistivity of each layer.

Table 3.5 - Varying Order of Increased Conductivity of Intermediate Layered Earth Model

Layer	Thickness [km]	Order 1 [Ωm]	Order 2 [Ωm]	Order 3 [Ωm]
Uniform Earth of 10,000 Ωm				
Surface	10	10,000	10,000	10,000
Intermediate	10	1,000	100	10
Half Space	-	10,000	10,000	10,000
Uniform Earth of 1,000 Ωm				
Surface	10	1,000	1,000	1,000
Intermediate	10	100	10	1
Half Space	-	1,000	1,000	1,000
Uniform Earth of 100 Ωm				
Surface	10	100	100	100
Intermediate	10	10	1	0.1
Half Space	-	100	100	100

Figure 3.9 shows the transfer function amplitude and phase for all the three Earth models, and the corresponding intermediate layer variability. It is seen that the shape of the transfer function as well as the phase is the same for each of the three Earth model cases. For amplitude, the resistivity of the Earth model is related to the relative amplitude and frequency at which Earth variation causes a difference in transfer function. That is, for increasing resistivity of the surface and half space, the relative amplitude increases, and the frequency at which the difference occurs also increases. For phase, the resistivity of the Earth model is related to the frequency at which the phase change occurs. That is, for increasing resistivity of the Earth model, the frequency at which the phase changes increases.

Furthermore, it is noticed that unlike the case of increasing the resistivity of the intermediate layer in Section 3.5, the order of decreased resistivity is related to the change in the amplitude and phase of the Earth transfer function. For higher order of decrease in resistivity, the change in the amplitude becomes greater and extends over more frequencies. The same is observed for phase, where for a greater order of smaller intermediate layer resistivity, the phase change is exaggerated and spans over a wider frequency range.

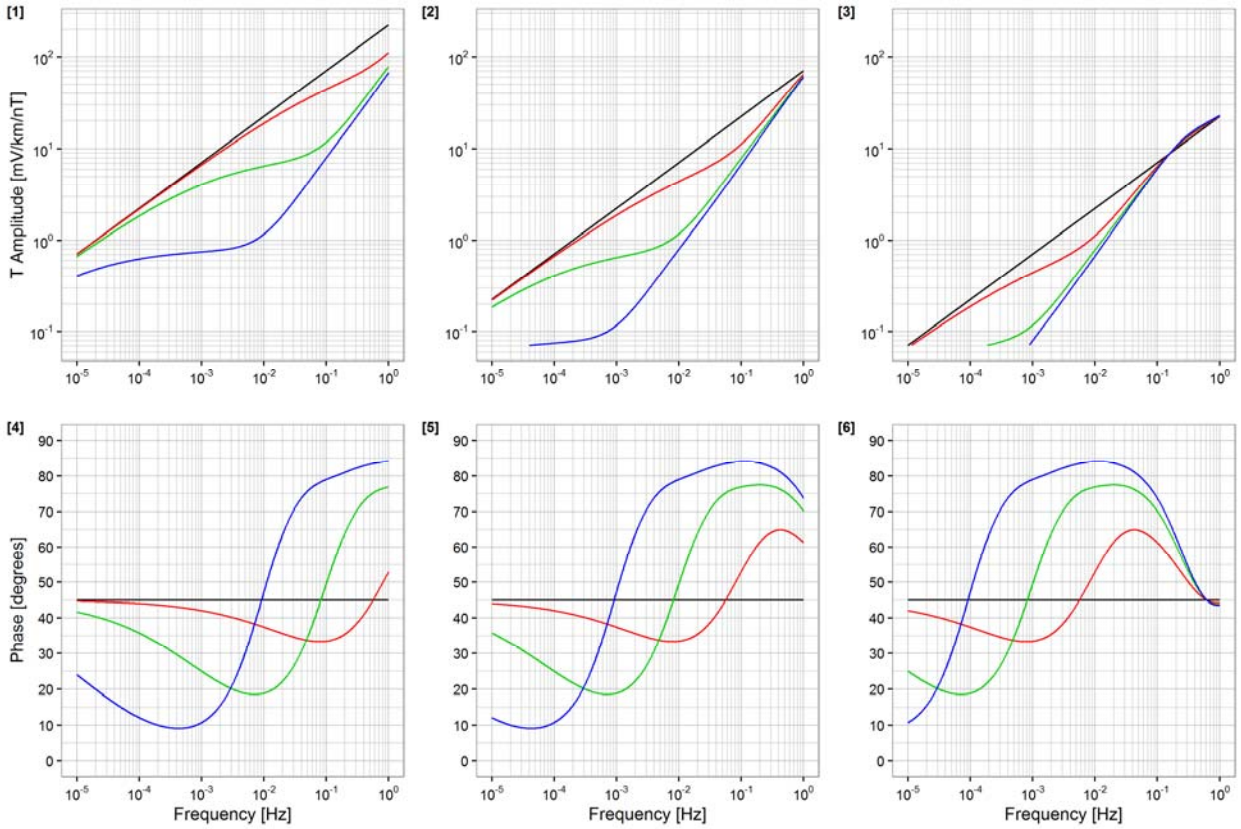

Figure 3.9 - Earth Model with Decreased Resistivity
Row one shows the transfer function amplitude of the Earth model with decreased resistivity of the intermediate layer by several orders of magnitude for a uniform Earth of [1] 10,000 Ωm, [2] 1,000 Ωm and [3] 100 Ωm. Row two shows the phases for the Earth model with decreased intermediate layer resistivity by several orders of magnitude for a uniform Earth of [4] 10,000 Ωm, [5] 1,000 Ωm, and [6] 100 Ωm. Ωm. [black] represents uniform Earth, and [red], [blue], and [green] represent a 1, 2, and 3 order of magnitude increase of conductivity.

3.7 Summary of Results

The study of general Earth models leads to several conclusions.

The uniform Earth models always have a linear transfer function in the log-frequency and log-amplitude domain, and the phase is always a constant 45˚. The difference in transfer function for each uniform Earth model is directly related to the resistivity of the Earth model.

For any variation in Earth model between two resistivity values, the Earth transfer function will be bound by the transfer function of uniform Earths of those two resistivity values, for frequencies approaching 0 and infinity. This means that the varying Earth model transfer function, will approach the transfer function of the uniform Earth with resistivity of the varying model half space layer for frequencies approaching 0, and will approach the transfer function of the uniform Earth with resistivity of the varying model surface layer for frequencies approaching infinity.

For a uniform Earth model with an upper and lower bound in resistivity per layer, the transfer function of a non-uniform Earth model with layer variability between the upper and lower resistivity, will be relatively well bound by the transfer function of the Earth with all upper and lower bound resistivity.

However, for any Earth with an increased or decreased resistivity the transfer function of that Earth may locally exceed the bounds determined by the transfer function of the Earth with all upper and lower bound resistivities.

For an Earth with an increased resistivity at some point moving from the depth to the surface, moving from low to high frequency will have a large increase in phase followed by a small decrease. The cycle of increased and decreased phase continues, but the magnitude of the phase change quickly approaches 0. The decrease in phase is related to the transfer function amplitude exceeding the upper bound.

For an Earth with a decreased resistivity at some point moving from depth to the surface, moving from low to high frequency will have a large decrease in phase followed by a small increase. The cycle of decreased and increased phase continues but the magnitude of the phase change quickly approaches 0. The increase in phase is related to the transfer function amplitude exceeding the lower bound.

For a layer between the surface and half space with increased resistivity, the amplitude and phase of the transfer function will be affected mainly by the thickness of the layer but not the magnitude of increased resistivity. For a layer between the surface and half space with decreased resistivity, the amplitude and phase will be affected by both the thickness of the layer and the magnitude of decreased resistivity.

The relative change in transfer function amplitude and phase for two earth models, one with equally scaled resistivity of the other, will be the same. However, the amplitude and frequency for which the change in transfer function occurs will shift, and frequency at which the transfer function phase will shift.

4.0 Effect of Varying Earth Models on Electric Field

The section applies the variety of the Earth model studied in Section 3 to a sample geomagnetic field to examine the effect of Earth variations on the resultant electric field.

The geomagnetic field variation used is artificial and constructed from six individual frequencies. Table 4.1 lists the frequencies and corresponding period, amplitude and phase. Figure 4.2 [1] in section 4.2 shows the corresponding total geomagnetic field amplitude in the time domain. The frequencies are used to construct the electric field in the time domain for a time step of 30 s. The particular frequencies were chosen to be close to equally spaces in log domain, with exponentially decreasing amplitudes and arbitrary phase shifts.

Table 4.1 - Artificial Geomagnetic Field Composition

k	Frequency [Hz]	Period [min]	Amplitude [nT]	Phase [degrees]
1	9.259×10^{-5}	180	200	10
2	2.083×10^{-4}	80	90	20
3	4.762×10^{-4}	35	30	30
4	1.111×10^{-3}	15	17	40
5	2.381×10^{-3}	7	8	50
6	5.556×10^{-3}	3	3.5	60

The Earth models used to calculate the electric field for the artificial geomagnetic field are based on the uniform Earth models studied in Section 3. The Earth model is composed of ten layers: nine layers of thickness of 10 km, and a resistivity per layer. The resistivity has two possible values, 100 Ωm and 1,000 Ωm, and the Earth model variations include all possible combinations of the two values for ten layers; there are 1024 different Earth models. Out of these models, two are unique: model 1 which has all resistivities of 100 Ωm, and model 1024 which has all resistivities of 1,000 Ωm. These two uniform Earth models form the standard lower and standard upper Earth model bounds, respectively. Table 4.2 lists the model properties for models 1, 1024, and a random variation model 712.

Table 4.2 - Standard Upper and Lower Models

Layer	Thickness [km]	Resistivity [Ωm]		
		Model 1	Model 1024	Model 712
1	10	100	1,000	1,000
2	10	100	1,000	100
3	10	100	1,000	1,000
4	10	100	1,000	1,000
5	10	100	1,000	100
6	10	100	1,000	100
7	10	100	1,000	100
8	10	100	1,000	1,000
9	10	100	1,000	1,000
10	-	100	1,000	1,000

This combination of parameters was chosen so that it would reflect on the variations studied in Section 3. I previous section there was a focus on two resistivity values: 100 Ωm and 1,000 Ωm. These two values represent conductive and resistive Earth structures. Furthermore, tests involved examining the

effect of changing thicknesses of the targeted resistive or conductive layers, generally between 10 km to 90 km. In reality, a single layer can be decomposed into a number of 10 km layers, with equal resistivity values. In general, the 1024 combinations of ten 10 km layers with two possible resistivity values include all the variations studied in section 3.

4.1 Transfer Function Amplitudes

As observed in Section 3, the Earth transfer function corresponding to the standard upper and lower Earth models is not the absolute maximum or minimum transfer function amplitude. By looking at all the possible Earth combinations collectively, it is possible to determine the maximum possible transfer function amplitude at any frequency. Figure 4.1 shows the transfer functions for standard upper and lower Earth models, as well the absolute maximum and minimum. It is seen that for frequencies ranging from 10^{-2} Hz to 1 Hz, there are models that can produce higher transfer function amplitudes, and from 10^{-3} Hz to 1 Hz there are models that can produce lower amplitudes. This is important if we make the assumption that higher transfer function amplitudes will cause higher electric field amplitudes in the time domain. Therefore it is expected that any changes in electric field will be caused by changes in amplitudes for frequencies only in these ranges.

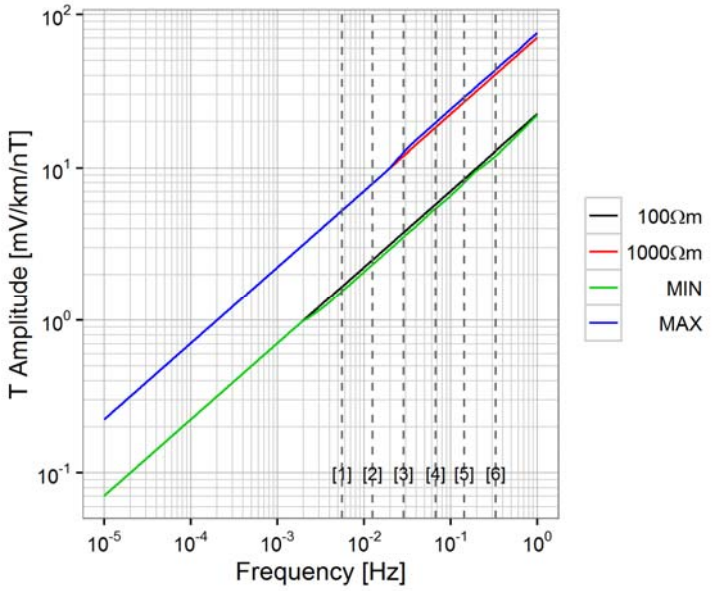

Figure 4.1 - Maximum and Minimum Transfer Function Amplitude Versus Frequency
The amplitude of a uniform 100 Ωm and 1,000 Ωm Earth which represent the standard lower and standard upper models, and the minimum and maximum observed amplitude at each frequency for all possible model combinations. Dotted lines and [k] represent the k^{th} frequency in Table 4.1. Note the slight increase and decrease in amplitude observed for the higher frequency ranges.

4.2 Electric Field

After the transfer function is determined for each Earth model combination, it is used to calculate the electric field. For each Earth model the maximum electric field amplitude is determined by taking the maximum of all the electric field values that occur for a particular geomagnetic field sample day. Figure 4.2 [1] shows the geomagnetic field amplitude in the time domain and [2] shows the calculated electric field amplitude in the time domain due to the standard upper limit Earth model, and all the

maximum electric field amplitudes for other models against their time of occurrence. Figure 4.3 shows the electric field amplitude for two hours during which the maximum observable electric field amplitude occurs. It compares electric field for standard upper and lower models, and the maximum electric field. The maximum is the highest electric field amplitude observable at any time, and is not particular to any model.

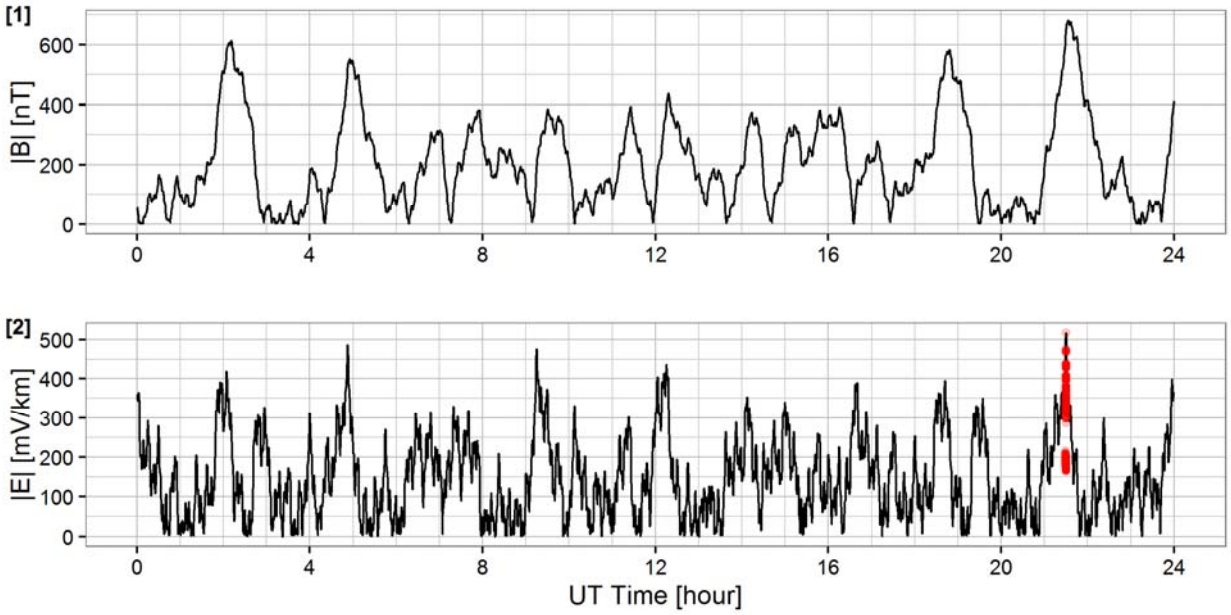

Figure 4.2 - Total Geomagnetic and Electric Field Amplitude
[1] Shows the total geomagnetic field amplitude measured as geomagnetic flux density, calculated from the Northward and Eastward components (equation 18). [2] Shows the total electric field amplitude due to the standard upper Earth model. Red dots represent the maximum electric field amplitude for all other Earth models, and their time of occurrence.

It is noticed in figure 4.2 that the time of occurrence of the maximum amplitude during the geomagnetic disturbance, is the same. This means that the maximum electric field would occur at the same time (at approximately 21:30 UT), regardless of the effect of changing Earth transfer function. The histogram of occurrences of the maximum amplitude values per specific bins is shown in section 4.3, figure 4.5.

In figure 4.3, one can see the electric field between 20:30 UT and 22:30 UT due to the standard upper (blue), and lower (red) Earth models. As expected, the upper bound electric field is generally higher than the lower bound electric field. However, it is seen that there are some times at which both models give similar values. Figure 4.3 also displays the maximum possible electric field (green), which is not represented by any specific model. In contrast, the upper bound electric field and maximum electric field are generally the same, with a few exceptions where the upper bound Earth model gives a significantly smaller electric field amplitude. It can be inferred that for the most part, the standard upper and lower Earth models serve as a standard upper and lower bound for the modelled E – field values. At some times, other models give more extreme modelled values.

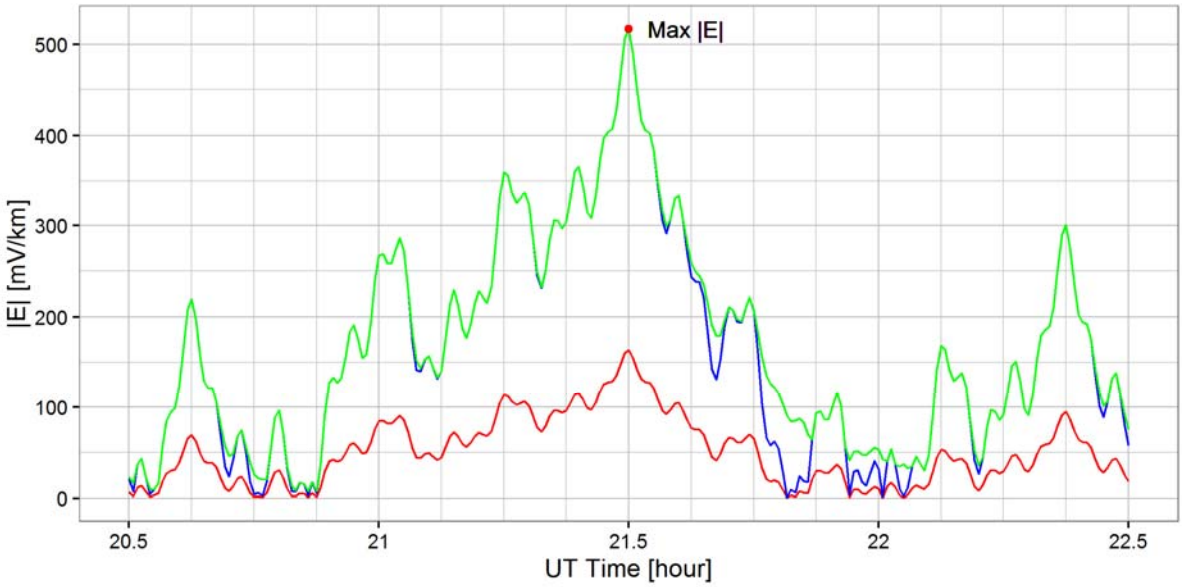

Figure 4.3 - Electric Field Amplitude During Maximum Occurrence
Electric fields for: standard lower [red], standard upper [blue] Earth models, and maximum [green]. [red dot] represents the maximum observable electric field amplitude for all of the models and times.

Generalised comparison of the electric field values obtained for three cases are shown in Figure 4.4. Plot [1] shows the standard upper bound, against itself (for reference) and the lower bound model. The distribution of data indicates a perfect linear agreement, suggesting that the electric field due to the standard lower bound Earth models is uniformly scaled from the standard upper Earth model. Plot [2] shows the standard upper bound, against itself (for reference) and against the maximum. This time the distribution of points is scattered, especially for amplitudes below 10^2 [mV/km], for which the standard upper Earth model gives significantly smaller electric field amplitude values. This is an interesting result that shows that the Earth model variations cannot be excluded from the electric field analysis.

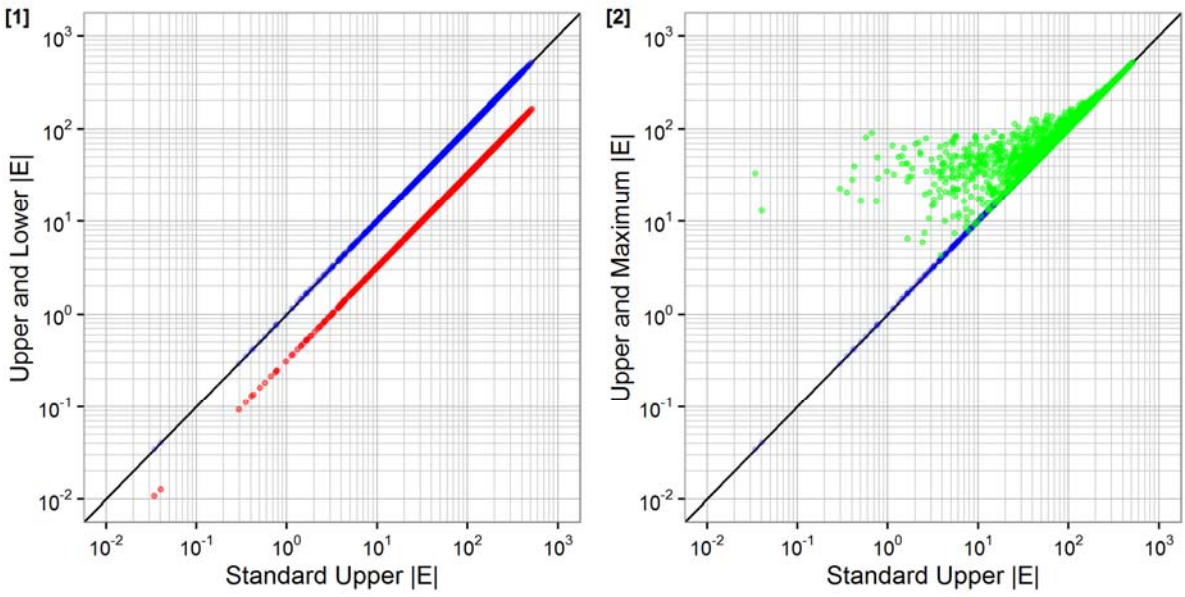

Figure 4.4 - One to One Plots of Electric Fields for Two Cases

[1] Standard upper electric field amplitudes vs itself [blue], and vs the standard lower electric field [red]. [2] Standard upper electric field amplitudes vs the artificial maximum electric field [green]. In all cases, each point represents a single time. For artificial maximum comparison, each point additionally represents an undetermined but different model. Black line represents a line of slope 1 and intercept 0.

4.3 Histogram of Maximum Electric Field Values

The maximum total electric field amplitudes obtained with the 100 Ωm and 1,000 Ωm uniform half-space models are compared against those of all possible combinations of layers, in a distribution histogram. Figure 4.5 shows the frequency of occurrence of the maximum total electric field amplitude values. It is clear that for the case of the Earth models considered, standard upper and lower models determine the upper and lower bounds of the maximum electric field amplitude, and that all other maximum electric field amplitudes fall within their range. However it is also worth noting that the distributions of data are separated into several discrete groups.

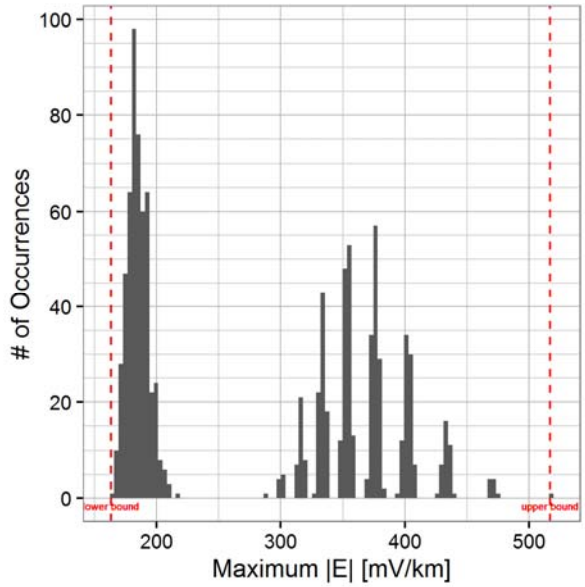

Figure 4.5 - Histogram of Maximum Electric Field Amplitudes

The bars show the frequency of occurrence of particular electric field amplitudes. The range between the minimum and maximum observed amplitudes is divided into 100 ranges of equal width (in linear space). The red vertical dashed lines represent the electric field amplitude corresponding to the standard upper and lower bound Earth models.

Figure 4.6 shows the distribution of transfer function amplitudes for each of the six frequencies from Table 4.1. The distribution of amplitudes from low frequency [1] to high frequency [6] changes from discrete to continuous. The distribution of the maximum electric field amplitudes in Figure 4.5 is most like the distribution from Figure 4.6 [1]. This would mean that the electric field amplitude is mainly affected by the geomagnetic field variations with low frequencies. The contributing factors to this effect may include the fact that the low frequencies of the geomagnetic field have naturally high amplitudes, and the way in which different frequencies interact with the shallow and deep Earth.

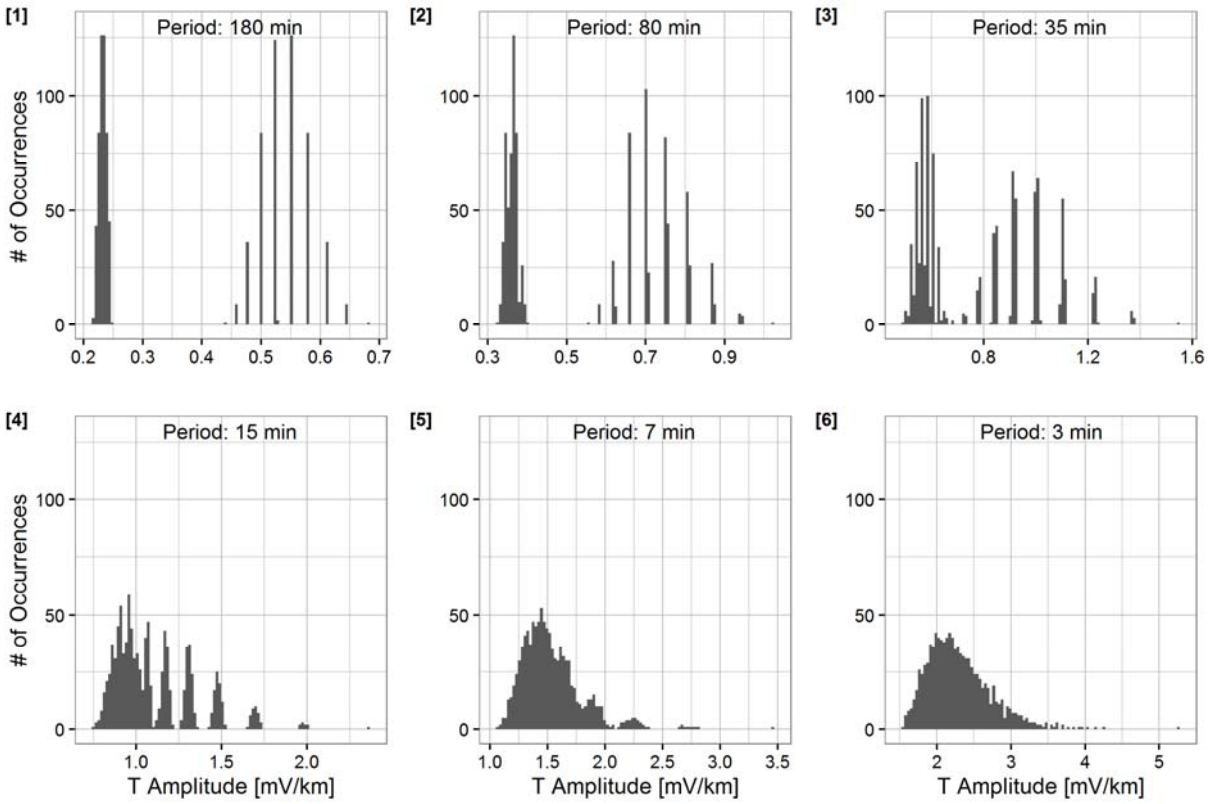

Figure 4.6 - Histogram of Transfer Function Amplitudes for Six Frequencies
[k] represents kth frequency from table 4.1 – Artificial Geomagnetic Field Composition. The range between the minimum and maximum transfer amplitude is divided into 100 bins of equal range length.

4.4 Variations of Geomagnetic and Electric Fields with Depth

The way the geomagnetic field interacts at depth within the shallow and deep Earth depends on the frequency of the variation. For the following example, in order to generalize the geomagnetic field frequencies, they have been adjusted according to values in table 4.3. Each frequency now has the same phase and amplitude. The Earth model used to calculate the change in electric field with depth, is model 1024, the standard upper bound Earth model, which is a uniform Earth model with a resistivity of 1,000 Ωm.

Table 4.3 - Properties of the New Geomagnetic Field

k	Frequency [Hz]	Period [min]	Amplitude [nT]	Phase [degrees]
1	9.259×10^{-5}	180	50	45
2	2.083×10^{-4}	80	50	45
3	4.762×10^{-4}	35	50	45
4	1.111×10^{-3}	15	50	45
5	2.381×10^{-3}	7	50	45
6	5.556×10^{-3}	3	50	45

Figure 4.7 presents [1] the electric field amplitude, and [2] the geomagnetic field amplitude, as a function of depth. The figures show that higher frequencies of the geomagnetic field diffuse into the Earth structure quicker than lower frequencies. This is also true for the electric field. However, for all

six frequencies the geomagnetic field amplitude is the same on the surface, but for the electric field, the surface amplitude is greater for the high frequency. This is related to the higher transfer function amplitude for higher frequencies. As a result, the electric field at high frequencies has high surface amplitudes but diffuses quickly, and low frequency electric fields have smaller surface amplitude but are more constant throughout the Earth. Note that this geomagnetic field does not represent a naturally occurring geomagnetic field. Normally the amplitudes at high frequencies are significantly smaller.

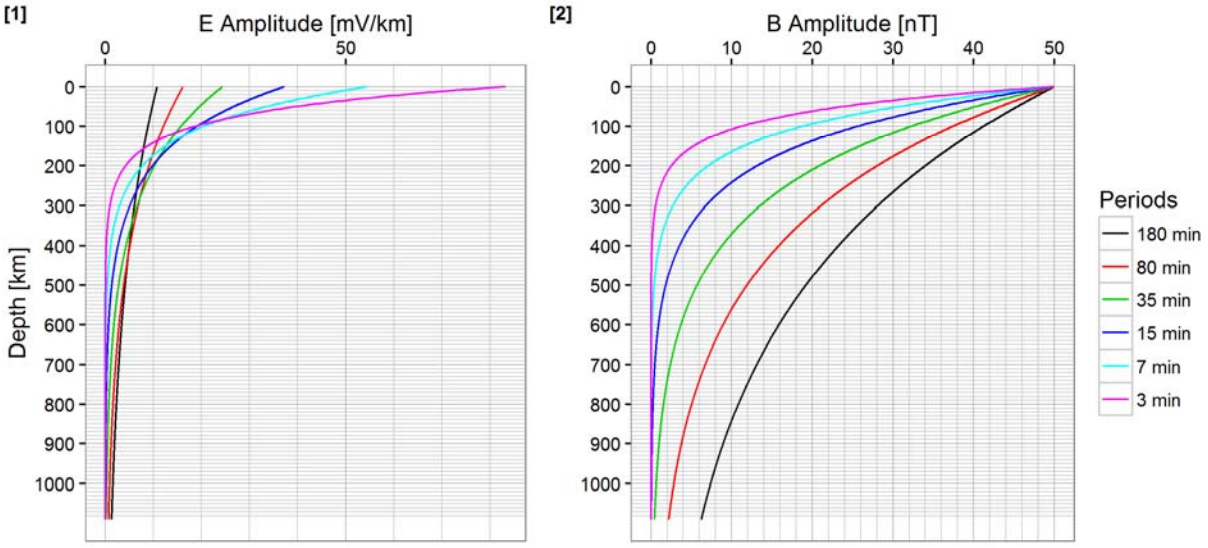

Figure 4.7 - Electric and Geomagnetic Fields at Depth
[1] shows the electric field amplitude for each of the six frequencies, and [2] shows the geomagnetic field amplitude for each of the six frequencies. The field amplitudes decay with depth.

5.0 Quebec Earth Model

In this section, analysis procedure used in Section 4 on the uniform Earth model is applied to the Quebec Earth model for several cases of real geomagnetic field records.

To examine how uncertainties in the Earth model affect the electric field we construct Earth models with standard layer resistivities multiplied by three and divided by three. The Quebec Earth model is constructed using seven layers. With a standard value, an upper value and lower value of resistivity for each of the seven layers, there are 2187 possible Earth model combinations. Out of all these, there are three special cases of Earth models, which include: the Upper Bound Earth Model (model 2187) – with all layer resistivity values increased by a factor of three, the Standard Earth Model (model 1094) – with all layer resistivity values standard, and the Lower Bound Earth Model (model 1) – with all layer resistivity values decreased by a factor of three. Table 5.1 lists the properties of each layer for the three special cases of Earth models.

Table 5.1 - Quebec Standard, Upper and Lower Earth Models

Layer	Thickness [km]	Resistivity [Ωm]		
		Lower Bound Model 1	Standard Quebec Model 1094	Upper Bound Model 2187
1	1	33	100	300
2	14	3,333	10,000	30,000
3	10	100	300	900
4	75	333	1000	3000
5	300	33	100	300
6	200	3.3	10	30
7	-	.33	1	3

Several sample geomagnetic records were selected for analysis, based on relative geomagnetic storm size, and range from quiet periods to large geomagnetic storms. Table 5.2 lists the geomagnetic storms analyzed for this study, their location, date and range of geomagnetic field components (North x, East y) in [nT]. Each record spans 24 hour, and contains 1440 data points with a 1 minute time step. For the analysis, this section will include graphs mainly for [1] OTT on 1989-03-13, and the remaining storms can be found in the appendices.

Table 5.2 - Geomagnetic Record Samples

Disturbance	Location	Date [yyyy-mm-dd]	Δx Range [nT]	Δy Range [nT]
1	OTT	1989-03-13	3019	1621
2	OTT	1995-09-28	119	128
3	OTT	2003-10-30	1739.4	1119.5
4	OTT	2012-03-09	680.5	388.6
5	OTT	2013-10-19	57.6	64.6
6	OTT	2014-06-08	128.4	278.5
7	OTT	2015-06-22	712.4	385.26

5.1 Transfer Function

Figure 5.1 shows the transfer function amplitude for the lower bound, standard Quebec and upper bound Earth models, as well as the maximum and minimum observable transfer function amplitude at each frequency. There are some frequencies at which the amplitude of the upper Earth model is not the highest amplitude, and amplitude of the lower Earth models is not the lowest. It is important to notice that these small differences occur across the entire frequency range, which is unlike the uniform Earth models tested in Section 4.0 which only affected higher frequencies (See figure 4.1). This could mean that the maximum electric field can be affected by both the low and high frequency waves.

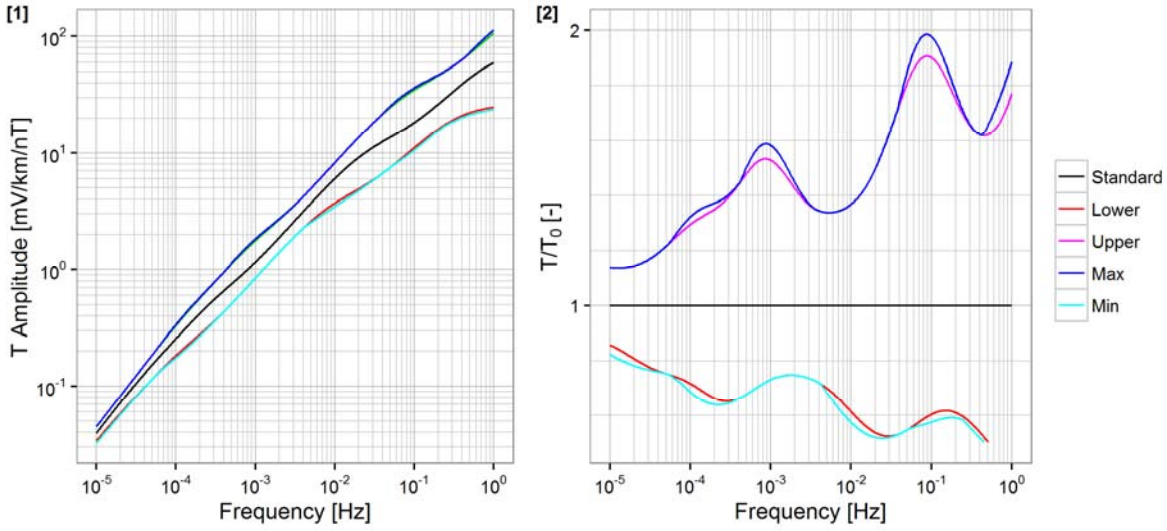

Figure 5.1 - Transfer Function Amplitude of the Quebec Earth Model

[1] The relationship between frequency and the amplitude of the Earth transfer functions due to the standard Quebec (model 1094), lower bound (model 1) and upper bound (model 2187) Earth models, as well as the maximum and minimum possible transfer amplitude for each frequency. [2] For a more clear view, the transfer function amplitude of each model divided by the transfer function amplitude of the standard model.

Figure 5.2 shows the phase of the lower bound, standard Quebec and upper bound Earth models. It is clear that the shape of the phase function is the same in all three cases, with the difference being the shift in frequencies. The phase of the transfer function from the upper bound Earth model is shifted to higher frequencies, and for the lower bound Earth models is shifted to lower frequencies. This means that for an Earth model with the same type of variation in the Earth, the phase will always be the same, and the frequency for which the phase occurs will be dependent on the relative resistivity of the Earth.

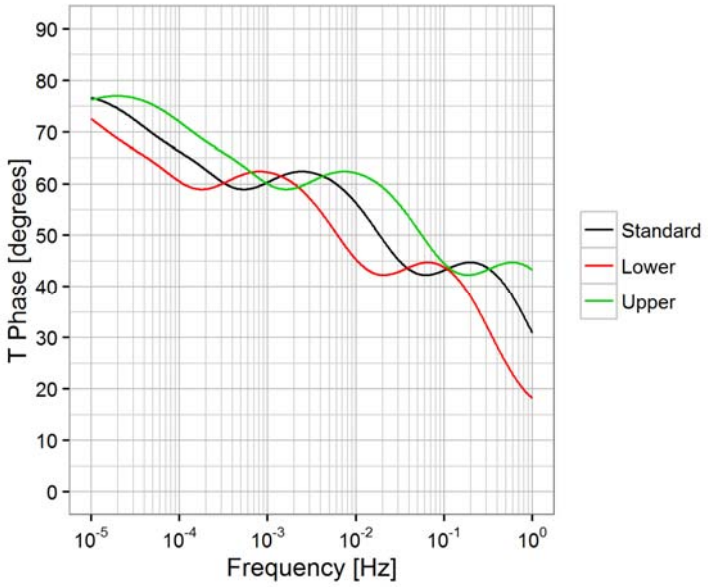

Figure 5.2 - Transfer Function Phase of the Quebec Earth Model
The relationship between frequency and phase of the Earth transfer functions due to the standard Quebec (model 1094), lower bound (model 1) and upper bound (model 2187) Earth models.

5.2 Electric Field

Figure 5.3 shows the geomagnetic and calculated electric field in the Northward (x) and Eastward (y) directions, for OTT 1989-03-13. The same data for other geomagnetic records are presented in Appendix A – Electric and Geomagnetic Fields. Graphs [1] and [2] show the geomagnetic flux density for Northward and Eastward component, and [3] and [4] show the electric field in Eastward and Northward directions, for the standard Quebec Earth model. Note that the E_x component is calculated from B_y and E_y is calculated from B_x.

The total geomagnetic and electric fields are displayed in figure 5.4. Graph [1] shows the total geomagnetic field and [2] the total electric field due to the standard Quebec Earth model. Figure 4.5 also shows the amplitude of the maximum total electric field for all other models, against time of occurrence. For other geomagnetic records, Northward and Eastward fields can be found in Appendix A – Electric and Geomagnetic Fields, and total electric and geomagnetic field amplitudes can be found in Appendix B – Total Electric and Geomagnetic Amplitude.

It is an interesting observation that the maximum E amplitudes for different models occur at different times. This is completely unlike the uniform Earth model studied in Section 4.0, where the peak electric field occurred only at one time (See figure 4.2). The occurrence of peaks at different times for different Earth models could suggest that the peak electric field is composed from different frequency components in each case, suggesting that variety in the Earth model interacts with the geomagnetic variation in different ways.

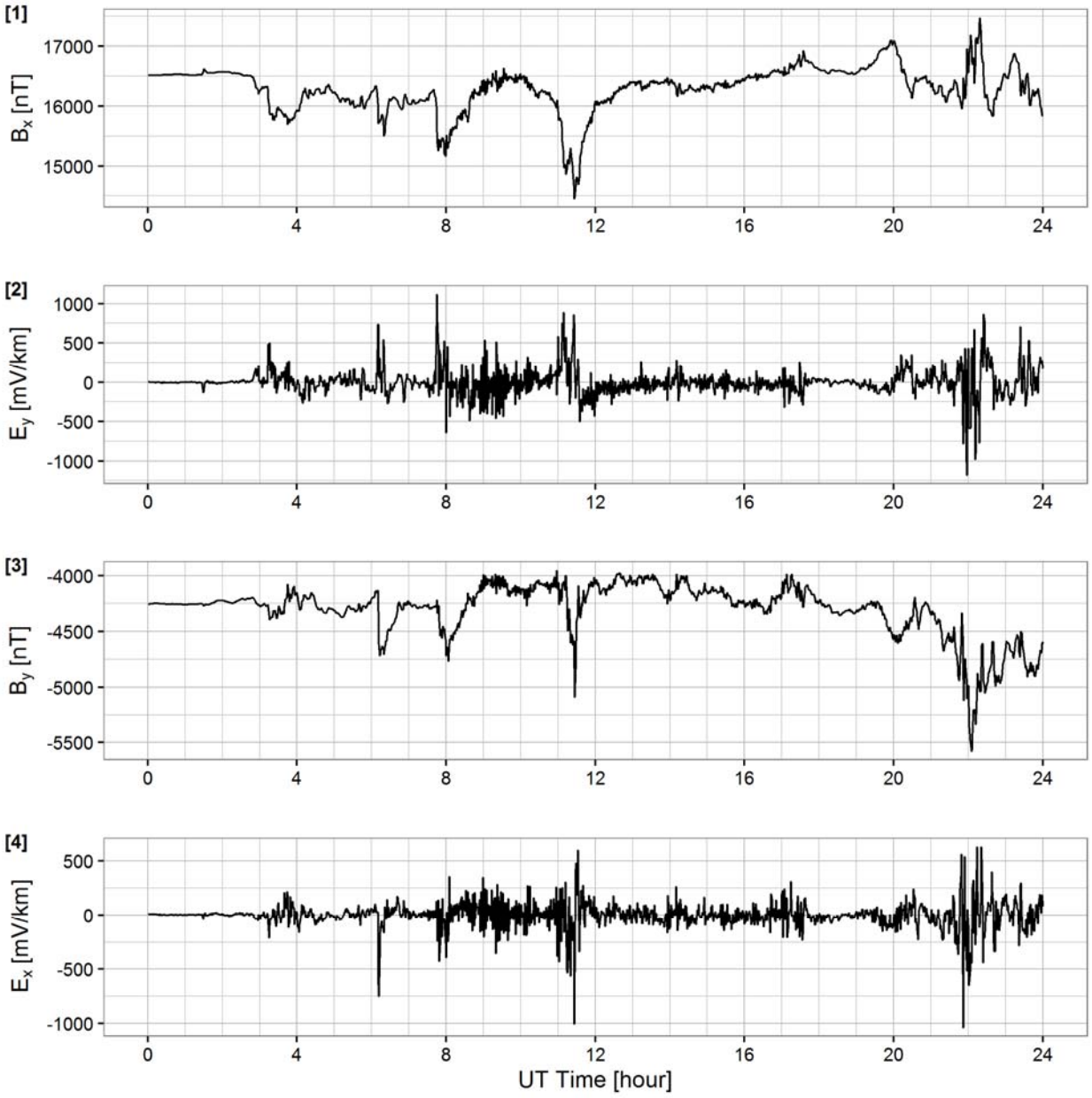

Figure 5.3 - Northward and Eastward Electric and Geomagnetic Fields for OTT 1989-03-13
[1] Eastward geomagnetic field, [2] Northward electric field, [3] Northward geomagnetic fields and [4] Eastward electric field, for the OTT magnetometer station in 1989-03-13. E_y is calculated from B_x, and E_x is calculated from B_y.

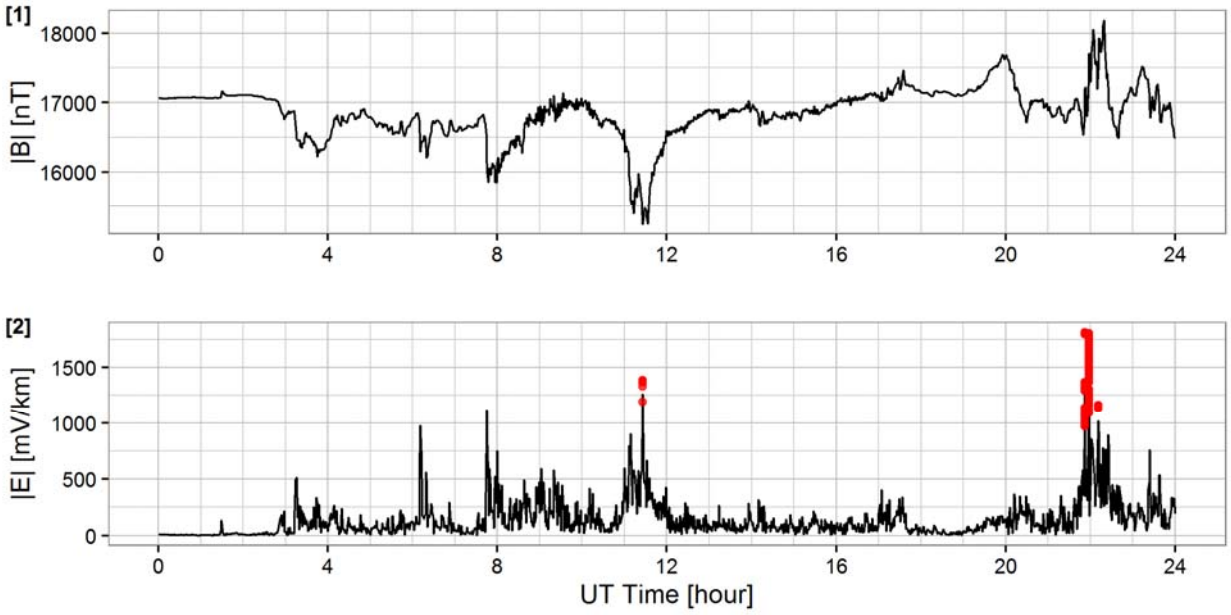

Figure 5.4 - Total B and E Amplitude for OTT on 1989-03-13
[1] Total geomagnetic field amplitude and [2] total electric field amplitude. Each red dot represents the maximum electric field amplitude at any time, observed for a particular model.

Figure 5.5 compares the total electric field from the lower, standard and upper Quebec Earth model, as well as the artificial maximum electric field, during the occurrence of the highest total electric field amplitude, for geomagnetic field recorded at OTT on 1989-03-13. Electric Field during maximum amplitude occurrence for several other events from table 5.2, can be found in Appendix C – Electric Field Sample During Peak.

The plots show the total electric field amplitude for the lower bound, standard Quebec and upper bound Earth models, as well as the maximum calculated electric field at any time, for 2 hours during the occurrence of the highest maximum. The pattern in the time series electric field is similar to the pattern observed in figure 4.3 for the uniform Earth model variation on the test geomagnetic field. However, it is worth noting that across all the events studied, there are particular times at which the electric field due to the upper bound Earth model is smaller in amplitude than the electric field due to the lower bound Earth model. Specifically, observe Figure C.3 for the event on 2012-03-09 at time UT 9:00, in Appendix C. In the general test case in Section 4, this effect was never observed, as according to figure 4.4 the electric fields amplitudes for the upper and lower bound models are clearly directly related. The same scatter plot for the Quebec Earth model variation electric field amplitudes is found in Figure 5.6 image [1], where the same relationship is clearly non-existent.

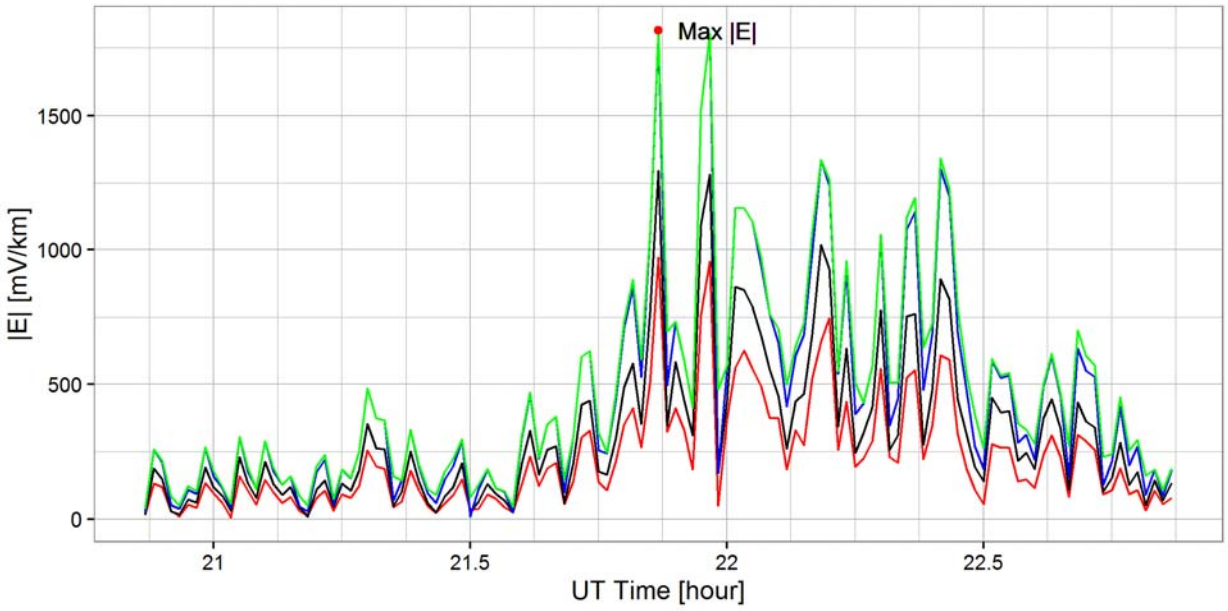

Figure 5.5 - Maximum Amplitude Occurrence for OTT at 1989-03-13
Electric Fields for [red] lower, [black] standard, [blue] upper Earth models, as well as [green] the artificial maximum. [red dot] represents the general maximum amplitude of the total electric field.

Figure 5.6 shows [1] the relationship between standard electric field and the lower and upper electric fields, as well as [2] the relationship between the standard electric field and the upper and artificial maximum electric fields, for geomagnetic field recorder located at OTT on 1989-03-13. The same plots for other geomagnetic field records are found in Appendix E – Scatter Plot of electric Field Cases. Each point on the scatter plot represents a single time for the electric field in the time domain. Note that, for the artificial maximum electric field amplitude, the points represent different models from all possible Earth variations.

For lower amplitudes of 10mV/km and less, it is seen that the [blue] point for the upper bound electric field versus the standard electric field, and the [red] point for the lower bound electric field versus the standard electric field, are mixed. It means that for a particular standard electric field, the electric field due to the upper bound Earth model gives smaller amplitudes, and the electric field due to the lower bound Earth model gives higher amplitudes. This pattern is observed across all the studied geomagnetic field samples. As a general rule, for increasing amplitude of the electric field, the upper and lower electric fields become more separated, giving electric field values higher and lower respectively. As well, in general the maximum observed field at each time shows more scatter in the lower amplitude region with often significantly higher electric field amplitudes, and converges with the upper electric field values for amplitudes 100mV/km and higher.

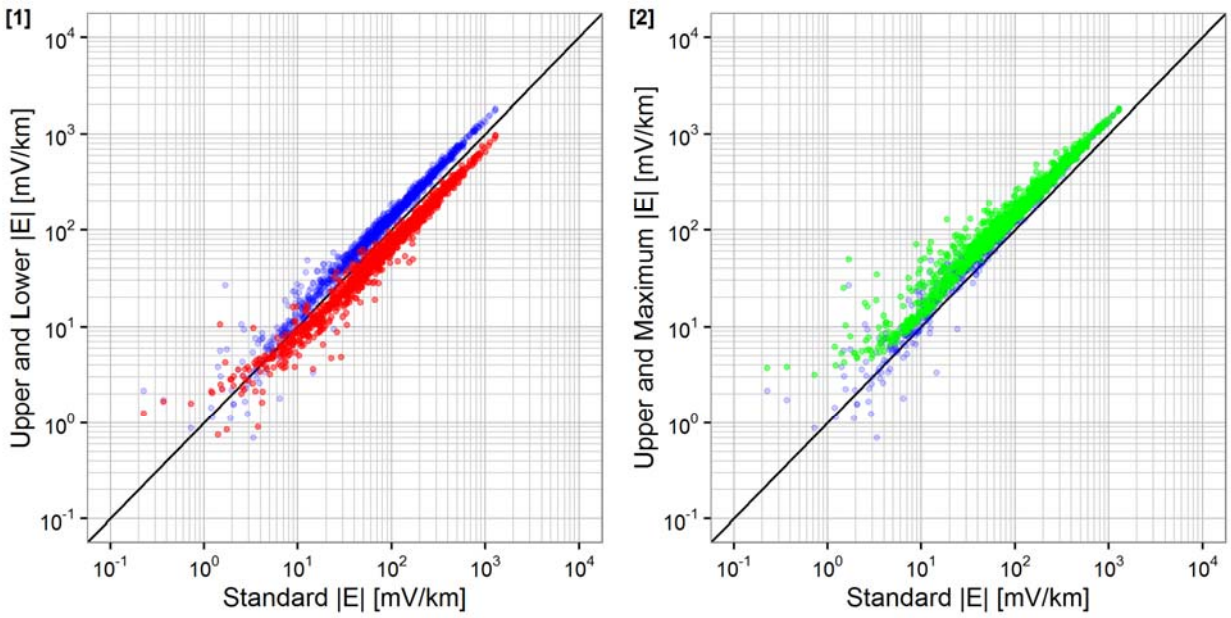

Figure 5.6 – Scatter Plot of E Fields at OTT on 1989-03-13
[1] shows the relationship between the standard electric field and, [blue] the upper bound electric field and [red] the lower bound electric field. [2] shows the relationship between the standard electric field and, [blue] the upper bound electric field and [green] the maximum electric field. Each point represents an individual time, and for the artificial maximum a different Earth variation.

5.3 Distribution of Maximum Electric Field Values

Figure 5.7 shows a histogram of the maximum total electric field values for all Earth models for the geomagnetic field recorded at OTT on 1989-03-13. Frequency distributions for the other events from table 5.2 can be found in Appendix D – Distribution of Maximum Electric Field Amplitudes.

It is observed that the range between the maximum and minimum peak electric field amplitude due to the upper bound and lower bound Earth models generally capture the majority of peak amplitudes that occur for the different models. There are some amplitudes however, that exceed these limits. This is unlike the uniform Earth model, where the E amplitudes due to Earth boundary models generally capture the entire range of possible peak amplitudes. This is especially evident for OTT on 2015-06-22, where there is a significant number of models that produced electric field amplitudes much greater than the upper bound Earth model. Refer to Appendix D.3 for distribution of peak electric field amplitudes of OTT on 2015-06-22. Section 5.5 focuses in detail on the upper bound Earth model and the model that produced the maximum electric field.

The distribution of the peak amplitude occurrences is also dependant on the geomagnetic record. For OTT on 1989-03-13, the occurrences fall into discrete categories like in figure 4.5 for the artificial geomagnetic field. However, for a geomagnetic field measured at OTT on 2013-10-19, the occurrence distribution of electric field peaks is continuous. Refer to Figure D.4 in Appendix D for frequency distribution at OTT on 2013-10-19.

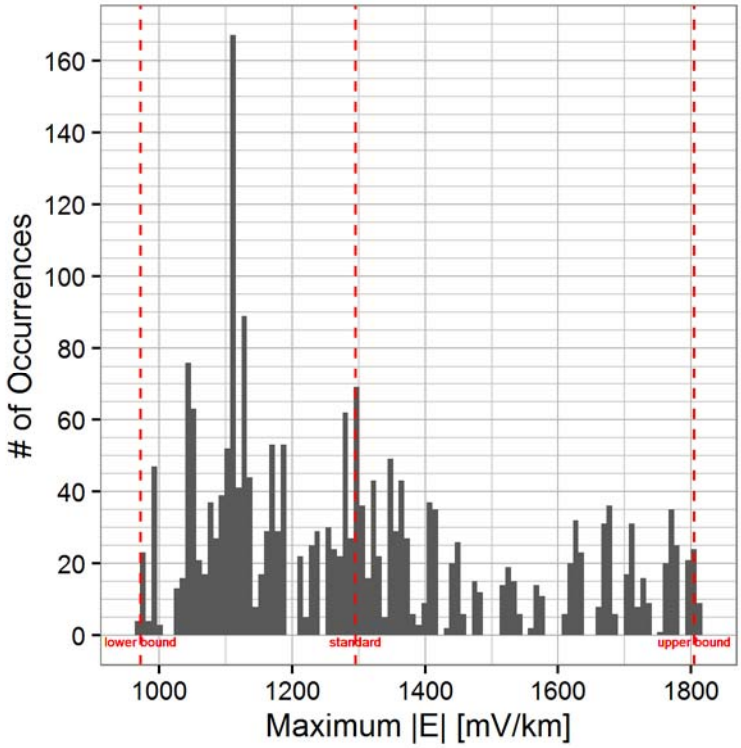

Figure 5.7 - Histogram of Maximum E Amplitude for OTT on 1989-03-13
Histogram of the maximum electric field amplitude for all 2187 Earth models. Range between minimum and maximum amplitude is divided into 100 bins of equal size. Red dotted lines represent the maximum amplitude for the lower, standard and upper Earth models.

5.4 Variations of Geomagnetic and Electric Fields at Depth

For the artificial geomagnetic field used in Section 4.4 (refer to Table 4.3 for the frequency components), the interaction of the geomagnetic and electric waves with the Quebec Earth can be calculated. Figure 5.8 shows the amplitude of the [1] electric field and [2] geomagnetic field with depth.

The electric and geomagnetic fields behave similarly to the uniform Earth structure, where amplitude from the high frequency variations diffuse in the Earth faster, and the amplitude of low frequency variations remain more constant throughout the depth of the Earth. The increasing amplitude of the Earth transfer function for higher frequencies indicates that the electric field amplitude at the surface for each frequency is not the sane. Furthermore, it is observed that the diffusion of each variation occurs individually for each layer, given by the observable changes in diffusion rate that would indicate change in Earth resistivity. A less resistive Earth will allow the electric or geomagnetic field variation to diffuse quicker as opposed to a more resistive Earth.

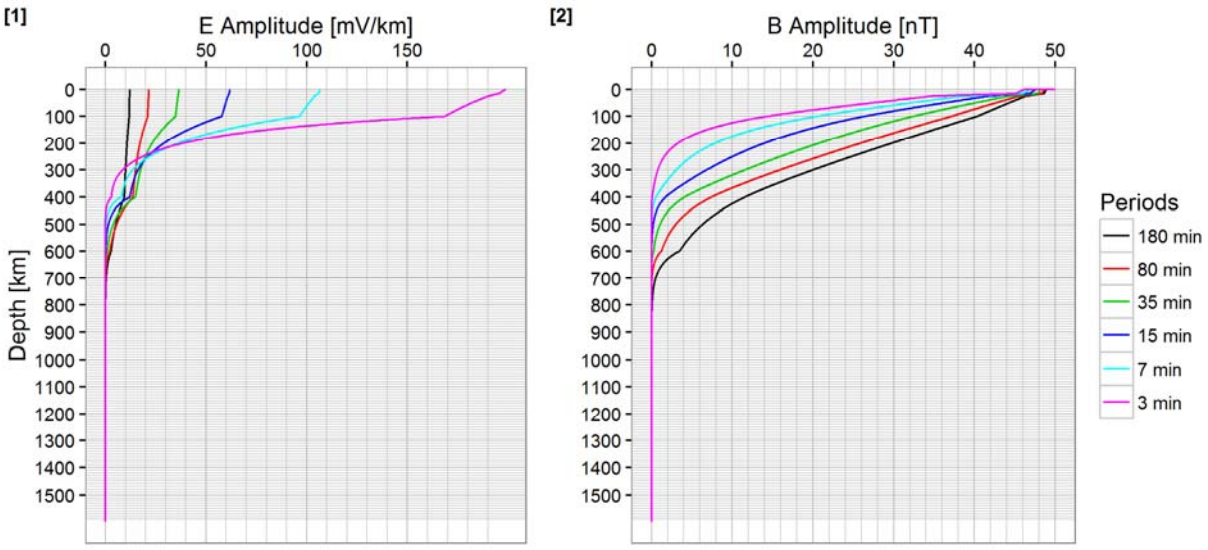

Figure 5.8 - Electric and Geomagnetic Field Amplitude at Depth for Quebec Earth Model
[1] shows the amplitude of the electric field at depth, and [2] shows the amplitude of the geomagnetic field at depth, calculated for the Quebec Earth model.

5.5 The Frequency Domain Data

In Section 5.3, it is explained that the upper and lower bound models, and the respective time domain maximum of the total electric field amplitudes capture the distribution of electric field peaks quite well. However, it should be noted that the distribution in some cases shows that the upper bound Earth model is not the Earth model that produced the highest total electric field amplitude. This is especially seen for the storm on 2015-06-22. The particular distribution of electric field peaks is found in Appendix D figure D.6, and it shows that there are close to 200 Earth models for which the maximum electric field amplitude is slightly higher than that of the upper Earth model. In order to determine the relationships that lead to this effect, the model that produces the maximum electric field peak is compared to the upper bound Earth model, in the frequency domain.

From the distribution data, it is determined that for 2015-06-22, the maximum electric field amplitude would occur due to Earth model 241. This model produces the maximum for this geomagnetic record. In figure 5.9, the frequency content for the geomagnetic field and the resultant electric field, are shown for the upper Earth model. For other geomagnetic records, refer to Appendix F – The frequency domain Data. Figure 5.10 shows the Earth structure information for maximum and upper Earth models of geomagnetic record on 2015-06-22. This includes the resistivity at depth and apparent resistivity as a function of frequency, as well as the transfer function amplitudes and phase. The Earth structure figures for other geomagnetic records are found in Appendix G – Earth Structure and Transfer Function.

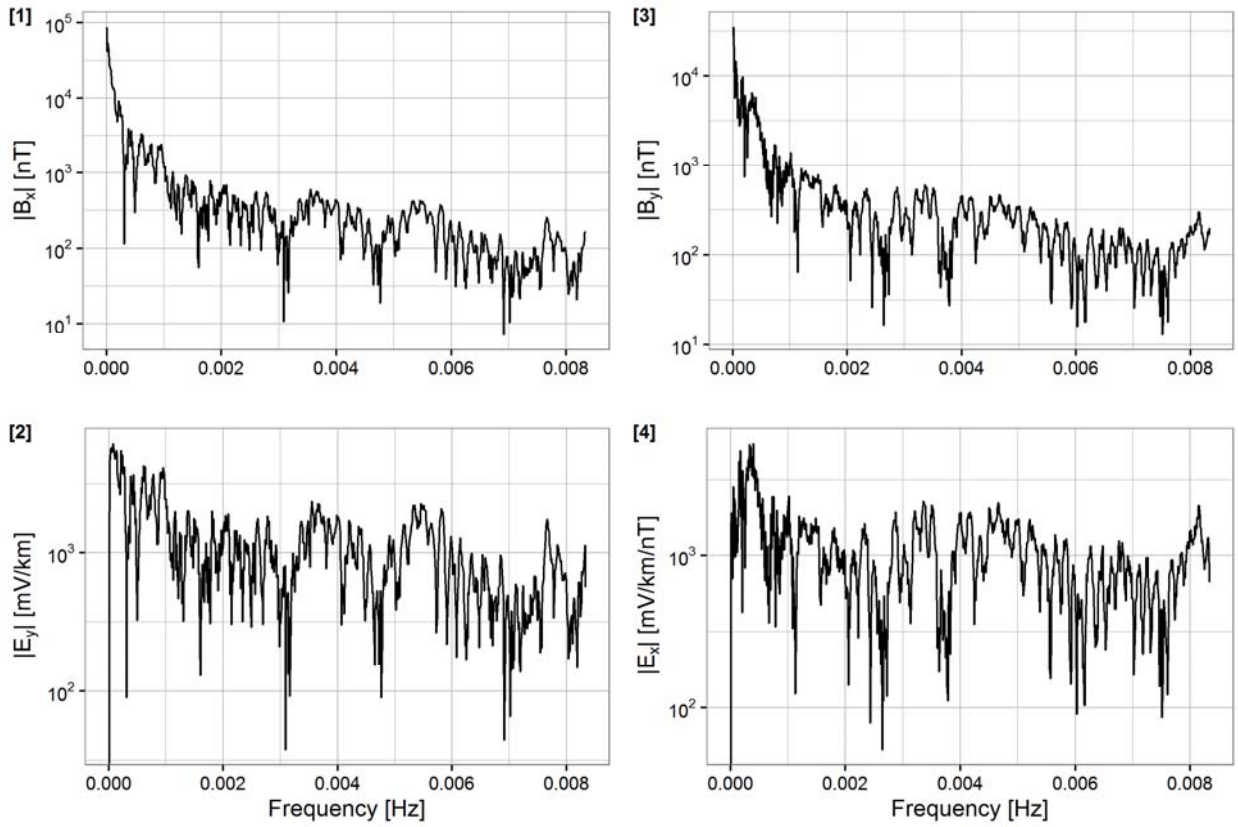

Figure 5.9 - The Frequency domain Geomagnetic and Electric Fields for 2015-06-22
The images show [1] the Northward geomagnetic field, [2] Eastward electric field, [3] Eastward geomagnetic field and [4] Northward electric field amplitudes in the frequency domain, for OTT on 2015-06-22. The Earth model used to calculate this electric field is the upper bound Earth model 2187.

In order to clarify the difference between the upper and maximum models, the transfer function due to both is divided by the transfer function of standard model 1094. The frequencies, for which this relationship is higher for the maximum model, meaning the transfer function is higher for the maximum model and not the upper model, are highlighted.

It is clear that the maximum model amplifies the electric field for specific frequencies. This is true for all geomagnetic records studied. This means that there must be a relationship between that frequency content and the increased electric field amplitude in the time domain, for the particular Earth model variations. Specifically, it is noticed that for 2015-06-22, the highlighted frequency region in 5.10 [4] would correspond to the higher electric field amplitudes in figure 5.9. It could be that the Earth models that produce the highest electric fields in the time domain are the models which amplify highest frequency domain amplitudes. This would also explain the variety of maximum Earth models for different geomagnetic records, since the frequency content of any electric field is dependent on the geomagnetic field itself.

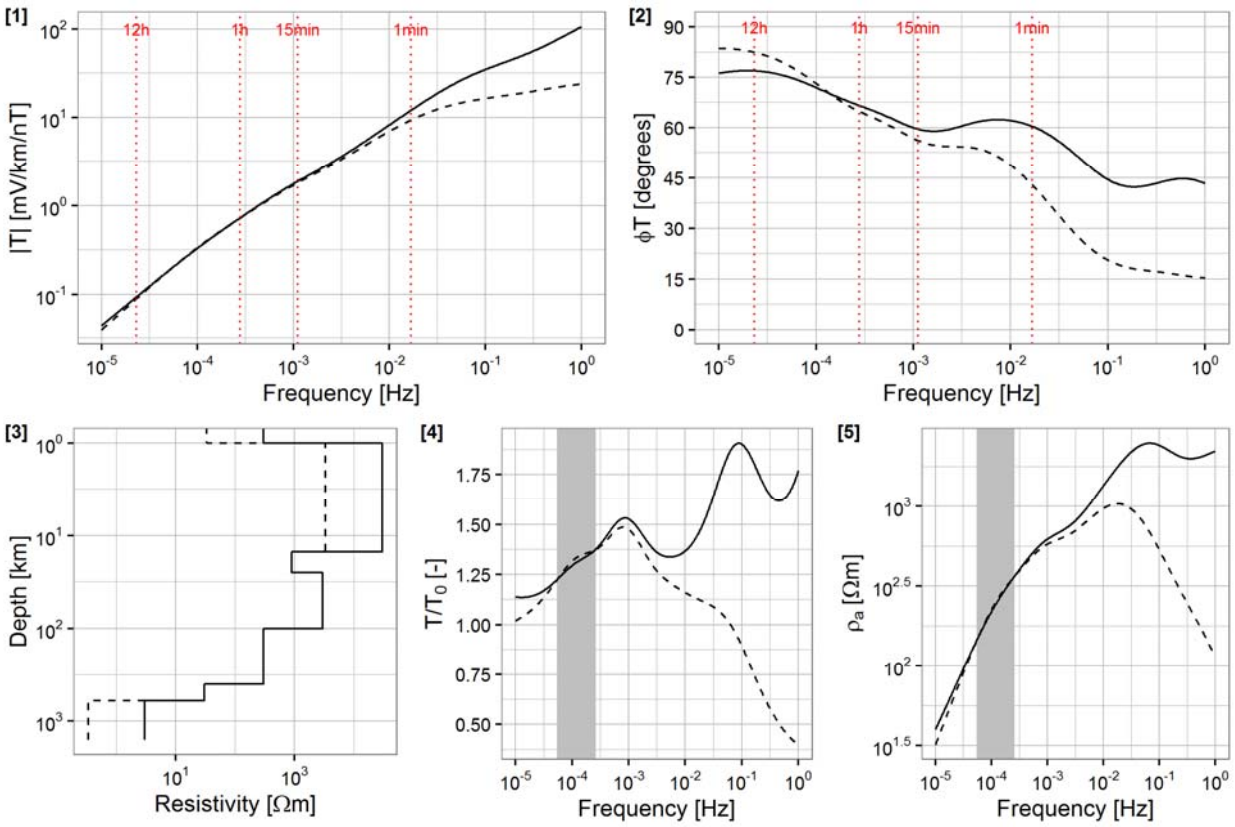

Figure 5.10 - Earth Structure and Transfer Function Data for 2015-06-22

Figures show, [1] transfer function amplitude, [2] transfer function phase, [3] resistivity of Earth with respect to depth, [4] transfer function amplitude of a model divided by standard model transfer function amplitude, and [5] the apparent resistivity per each frequency. On figures [1] and [2] highlighted vertical lines correspond to specific periods, and on figures [4] and [5] highlighted regions mark the frequencies where the maximum model gives higher amplitude. In all figures, solid lines represent the upper bound Earth model, and dashed lines represent the maximum Earth model.

In figure 5.11, the relationship between the frequency domain upper and maximum model electric field amplitudes is shown, for both the x and y components from values in the frequency domain. Highlighted are amplitudes which are greater for the maximum model, and black are amplitudes which are greater for the upper model. As expected, the relationship shows a tight fit. However, it is important to notice that especially for the Northward electric field for 2015-06-22, the red highlighted amplitudes are found in the upper end of the point distribution. The upper model versus maximum model the frequency domain amplitude scatter plots for the other geomagnetic records listed in table 5.2 are found in Appendix H. It is observed that for all the dates analysed there are some frequencies for which the maximum model produced higher amplitudes than the upper model (marked in red), except in the case of 2013-10-09 in figure H.5 for which the maximum model is the upper model. It is further seen that in all the cases the increased amplitudes include the highest amplitudes in at least one of the electric field components x or y.

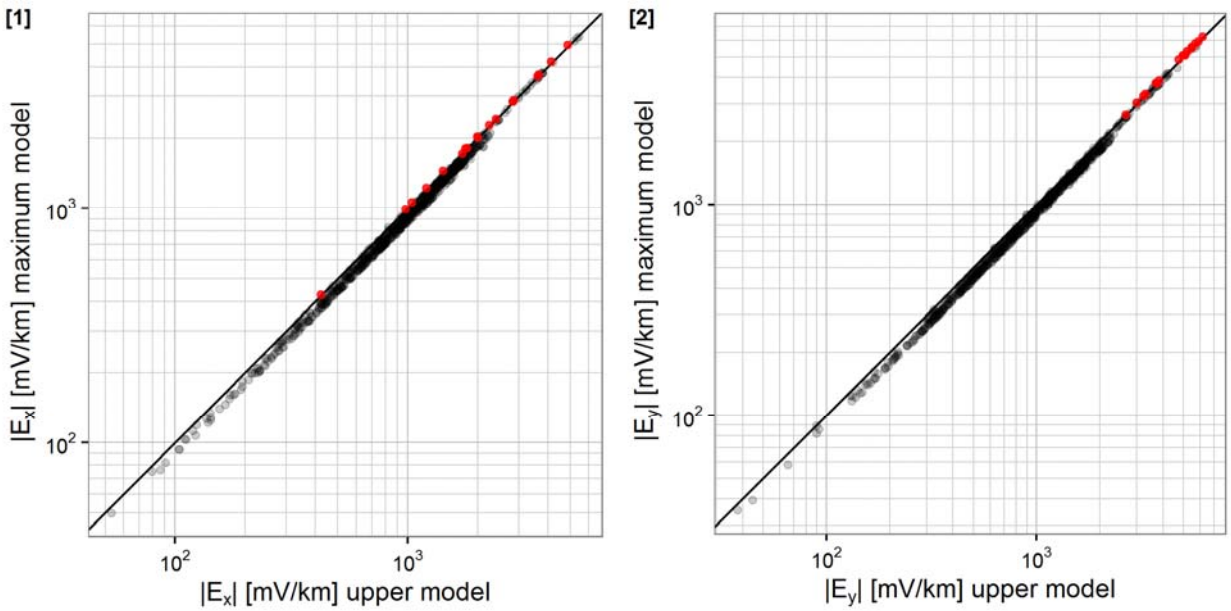

Figure 5.11 - Upper model versus Maximum model amplitudes for 2015-06-22
[1] Northward electric field, and [2] Eastward electric field for the upper versus maximum Earth models. Highlighted in red are points for which the maximum Earth model produces higher amplitudes and in black for which the upper Earth model produces higher amplitudes. Amplitudes are in the frequency domain.

As seen in figure F.4, the maximum Earth model produces higher amplitudes for a wide frequency band. This band captures most of the electric field amplitudes, including some of the highest values. Further in Appendix F figure F.5, it is seen in the upper model versus maximum model electric field plots, that the amplitudes which are higher for the maximum model (highlighted in red), are spread across all possible amplitude values. These excited frequencies are likely to contribute to the higher electric field amplitude in the time domain. For further information, table 5.3 lists the time domain maximum total electric field amplitude per specific models, for 1989-03-13 and 2015-06-22.

Table 5.3 - Peak Electric Field in The time domain

Model	**Electric Field Peak [mV/km]**	
	1989-03-13	**2015-06-22**
Standard (1094)	1295.35	439.556
Upper (2187)	1804.21	605.623
Maximum	1815.12	626.796

6.0 Conclusions

From the study of Earth transfer functions for various simple earth models, several conclusions can be drawn:

1. In general, a more resistive earth model will generate an earth transfer function with higher amplitudes for all frequencies. However, there are possible combinations of more resistive and more conductive layers that can produce even higher earth transfer function amplitudes for a small frequency range.
2. Similarly, a less resistive earth model will generate an earth transfer function with lower amplitudes for all frequencies. However, there ae possible combinations of more resistive and more conductive layers that can produce even lower earth transfer function amplitudes for a small frequency range.
3. All the possible earth transfer function amplitudes for a varying earth structure can be relatively well bound by the upper bound earth model and lower bound earth model. The upper bound earth model represents the highest resistivity of the varying earth model, and the lower bound earth model represents the lowest resistivity of the varying earth model.

From the study of the Earth transfer function and geomagnetic and electric fields in time and the frequency domain, several conclusions can be drawn:

1. It has been determined that for a 1-D Earth model composed of several layers, where each layer has a range of possible resistivity values, there are possible Earth models within the resistivity bounds that can produce Earth transfer function amplitudes in certain frequency ranges, higher than the Earth transfer function amplitude due to the general Earth model with the boundary values of resistivity.
2. There is a link between the increased transfer amplitude by the maximum Earth model, and the resultant electric field amplitude in the time domain. Specifically, it has been found that the electric field amplitudes in the frequency domain that have been amplified by the maximum Earth model's transfer function, tend to be the highest amplitudes from the electric field.
3. Since the frequency composition of the geomagnetic storm varies on each day, the electric field amplitudes in the frequency domain will also vary, and thus the specific Earth transfer function that will cause the highest electric field amplitudes in the time domain is dependent on the particular day. The frequencies for which the amplitudes are increased are directly related to the variation in resistivity of particular layers in the Earth model.
4. The time domain electric field analysis showed that the maximum electric field amplitude does not occur at the same time depending on the Earth model and particular geomagnetic field composition.
5. In general, it was seen that the maximum Earth model is dependent on the geomagnetic storm, and cannot be previously determined if the geomagnetic storm frequency composition is not previously known. However, it has also been determined that the bounds on the amplitudes of

the electric field in the time domain, although dependent on the geomagnetic storm, can be relatively well determined by the boundary Earth models.

These results indicate that the GIC, which are dependent on the electric fields occurring during geomagnetic storms, will vary according to the variation in Earth conductivity structures. In general the upper and lower bound Earth models can be used to determine the overall upper and lower bounds on the electric fields, and thus the upper and lower bounds on the GIC. It is also determined that there are other possible Earth conductivity models that can be used to calculate higher electric fields and GIC, however it was shown that even though these models exist, they are not easily determined in advance of the geomagnetic storm. In practice the boundary Earth models can be used to determine bounds on electric fields in the time domain, and more in depth analysis of Earth conductivity model variety can be used to determine expected maximums.

References

Beggan, C. D., Sensitivity of Geomagnetically Induced Currents to Varying Auroral Electrojet and Conductivity Models, Planets and Space, 67:24, 2015. Doi 10.1186/s40623-014-0168-9.

Boteler, D.H., Geomagnetic Effects on Power Systems, IEEE Electrification Magazine, December 2015, p 4-7, doi: 10.1109/MELW.2015.2480555.

Boteler, D.H., The Evolution of Québec Earth Models used in Modelling Geomagnetically Induced Currents, IEEE Transactions on Power Delivery, 30, 5, 2171-2178, 2015.

Boteler, D.H. and Trichtchenko, L., Telluric Influence on Pipelines, Chapter 21, Oil and Gas Pipelines: Integrity and Safety Handbook, edited by R. Winston Revie, John Wiley & Sons, Inc., Hoboken, p 275-288, 2015.

Boteler, D.H., The impact of space weather on the electric power grid, p 74-95, HELIOPHYSICS V. SPACE WEATHER AND SOCIETY, edited by C.J. Schrijver, F. Bagenal and J.J. Sojka, Early chapter collection V. Jan 5, 2015.

Boteler, D.H., Assessment of Geomagnetic Hazard to Power Systems in Canada, Natural Hazards, 13, 101-120, 2001.

Bracewell, R. N., The Fourier transform and its applications, New York, McGraw-Hill, 1978.

Fiori, R.A.D., D.H. Boteler, L. Trichtchenko, L. Nikolic, H.-L. Lam, D. Danskin, L. McKee, An Overview of Space Weather and Potential Impacts on Power Systems –A Canadian Perspective, Infrastructure Resilience Risk Reporter (IR3), Vol 1, Issue 3, p18-25, June 2015.

Kaufman, A. A., Keller, G. V., The magnetotelluric Sounding Method, Amsterdam, Elsevier Scientific Pub. Co., 1981.

Simpson, F., Bahr, K., Practical Magnetotellurics, Cambridge, Cambridge University Press, 2005.

Weaver, J. T., Mathematical Methods for Geo-Electromagnetic Induction, New York, Wiley, 1994.

Zheng, K., Trichtchenko, L., Pirjola, R. J., Liu, L.-G., Effects of Geophysical Parameters on GIC Illustrated by Benchmark Network Modeling, IEEE Transactions on Power Delivery, 28, 2, 0885-8977, 2013.

Appendix A Electric and Geomagnetic Fields

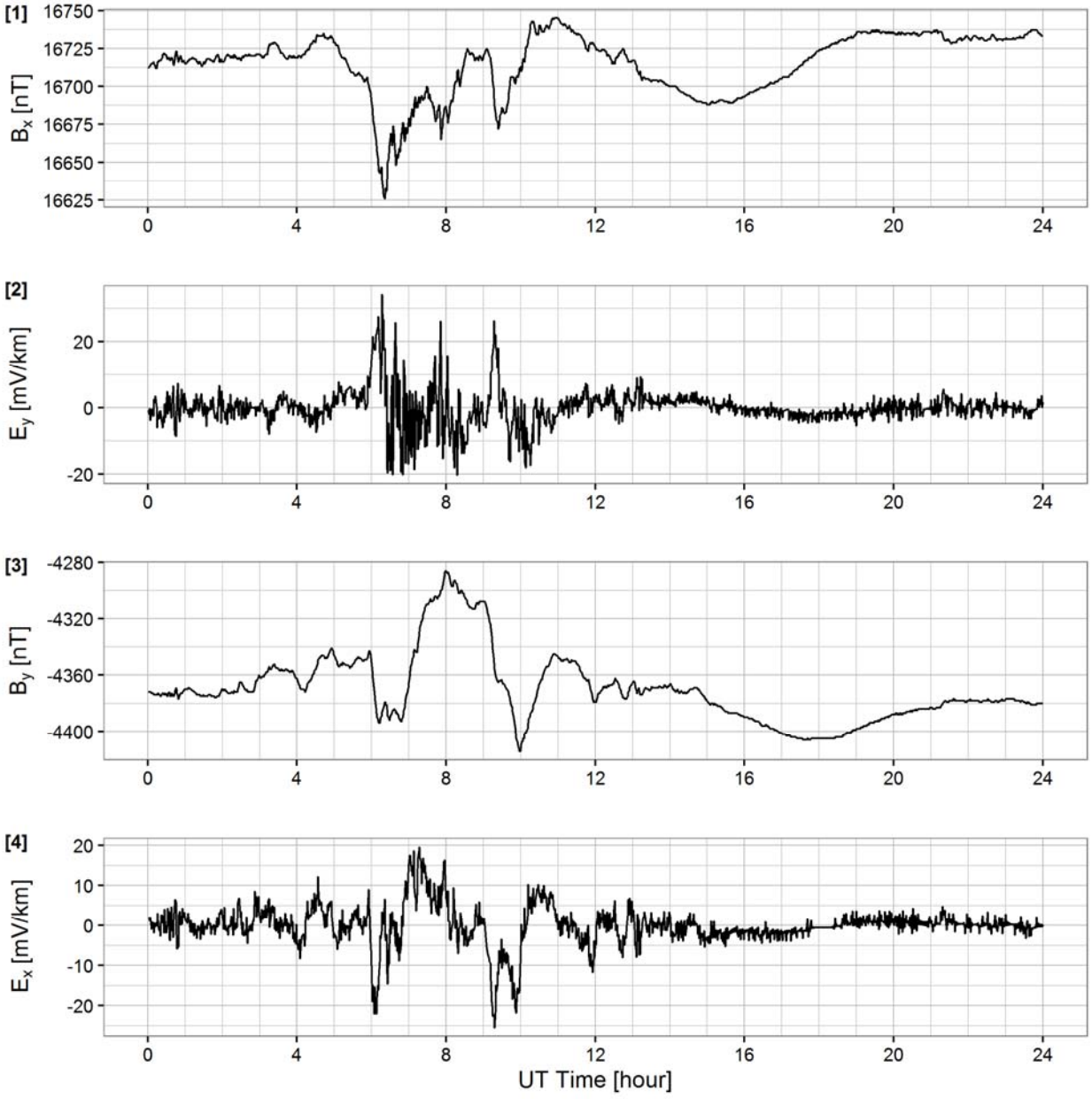

Figure A.1 - Northward and Eastward E and B Fields for OTT 1995-09-28
[1] Northward geomagnetic field, [2] Eastward electric field, [3] Eastward geomagnetic field and [4] Northward electric field in the time domain.

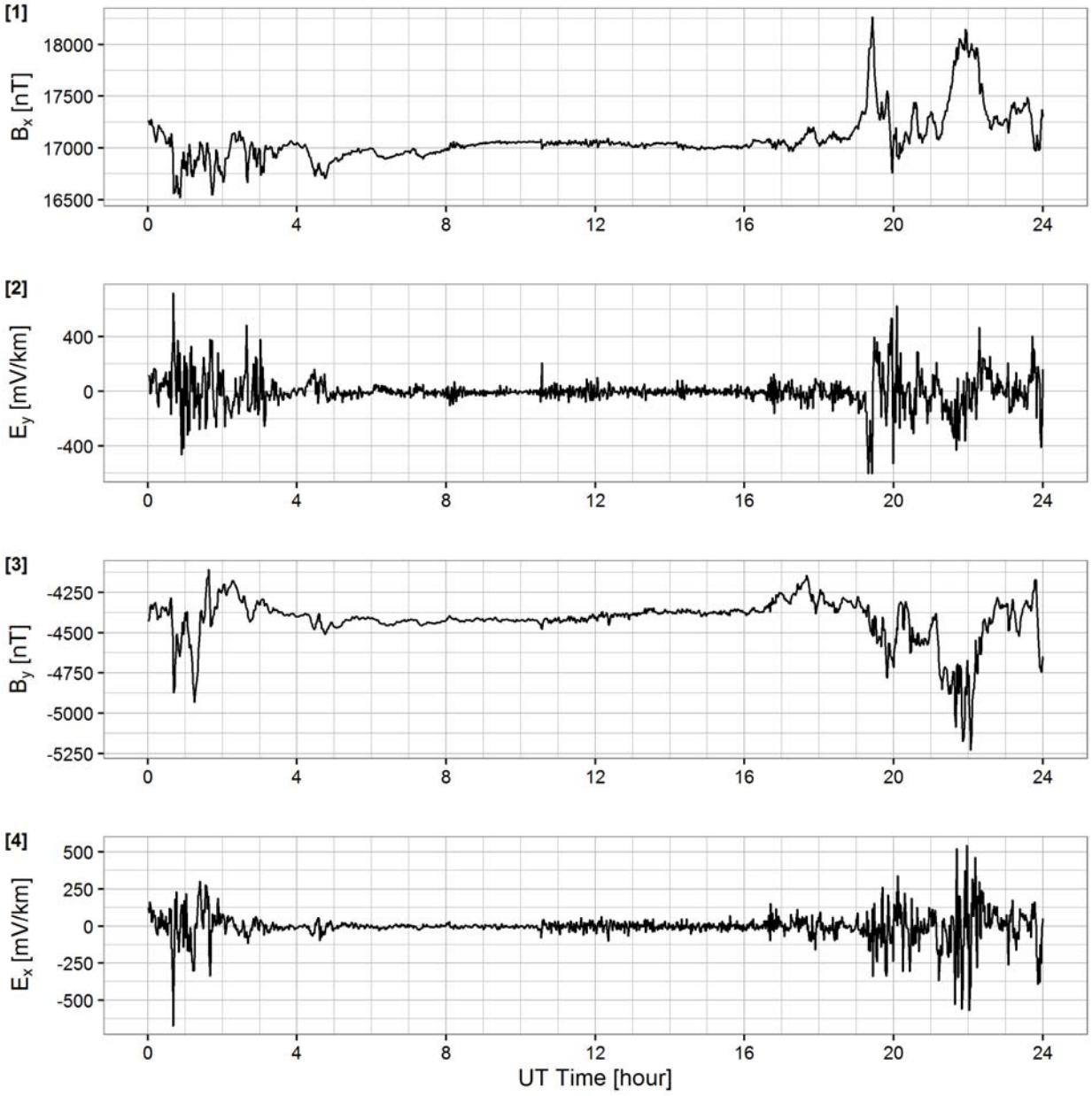

Figure A.2 - Northward and Eastward E and B Fields for OTT 2003-10-30
[1] Northward geomagnetic field, [2] Eastward electric field, [3] Eastward geomagnetic field and [4] Northward electric field in the time domain.

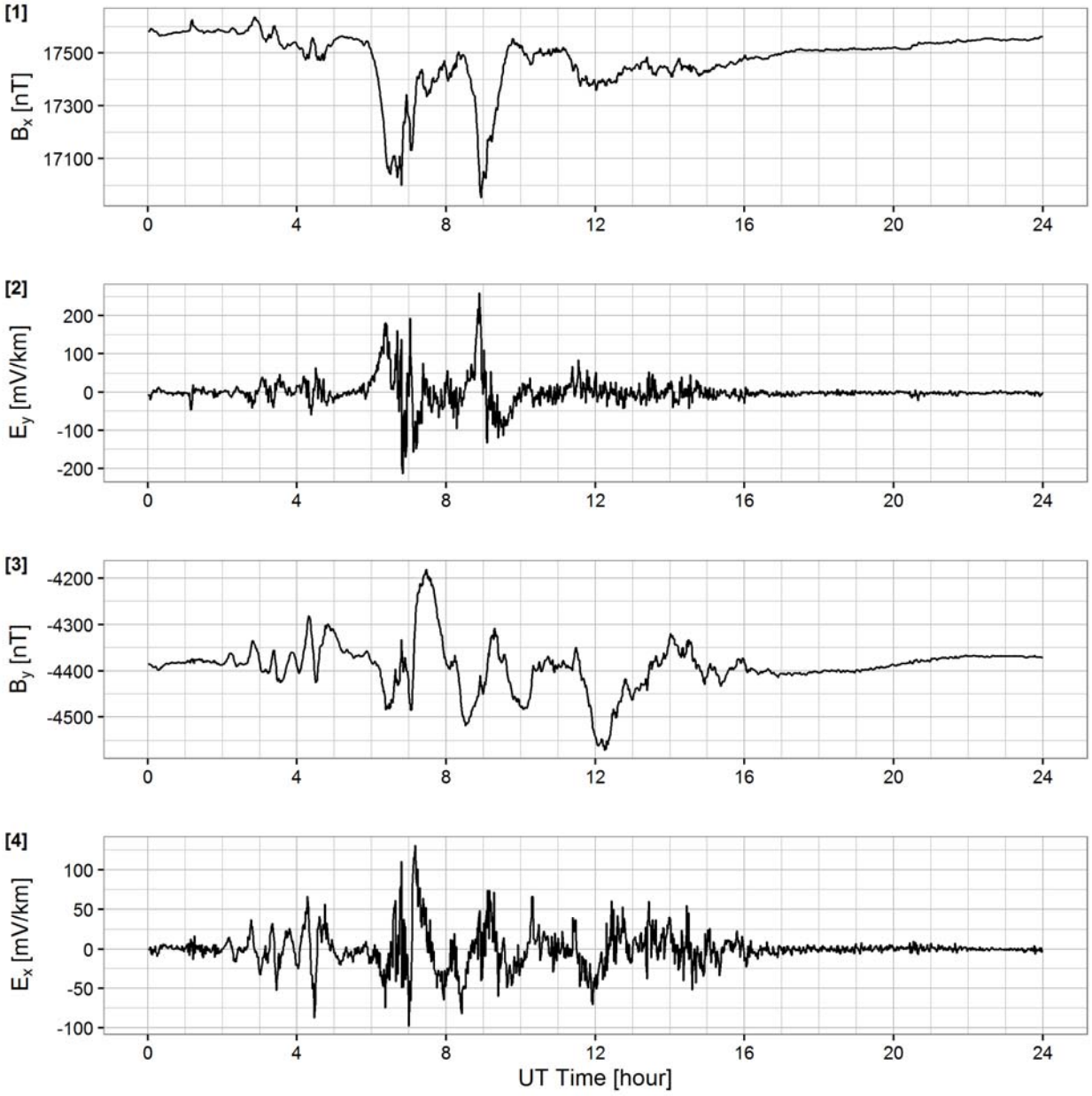

Figure A.3 - Northward and Eastward E and B Fields for OTT 2012-03-09
[1] Northward geomagnetic field, [2] Eastward electric field, [3] Eastward geomagnetic field and [4] Northward electric field in the time domain.

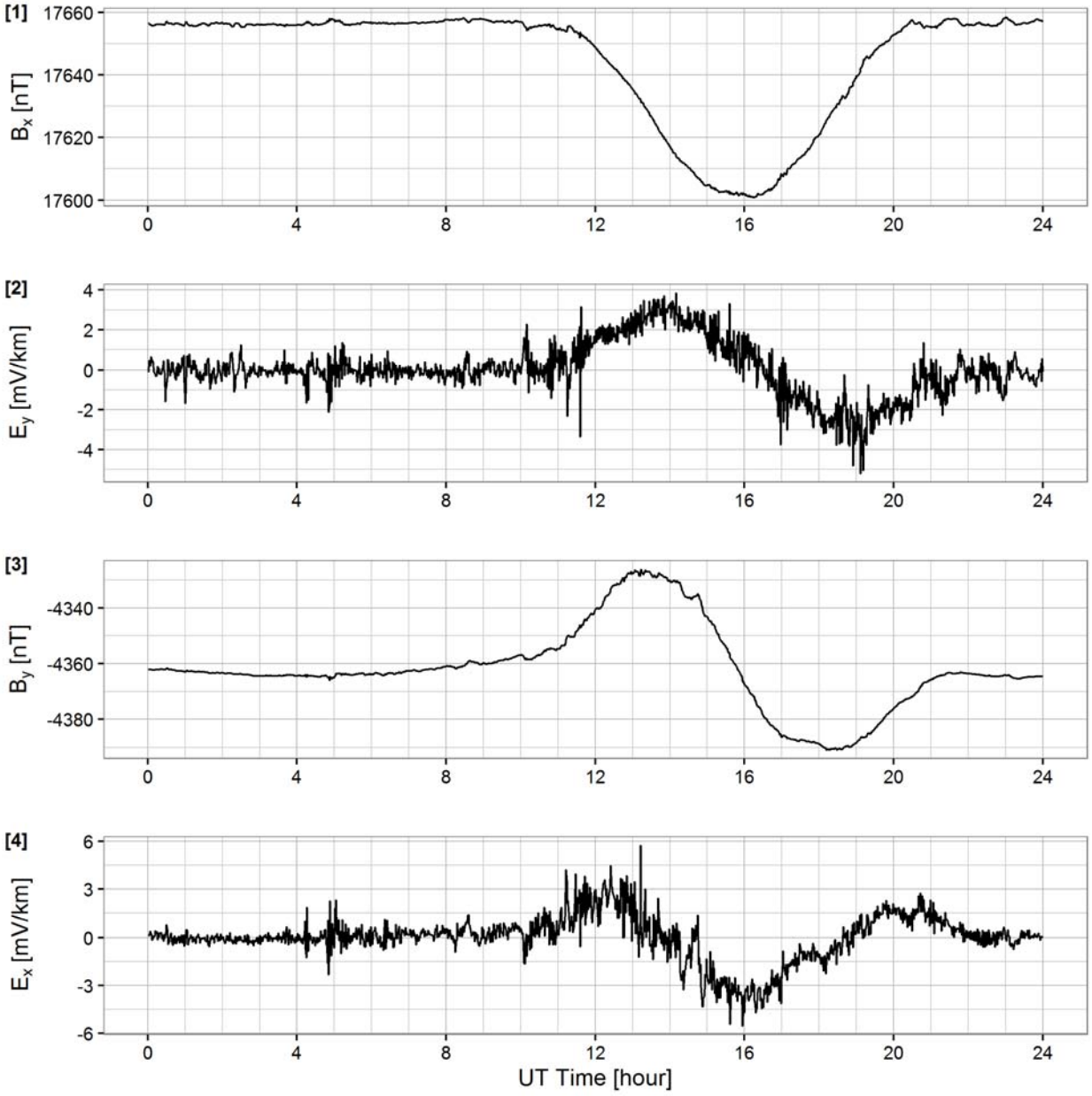

Figure A.4 - Northward and Eastward E and B Fields for OTT 2013-10-19
[1] Northward geomagnetic field, [2] Eastward electric field, [3] Eastward geomagnetic field and [4] Northward electric field in the time domain.

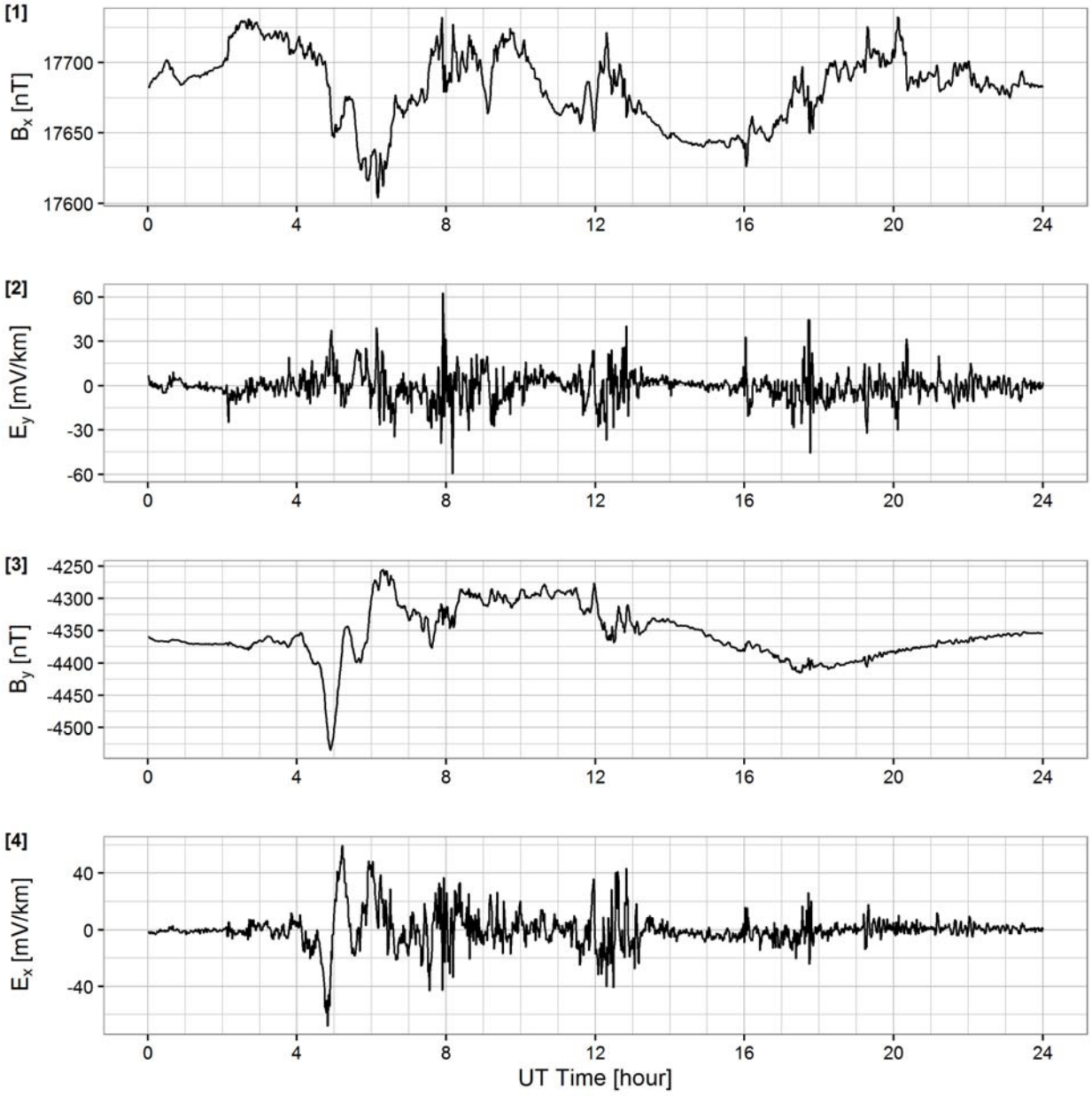

Figure A.5 - Northward and Eastward E and B Fields for OTT 2014-06-08
[1] Northward geomagnetic field, [2] Eastward electric field, [3] Eastward geomagnetic field and [4] Northward electric field in the time domain.

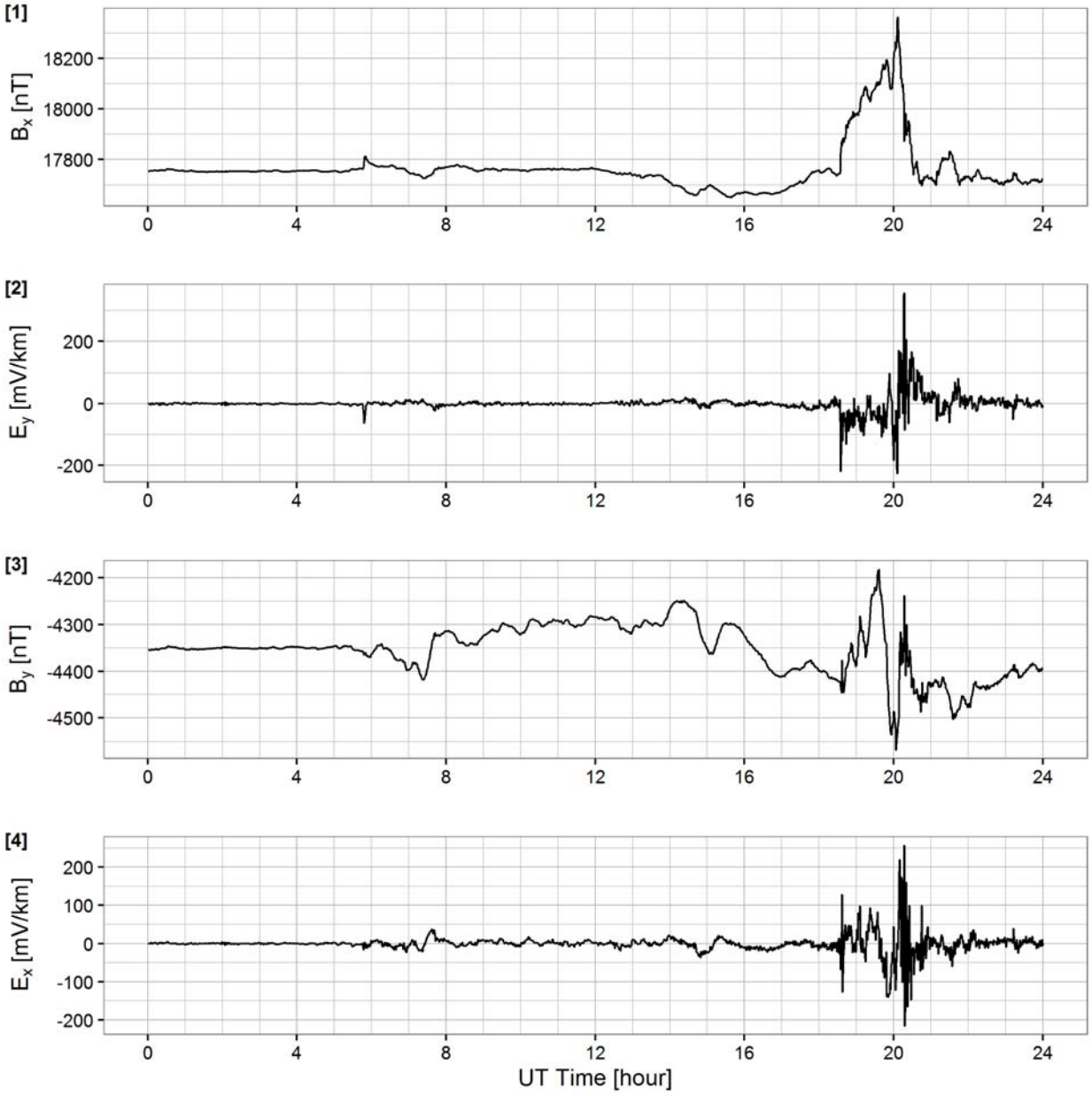

Figure A.6 - Northward and Eastward E and B Fields for OTT 2015-06-22
[1] Northward geomagnetic field, [2] Eastward electric field, [3] Eastward geomagnetic field and [4] Northward electric field in the time domain.

Appendix B Total Electric and Geomagnetic Amplitude

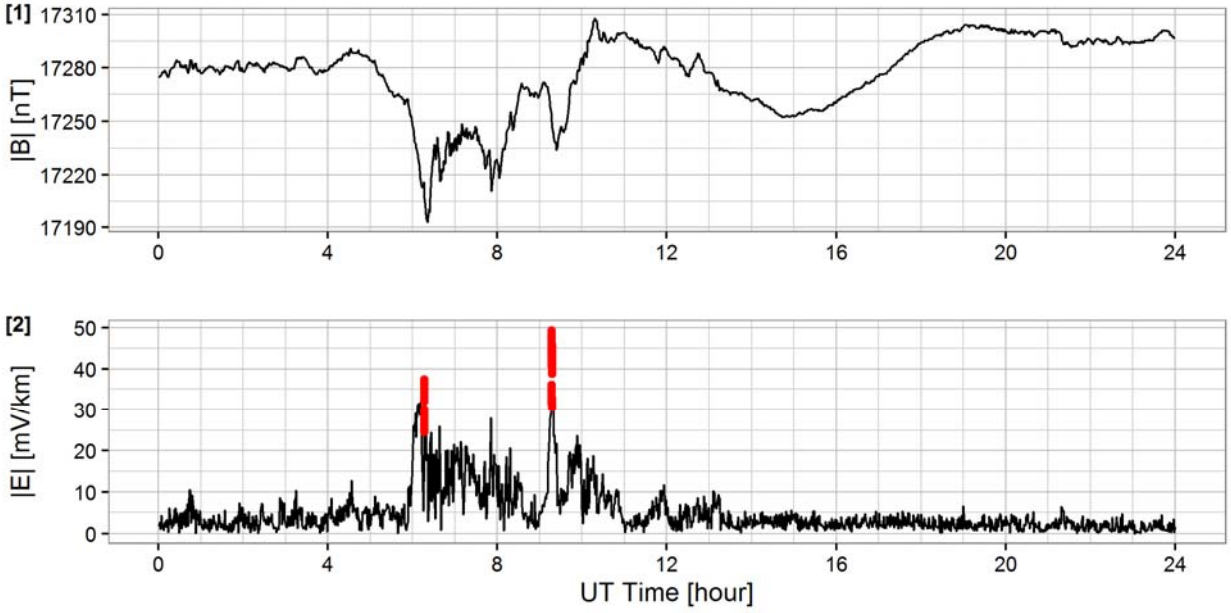

Figure B.1 - Total E and B Field Amplitude for OTT on 1995-09-28
[1] Total geomagnetic field and [2] total electric field in the time domain. Red dot represents the maximum modelled electric field amplitude per model, and is displayed for the time of its occurrence.

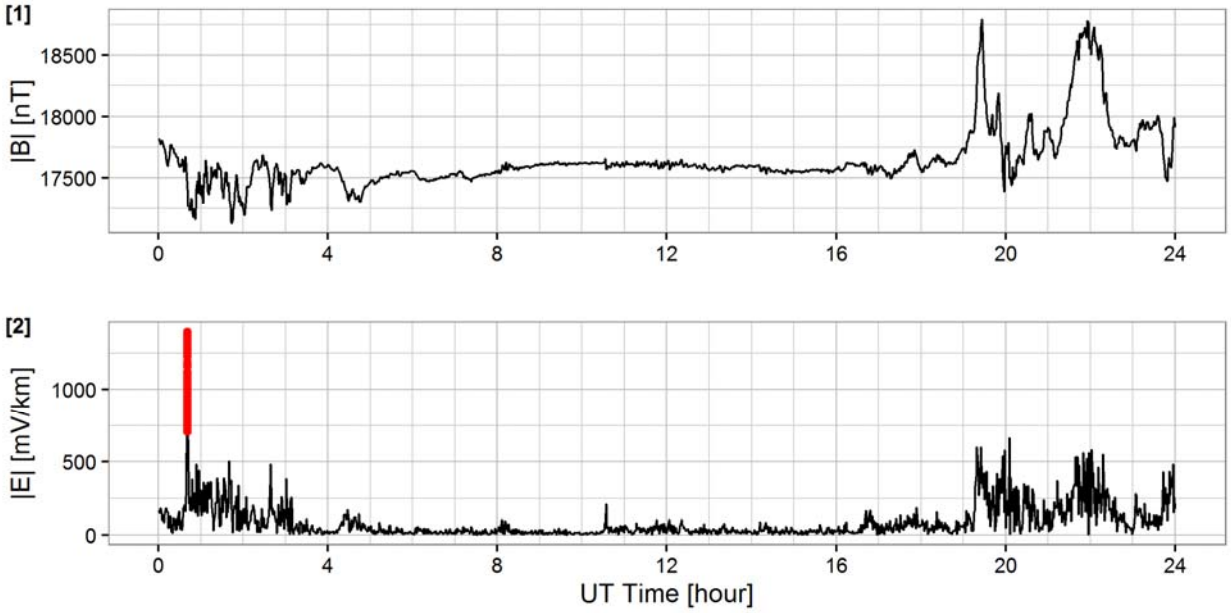

Figure B.2 - Total E and B Field Amplitude for OTT on 2003-10-30
[1] Total geomagnetic field and [2] total electric field in the time domain. Red dot represents the maximum modelled electric field amplitude per model, and is displayed for the time of its occurrence.

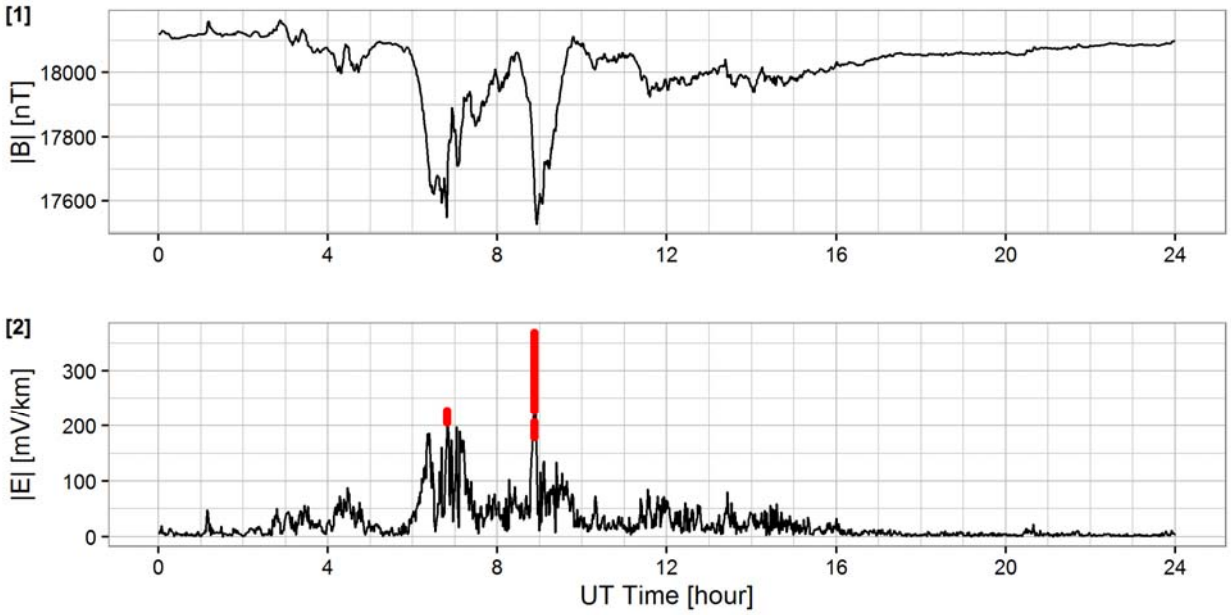

Figure B.3 - Total E and B Field Amplitude for OTT on 2012-03-09
[1] Total geomagnetic field and [2] total electric field in the time domain. Red dot represents the maximum modelled electric field amplitude per model, and is displayed for the time of its occurrence.

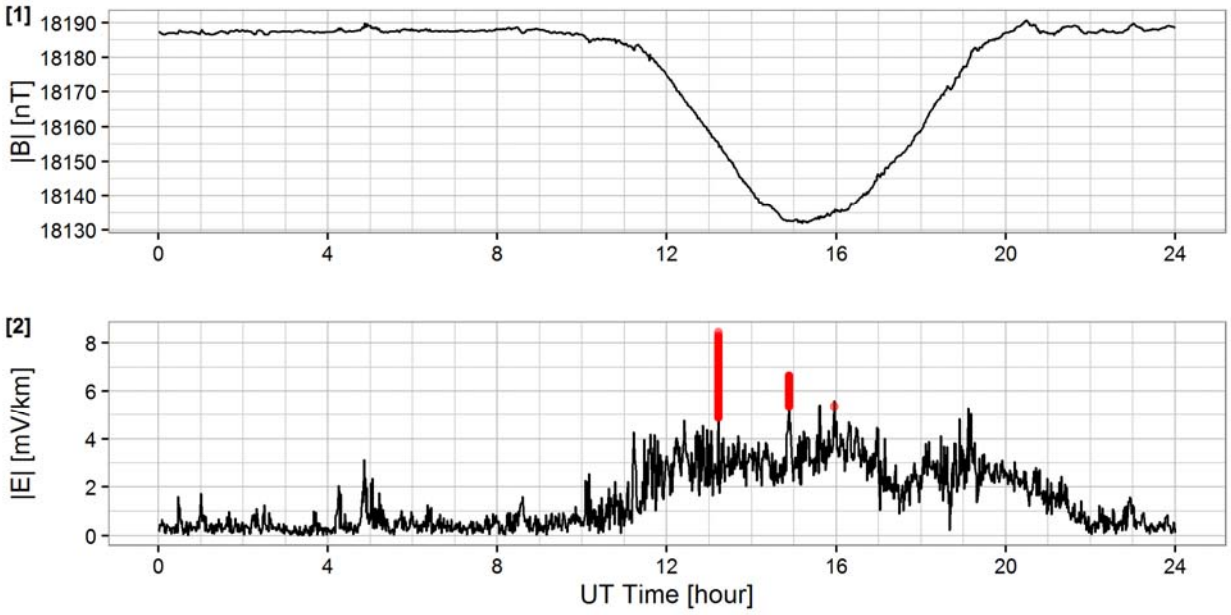

Figure B.4 - Total E and B Field Amplitude for OTT on 2013-10-19
[1] Total geomagnetic field and [2] total electric field in the time domain. Red dot represents the maximum modelled electric field amplitude per model, and is displayed for the time of its occurrence.

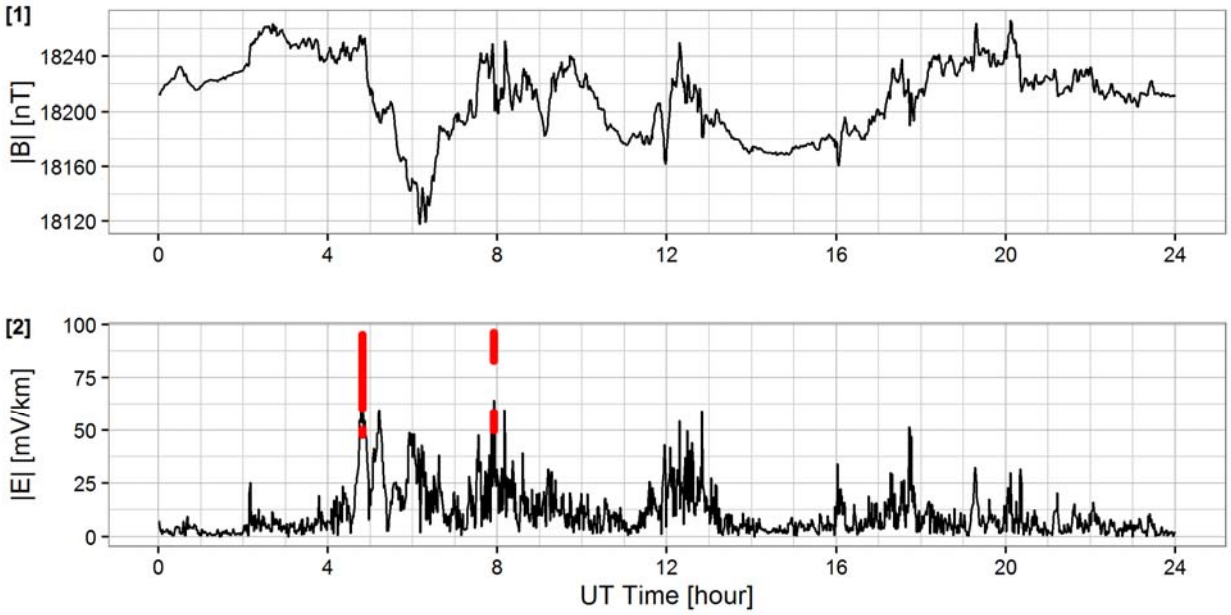

Figure B.5 - Total E and B Field Amplitude for OTT on 2014-06-08
[1] Total geomagnetic field and [2] total electric field in the time domain. Red dot represents the maximum modelled electric field amplitude per model, and is displayed for the time of its occurrence.

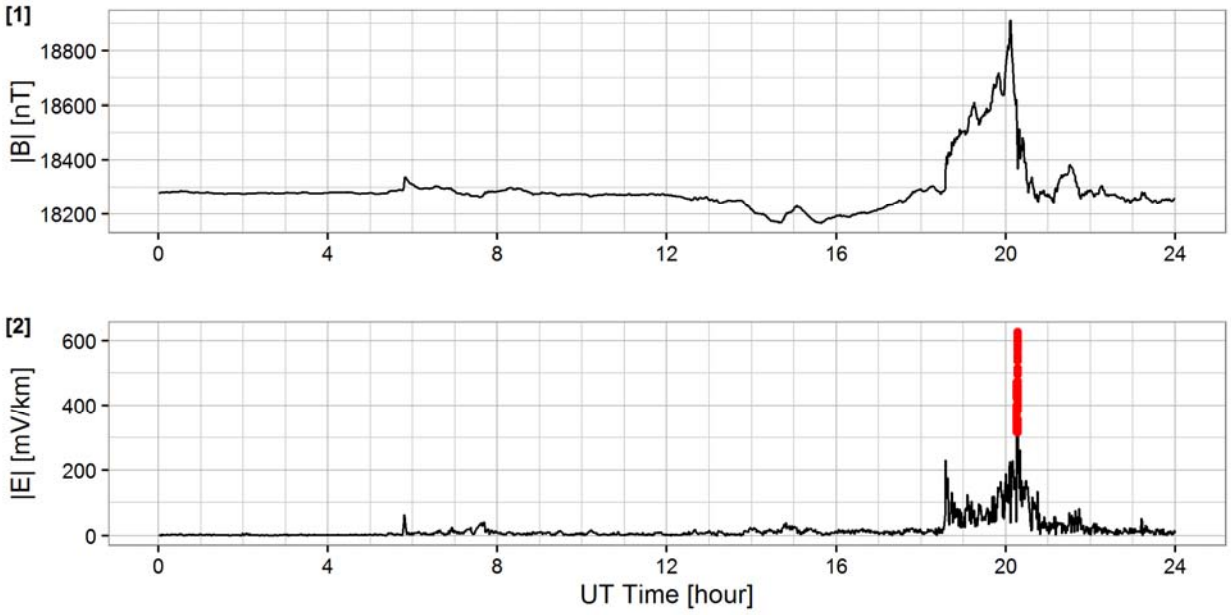

Figure B.6 - Total E and B Field Amplitude for OTT on 2015-06-22
[1] Total geomagnetic field and [2] total electric field in the time domain. Red dot represents the maximum modelled electric field amplitude per model, and is displayed for the time of its occurrence.

Appendix C Electric Field Sample During Peak

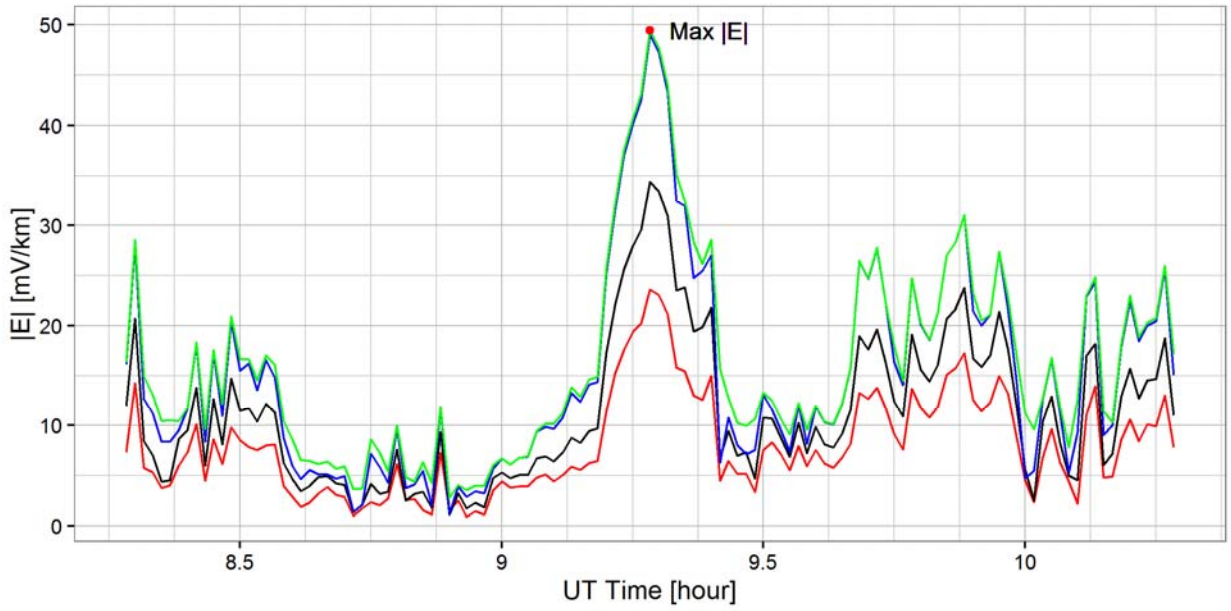

Figure C.1 - Maximum Amplitude Occurrence for OTT on 1995-09-28
Red – lower bound, black – standard, blue – upper bound and green maximum, modelled electric field in the time domain, during the occurrence of the overall maximum electric field.

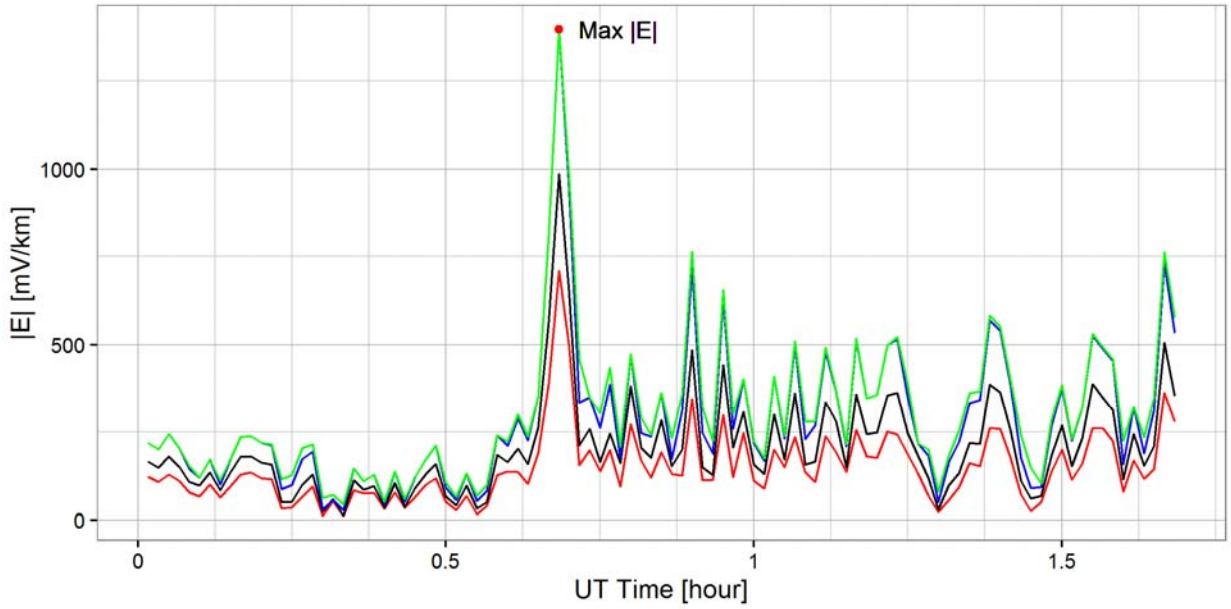

Figure C.2 - Maximum Amplitude Occurrence for OTT 2003-10-30
Red – lower bound, black – standard, blue – upper bound and green maximum, modelled electric field in the time domain, during the occurrence of the overall maximum electric field.

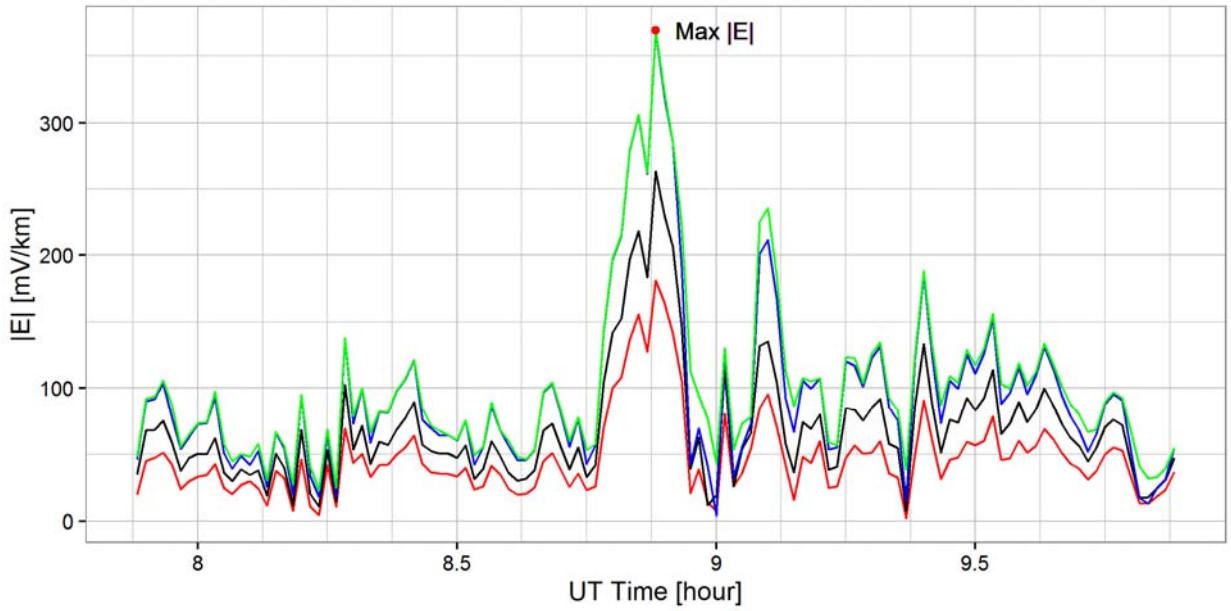

Figure C.3 - Maximum Amplitude Occurrence for OTT on 2012-03-09
Red – lower bound, black – standard, blue – upper bound and green maximum, modelled electric field in the time domain, during the occurrence of the overall maximum electric field.

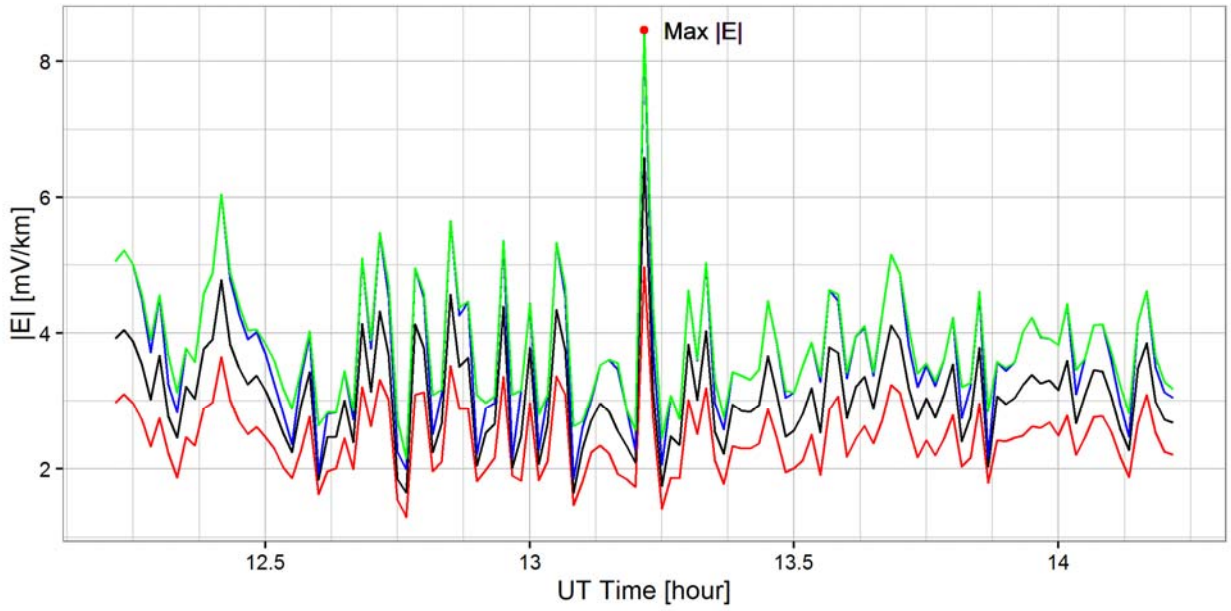

Figure C.4 - Maximum Amplitude Occurrence for OTT on 2013_10_19
Red – lower bound, black – standard, blue – upper bound and green maximum, modelled electric field in the time domain, during the occurrence of the overall maximum electric field.

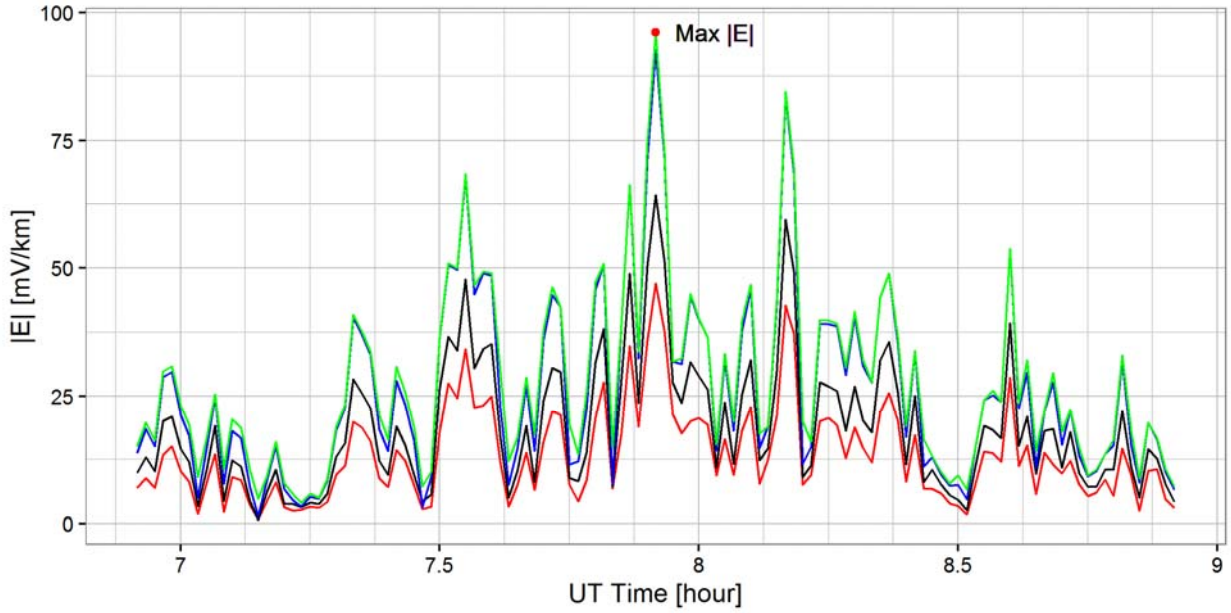

Figure C.5 - Maximum Amplitude Occurrence for OTT on 2014-06-08
Red – lower bound, black – standard, blue – upper bound and green maximum, modelled electric field in the time domain, during the occurrence of the overall maximum electric field.

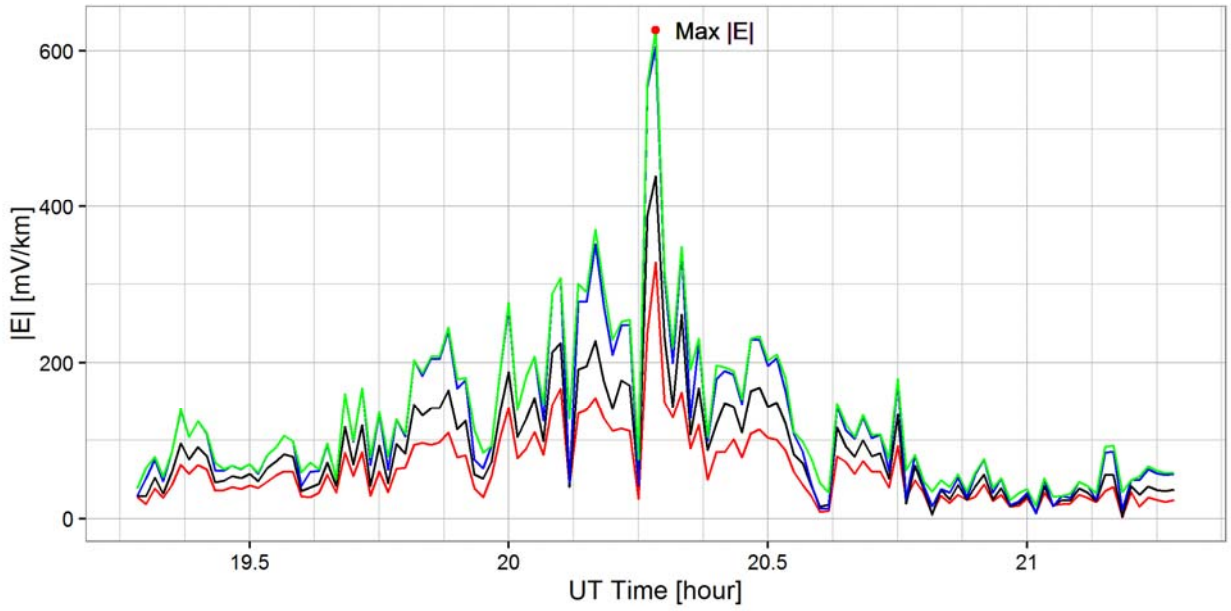

Figure C.6 - Maximum Amplitude Occurrence for OTT on 2015-06-22
Red – lower bound, black – standard, blue – upper bound and green maximum, modelled electric field in the time domain, during the occurrence of the overall maximum electric field.

Appendix D Distribution of Max Electric Field Amplitudes

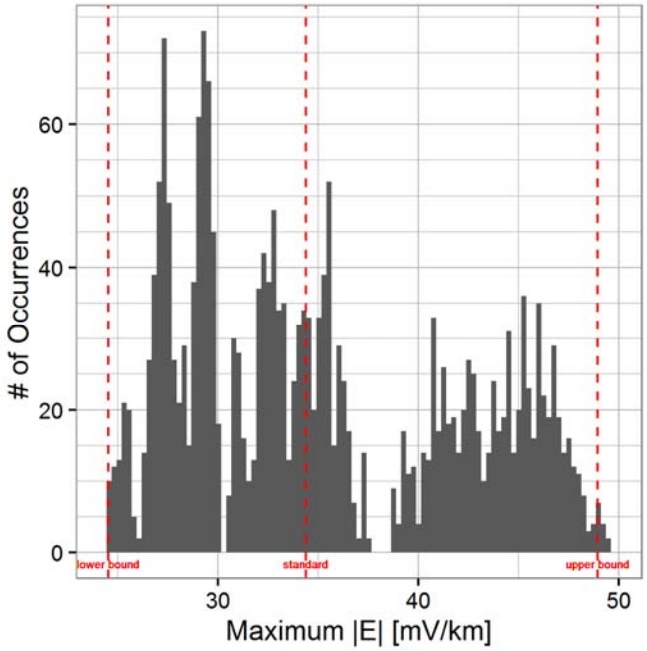

Figure D.1 - Histogram of Maximum E Amplitudes for OTT on 1995-09-28
Maximum modelled electric field per model occurrences. Histogram shows 100 bins of equal width in linear space. Red dotted lines represent the maximum modelled electric field amplitude for three models: lower, standard and upper.

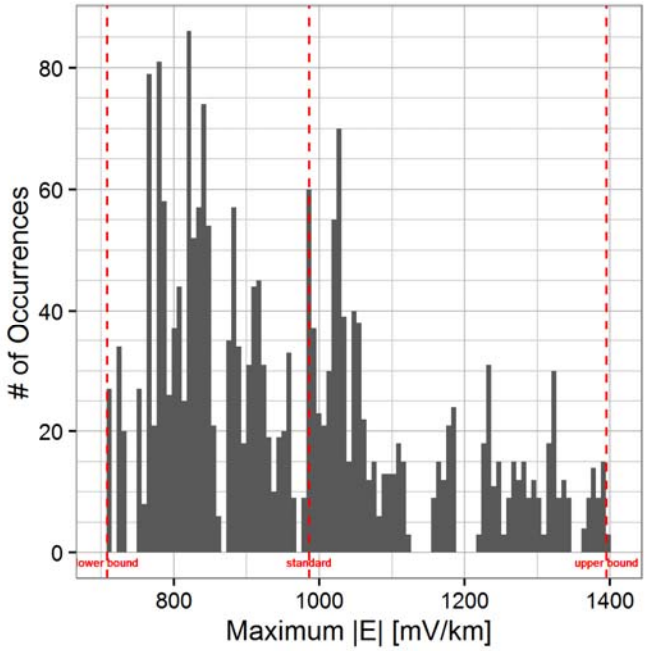

Figure D.2 - Histogram of Maximum E Amplitudes for OTT on 2003-10-30
Maximum modelled electric field per model occurrences. Histogram shows 100 bins of equal width in linear space. Red dotted lines represent the maximum modelled electric field amplitude for three models: lower, standard and upper.

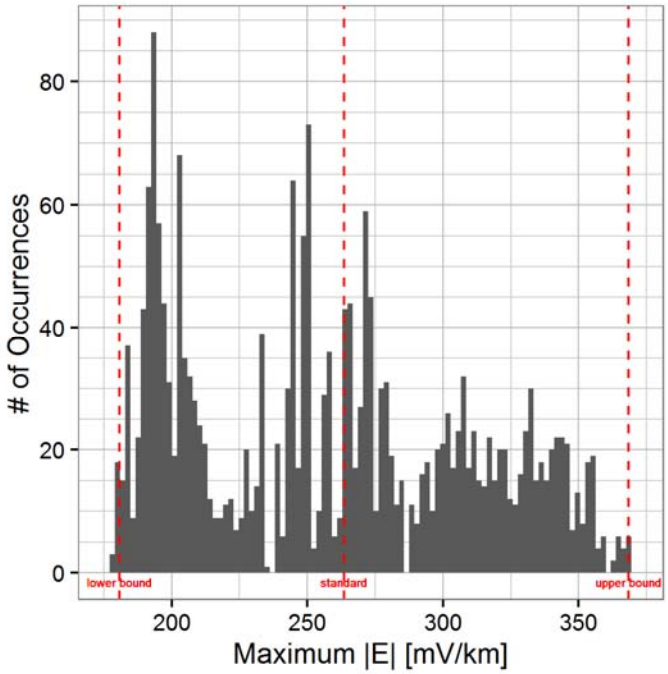

Figure D.3 - Histogram of Maximum E Amplitudes for OTT on 2012-03-09
Maximum modelled electric field per model occurrences. Histogram shows 100 bins of equal width in linear space. Red dotted lines represent the maximum modelled electric field amplitude for three models: lower, standard and upper.

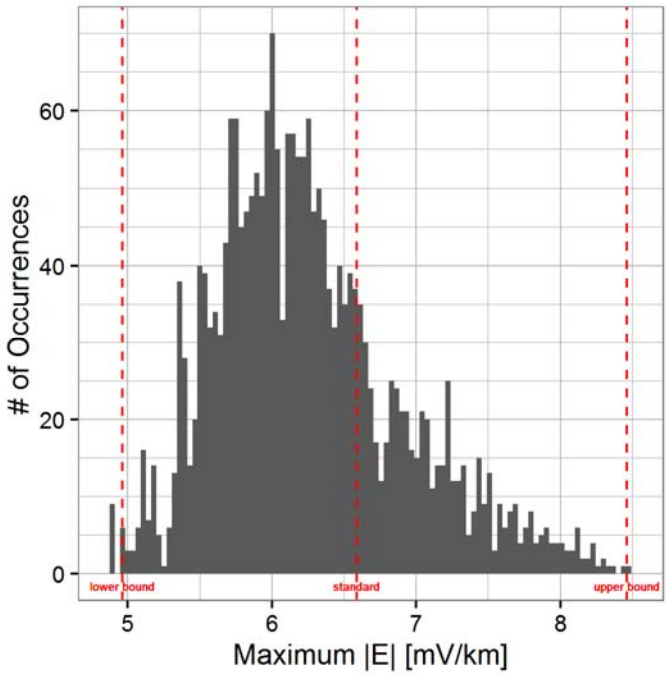

Figure D.4 - Histogram of Maximum E Amplitudes for OTT on 2013-10-19
Maximum modelled electric field per model occurrences. Histogram shows 100 bins of equal width in linear space. Red dotted lines represent the maximum modelled electric field amplitude for three models: lower, standard and upper.

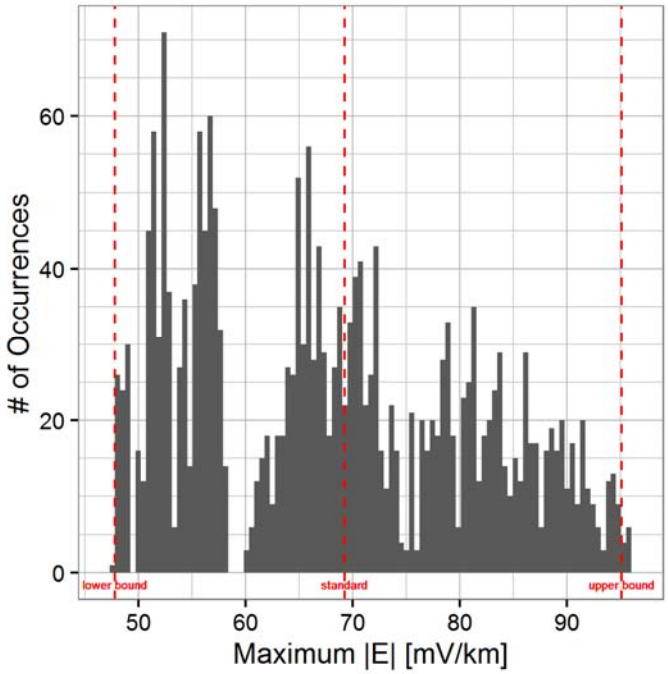

Figure D.5 - Histogram of Maximum E Amplitudes for OTT on 2014-06-08
Maximum modelled electric field per model occurrences. Histogram shows 100 bins of equal width in linear space. Red dotted lines represent the maximum modelled electric field amplitude for three models: lower, standard and upper.

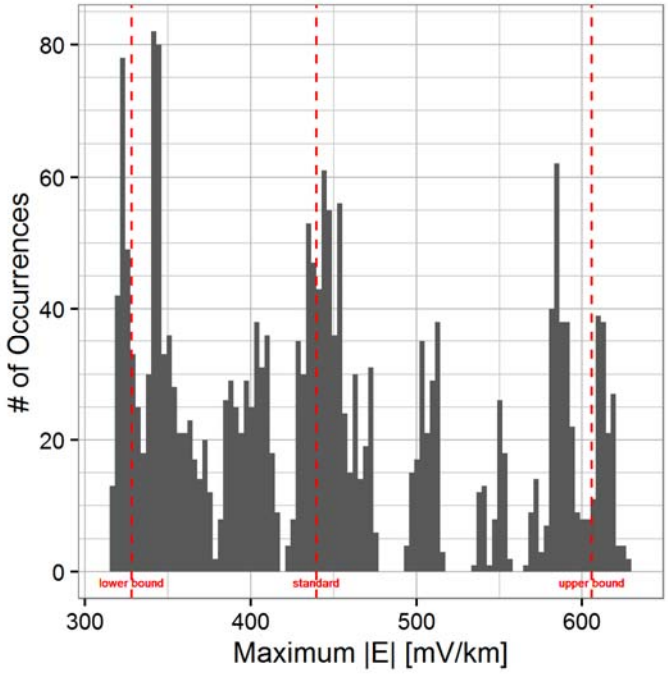

Figure D.6 - Histogram of Maximum E Amplitudes for OTT on 2015-06-22
Maximum modelled electric field per model occurrences. Histogram shows 100 bins of equal width in linear space. Red dotted lines represent the maximum modelled electric field amplitude for three models: lower, standard and upper.

Appendix E Scatter Plot of Electric Field Cases

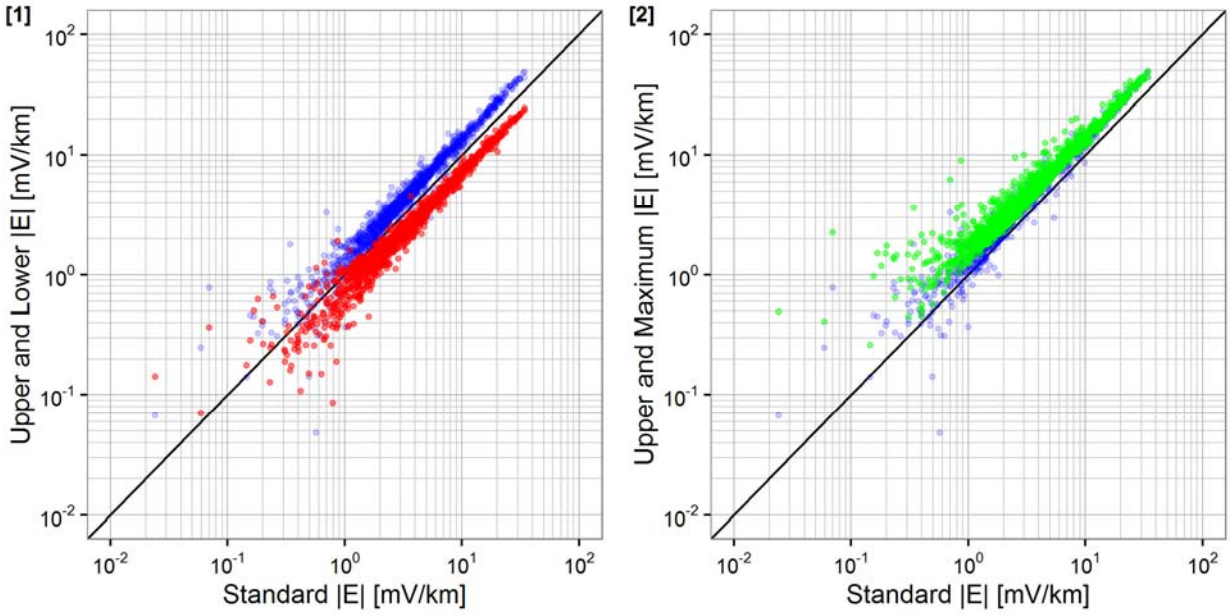

Figure E.1 - Scatter Plot of E Fields at OTT on 1995-09-28
[1] Blue - upper and red - lower model electric field versus black - standard model electric field, and [2] blue - upper model and green - maximum electric field versus black - standard model electric field.

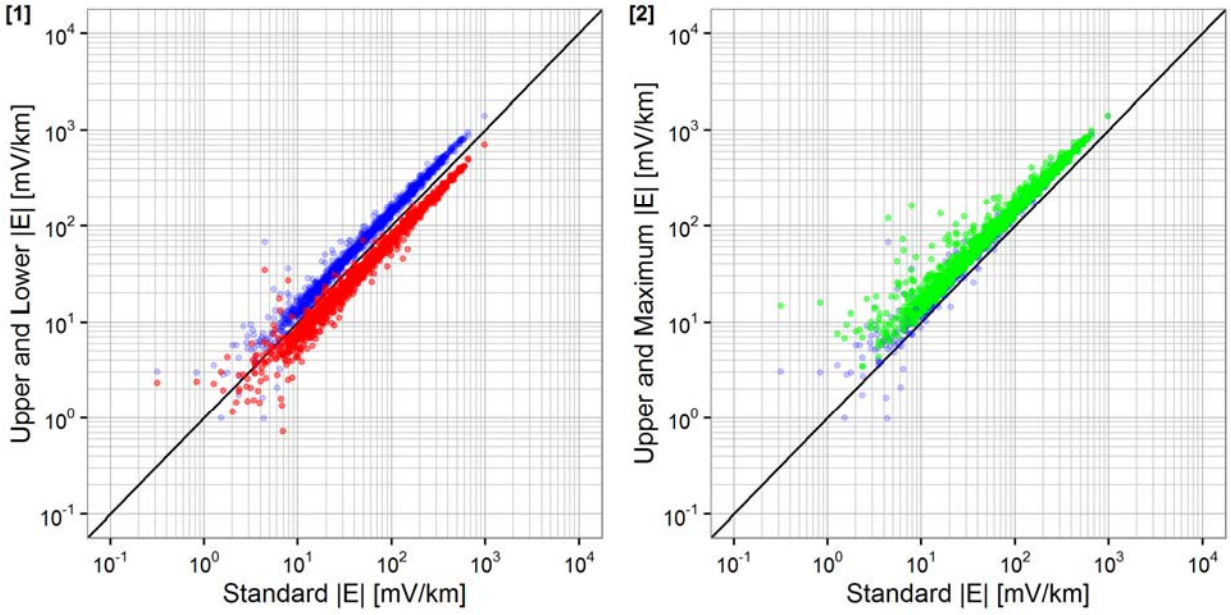

Figure E.2 - Scatter Plot of E Fields at OTT on 2003-10-30
[1] Blue - upper and red - lower model electric field versus black - standard model electric field, and [2] blue - upper model and green - maximum electric field versus black - standard model electric field.

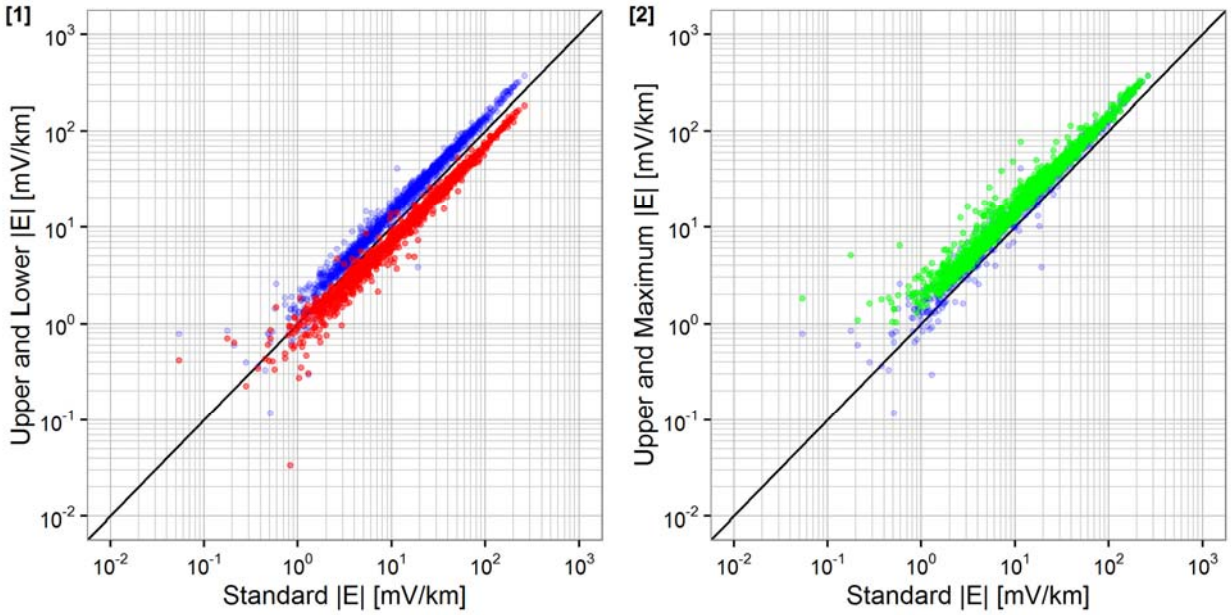

Figure E.3 - Scatter Plot of E Fields at OTT on 2012-03-09
[1] Blue - upper and red - lower model electric field versus black - standard model electric field, and [2] blue - upper model and green - maximum electric field versus black - standard model electric field.

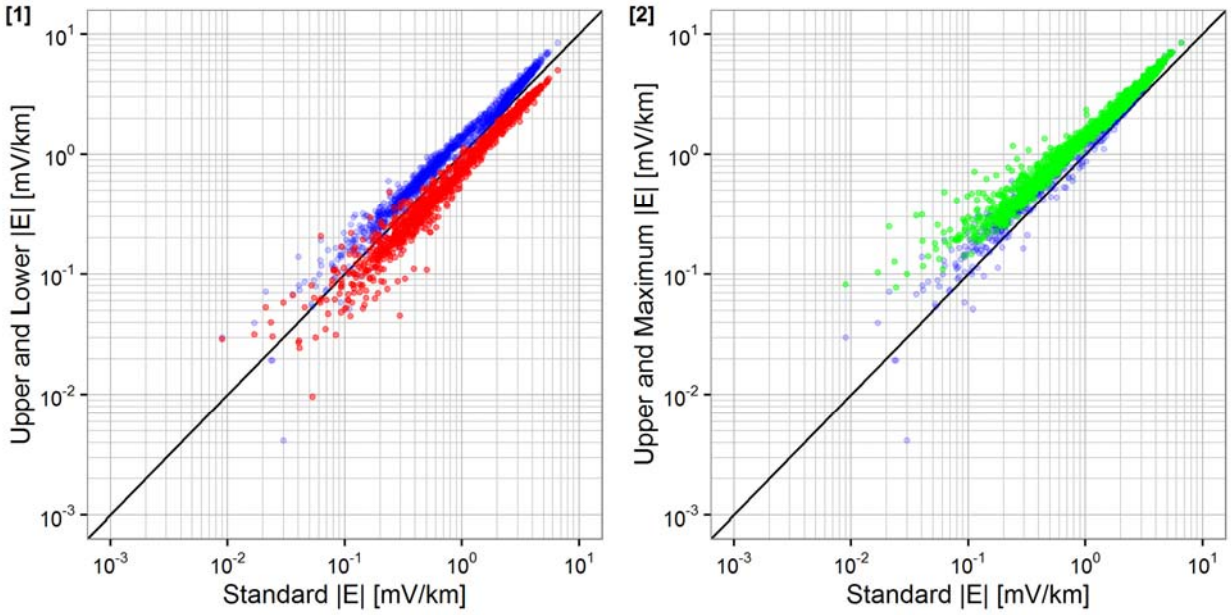

Figure E.4 - Scatter Plot of E Fields at OTT on 2013-09-19
[1] Blue - upper and red - lower model electric field versus black - standard model electric field, and [2] blue - upper model and green - maximum electric field versus black - standard model electric field.

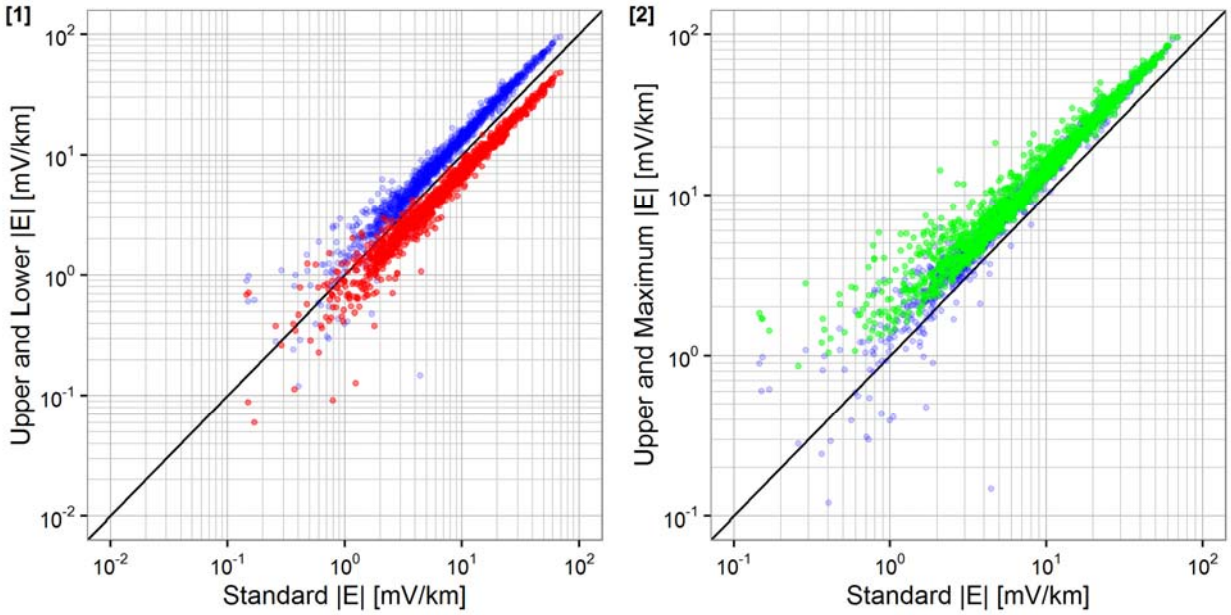

Figure E.5 - Scatter Plot of E Fields at OTT on 2014-06-08
[1] Blue - upper and red - lower model electric field versus black - standard model electric field, and [2] blue - upper model and green - maximum electric field versus black - standard model electric field.

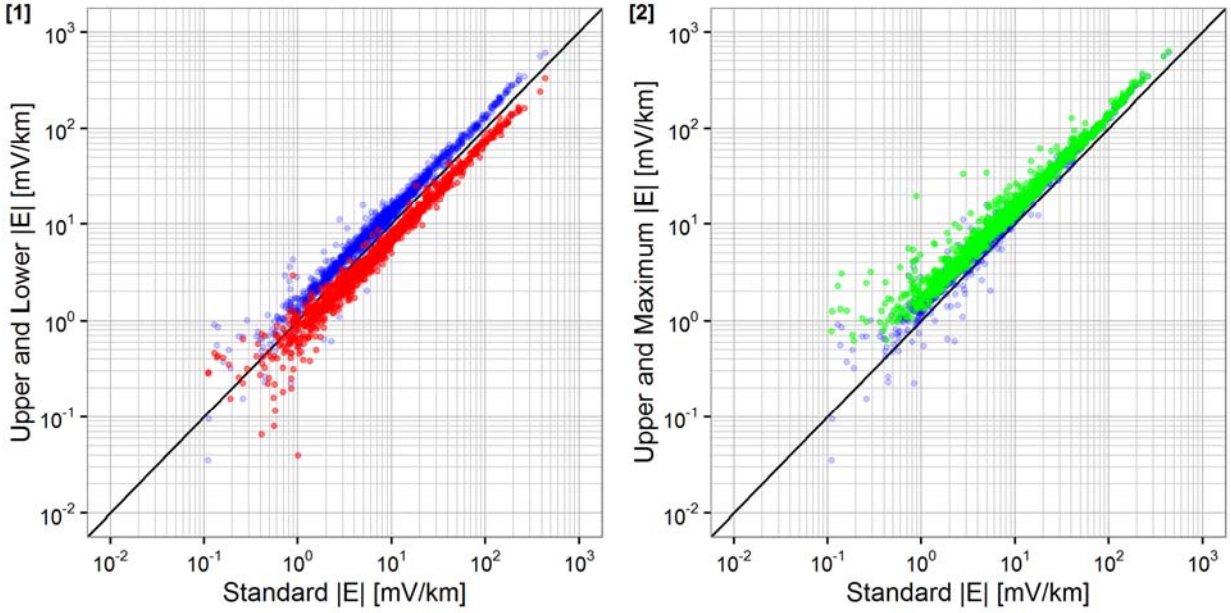

Figure E.6 - Scatter Plot of E Fields at OTT on 2015-06-22
[1] Blue - upper and red - lower model electric field versus black - standard model electric field, and [2] blue - upper model and green - maximum electric field versus black - standard model electric field.

Appendix F The Frequency Domain Data

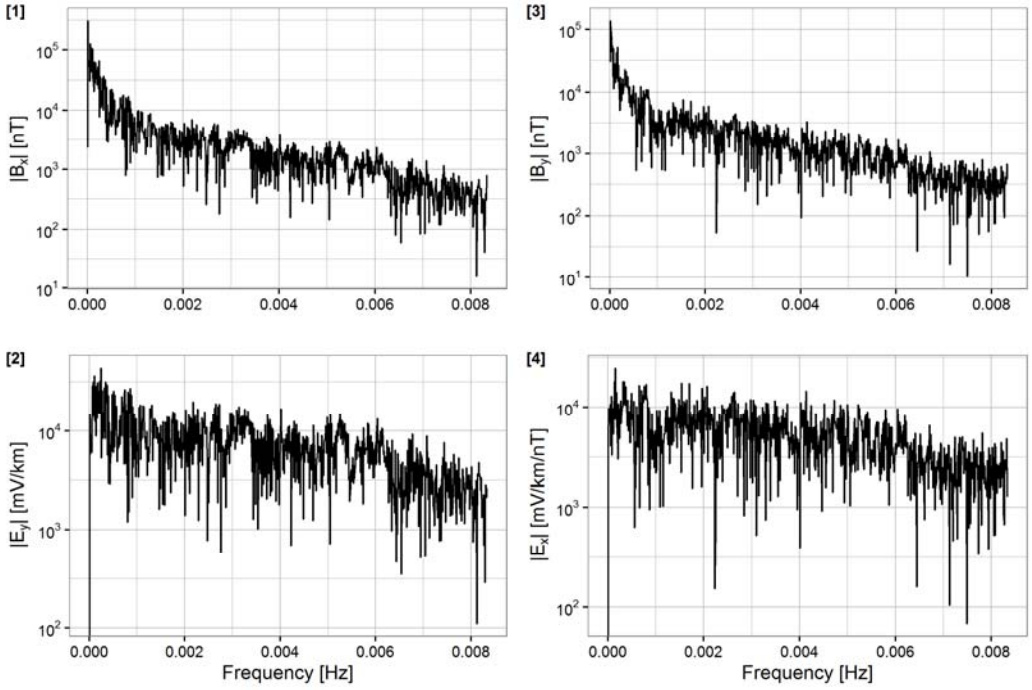

Figure F.1 - B and E Frequency Domain Components for 1989-03-13
[1] Eastward geomagnetic field amplitude, [2] Northward electric field amplitude, [3] Northward geomagnetic electric field amplitude, and [4] Eastward electric field amplitude.

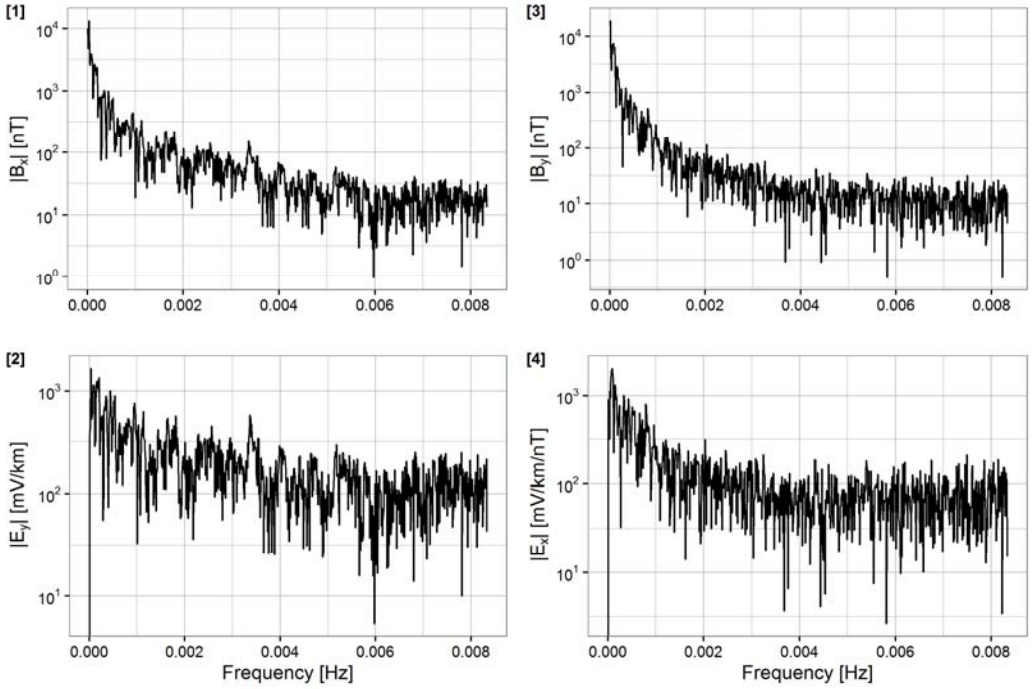

Figure F.2 - B and E Frequency Domain Components for 1995-09-28
[1] Eastward geomagnetic field amplitude, [2] Northward electric field amplitude, [3] Northward geomagnetic electric field amplitude, and [4] Eastward electric field amplitude.

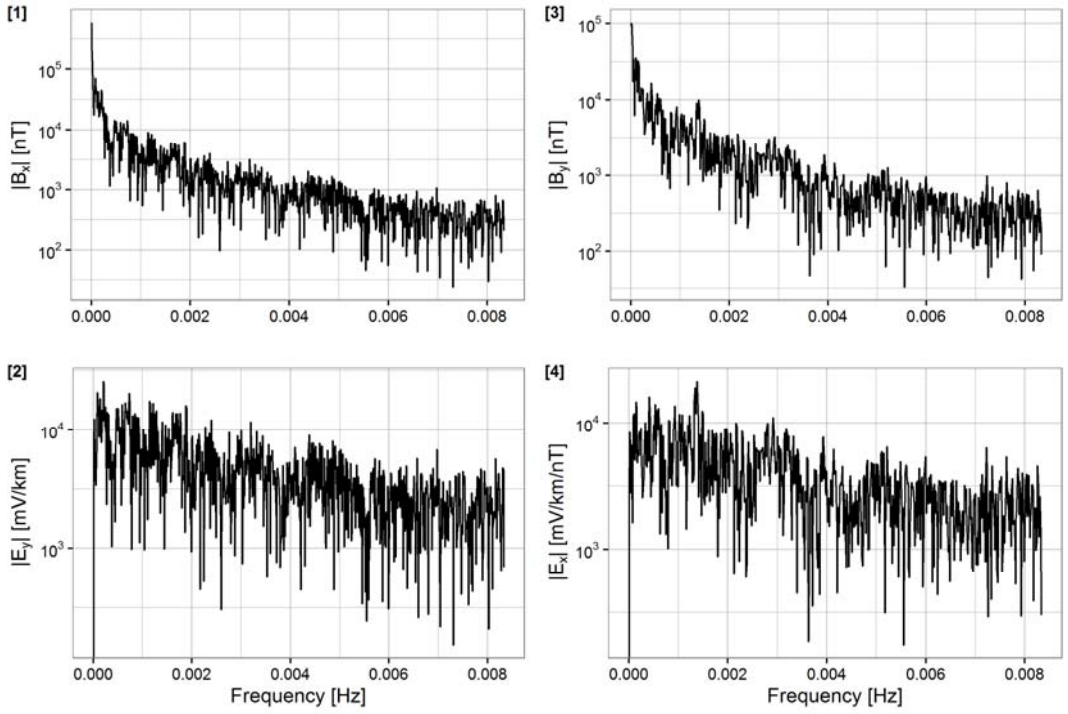

Figure F.3 - B and E Frequency Domain Components for 2003-10-30
[1] Eastward geomagnetic field amplitude, [2] Northward electric field amplitude, [3] Northward geomagnetic electric field amplitude, and [4] Eastward electric field amplitude.

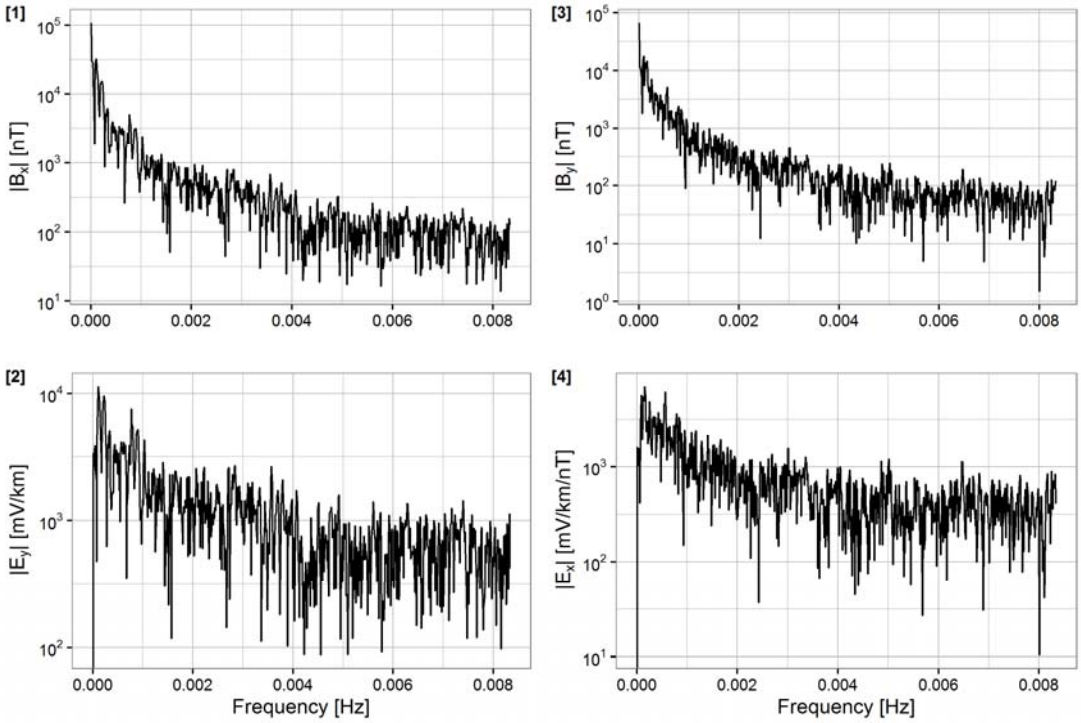

Figure F.4 - B and E Frequency Domain Components for 2012-03-09
[1] Eastward geomagnetic field amplitude, [2] Northward electric field amplitude, [3] Northward geomagnetic electric field amplitude, and [4] Eastward electric field amplitude.

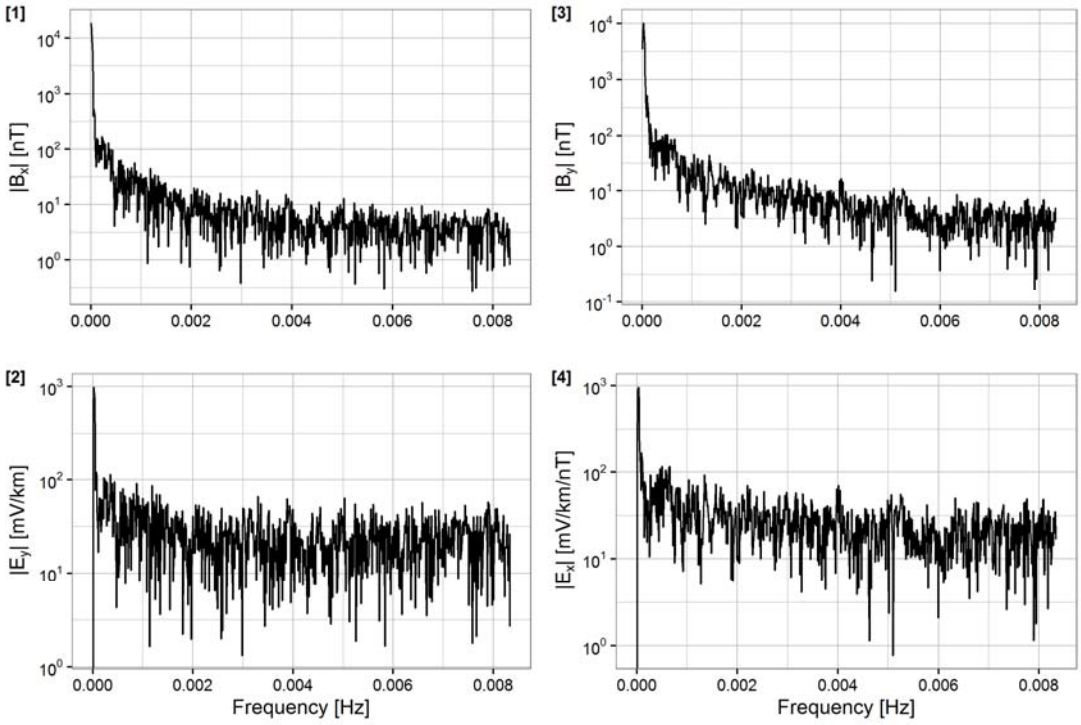

Figure F.5 - B and E Frequency Domain Components for 2013-10-19
[1] Eastward geomagnetic field amplitude, [2] Northward electric field amplitude, [3] Northward geomagnetic electric field amplitude, and [4] Eastward electric field amplitude.

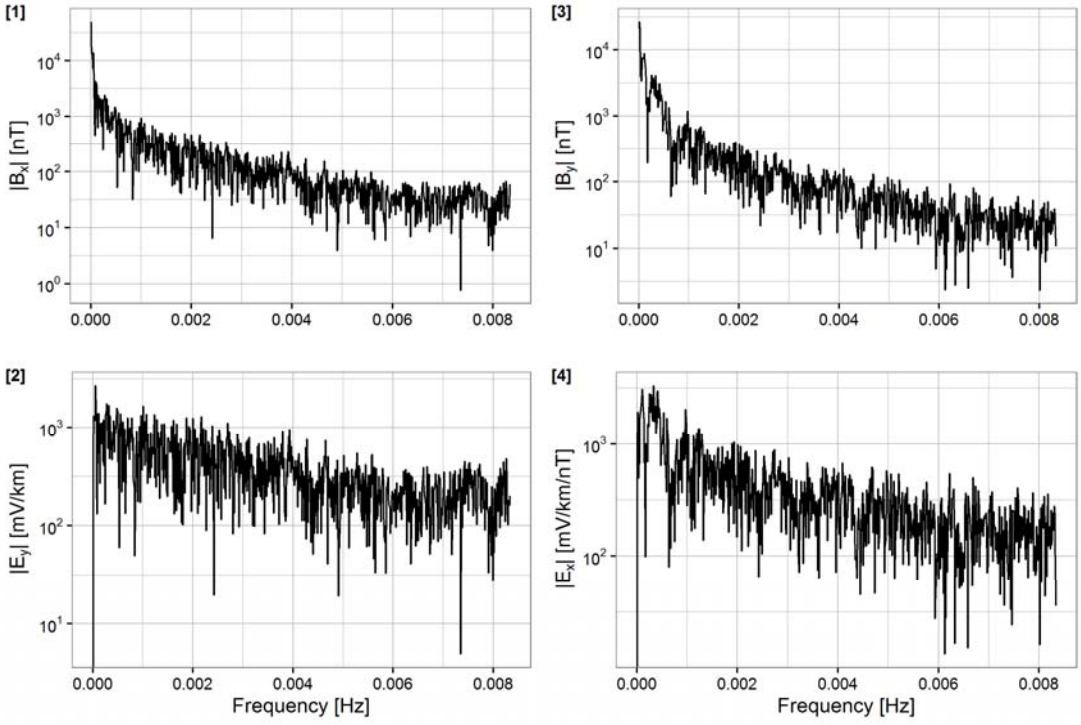

Figure F.6 – B and E Frequency Domain Components for 2014-05-08
[1] Eastward geomagnetic field amplitude, [2] Northward electric field amplitude, [3] Northward geomagnetic electric field amplitude, and [4] Eastward electric field amplitude.

Appendix G Earth Structure and Transfer Functions

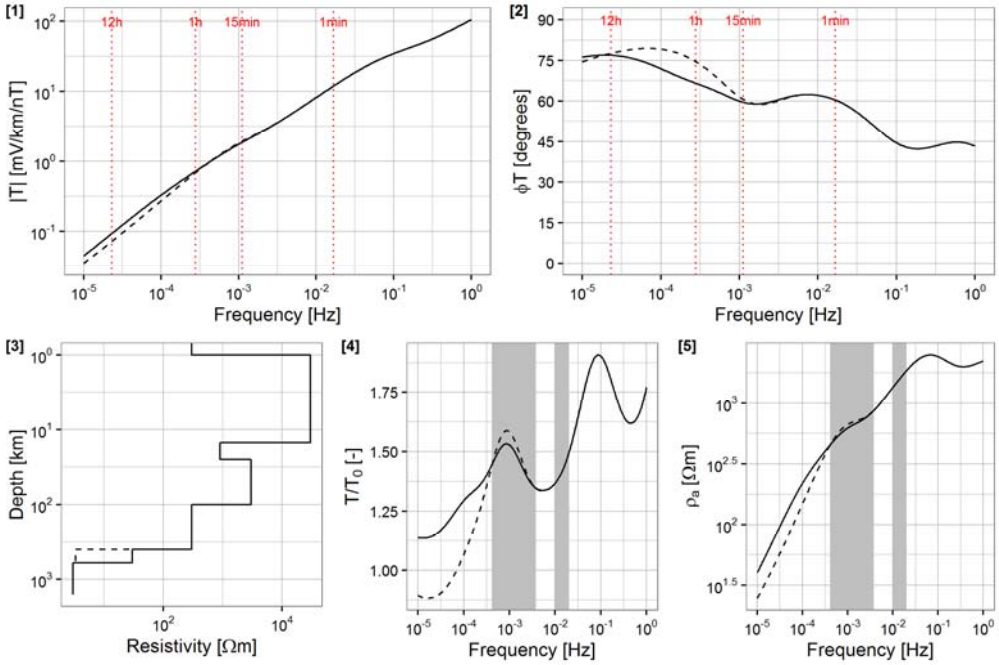

Figure G.1 - Resistivity and Transfer Function of Upper and Maximum for 1989-03-13
Solid represents upper bound, and dashed represents the maximum Earth model. Plot [1] shows the transfer function amplitude, [2] the transfer function phase, [3] resistivity with depth, [4] model over standard transfer amplitude, and [5] apparent resistivity

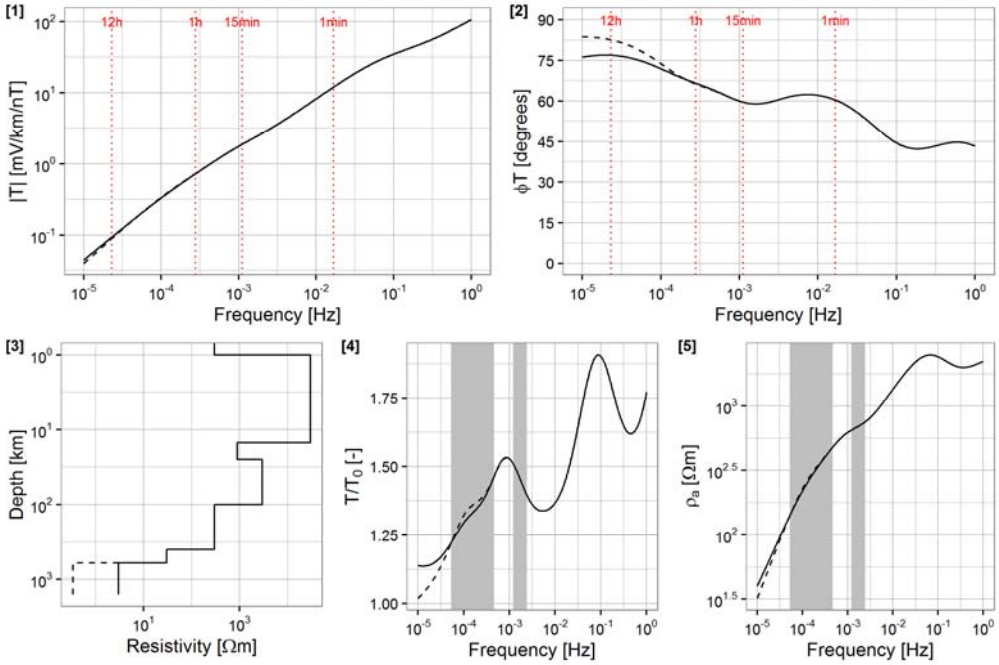

Figure G.2 - Resistivity and Transfer Function of Upper and Maximum for 1995-09-28
Solid represents upper bound, and dashed represents the maximum Earth model. Plot [1] shows the transfer function amplitude, [2] the transfer function phase, [3] resistivity with depth, [4] model over standard transfer amplitude, and [5] apparent resistivity

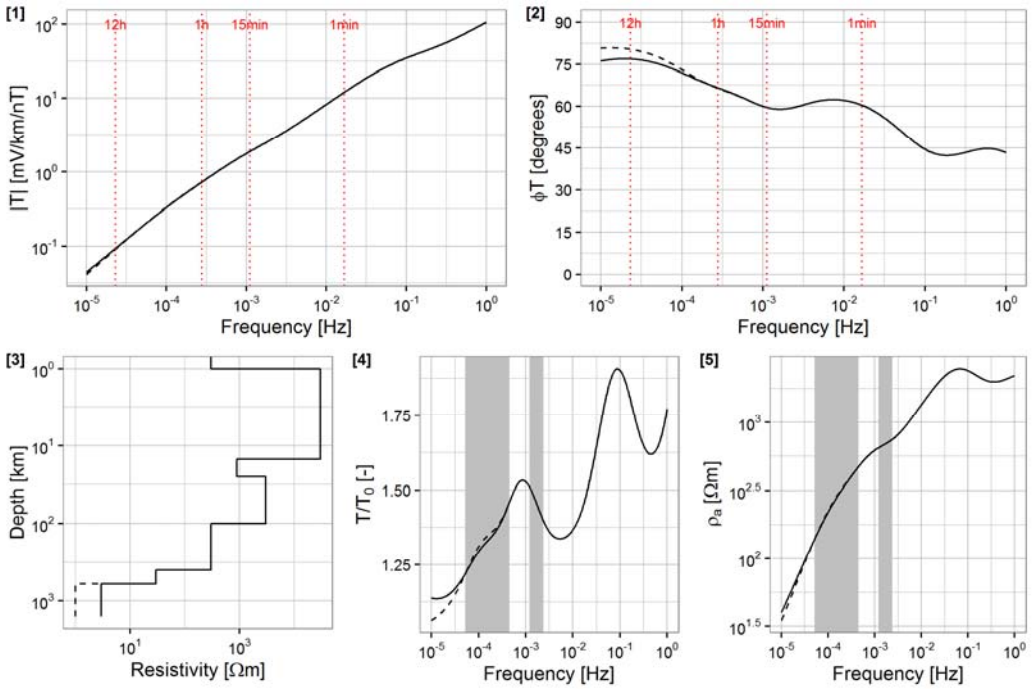

Figure G.3 - Resistivity and Transfer Function of Upper and Maximum for 2003-10-30
Solid represents upper bound, and dashed represents the maximum Earth model. Plot [1] shows the transfer function amplitude, [2] the transfer function phase, [3] resistivity with depth, [4] model over standard transfer amplitude, and [5] apparent resistivity

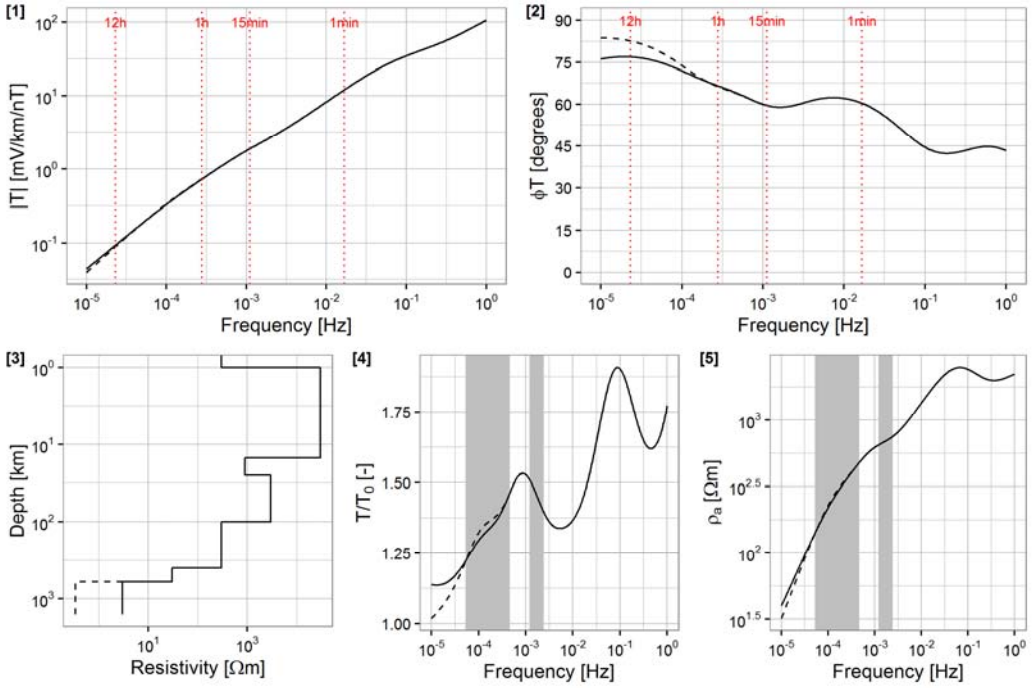

Figure G.4 - Resistivity and Transfer Function of Upper and Maximum for 2012-03-09
Solid represents upper bound, and dashed represents the maximum Earth model. Plot [1] shows the transfer function amplitude, [2] the transfer function phase, [3] resistivity with depth, [4] model over standard transfer amplitude, and [5] apparent resistivity

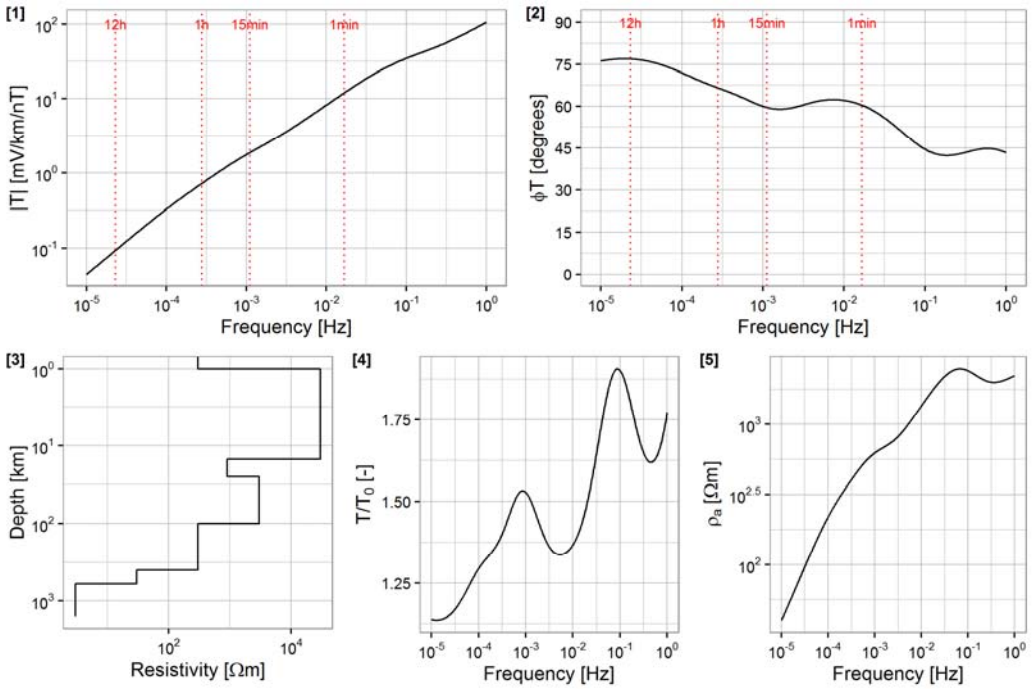

Figure G.5 - Resistivity and Transfer Function of Upper and Maximum for 2013-10-19
Solid represents upper bound, and dashed represents the maximum Earth model. Plot [1] shows the transfer function amplitude, [2] the transfer function phase, [3] resistivity with depth, [4] model over standard transfer amplitude, and [5] apparent resistivity

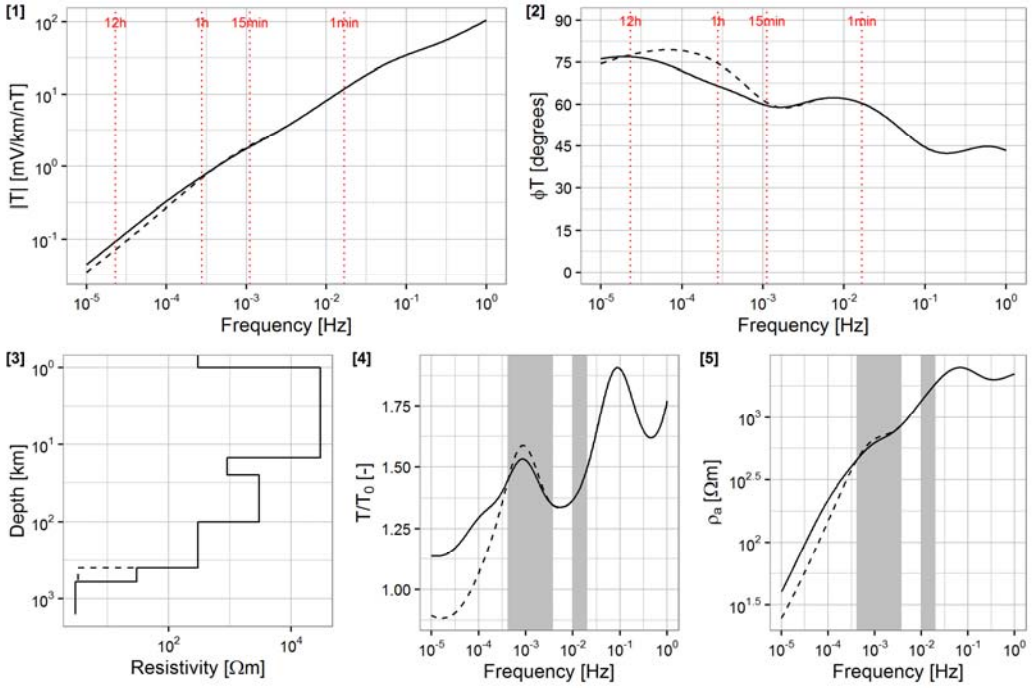

Figure G.6 - Resistivity and Transfer Function of Upper and Maximum for 2014-06-22
Solid represents upper bound, and dashed represents the maximum Earth model. Plot [1] shows the transfer function amplitude, [2] the transfer function phase, [3] resistivity with depth, [4] model over standard transfer amplitude, and [5] apparent resistivity

Appendix H Upper Versus Maximum Model The frequency domain Amplitude

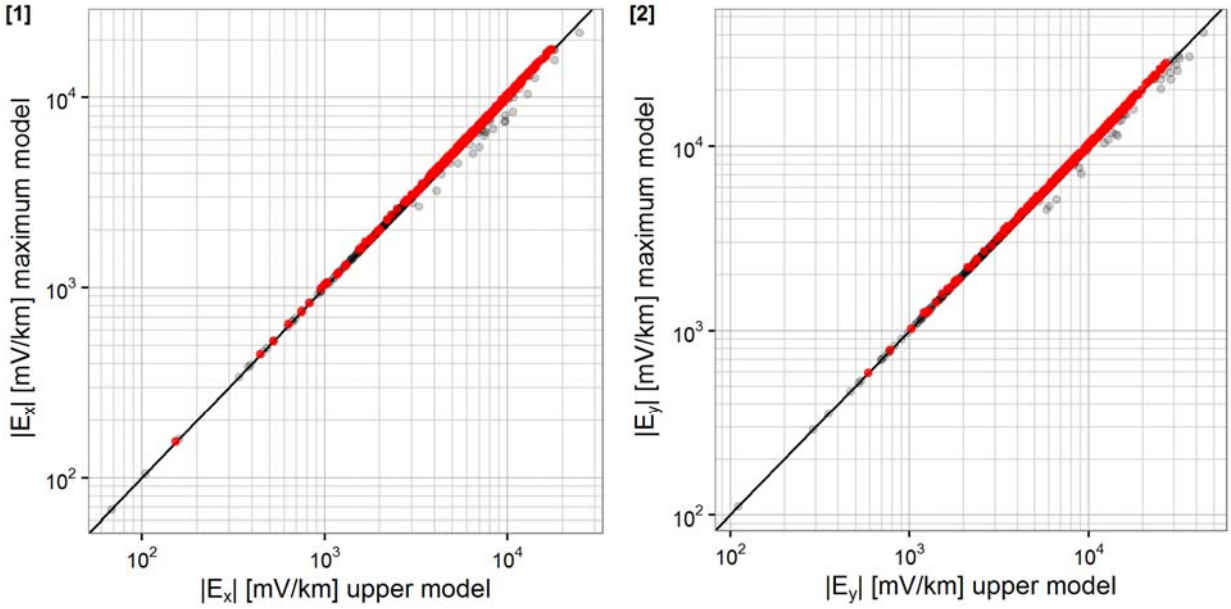

Figure H.1 - Upper Model versus Maximum Model Amplitudes for 1989-03-13
[1] Northward electric field, and [2] Eastward electric field for the upper versus maximum Earth models. Highlighted in red are points for which maximum Earth model produces higher amplitudes and in black for which upper Earth model produces higher amplitudes. Amplitudes are in the frequency domain.

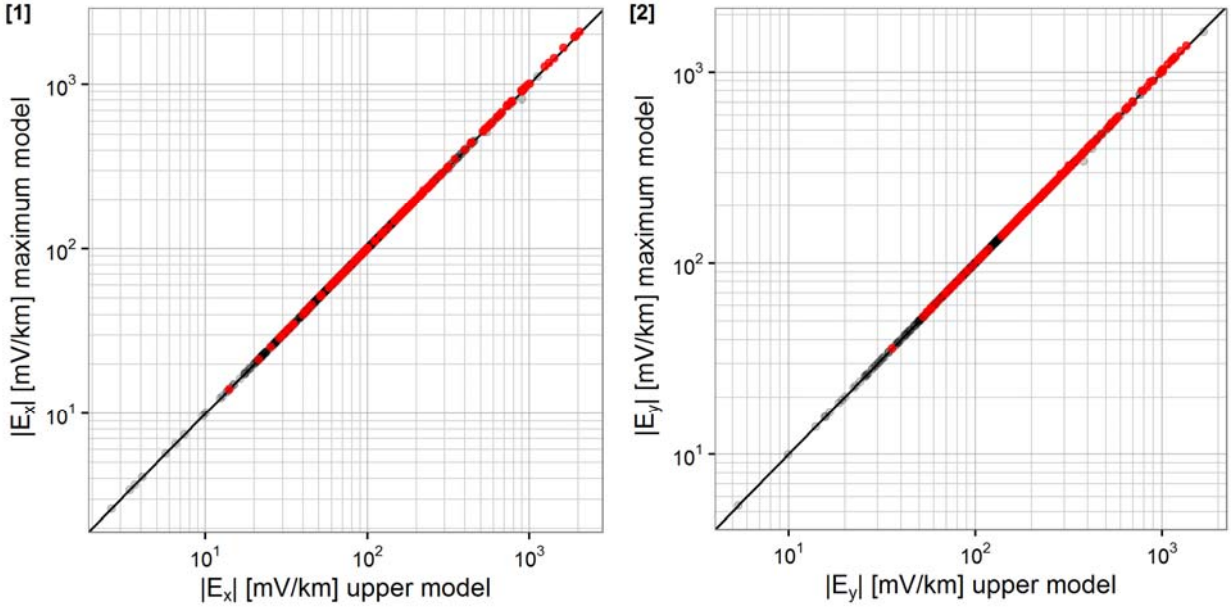

Figure H.2 - Upper Model versus Maximum Model Amplitudes for 1886-09-28
[1] Northward electric field, and [2] Eastward electric field for the upper versus maximum Earth models. Highlighted in red are points for which maximum Earth model produces higher amplitudes and in black for which upper Earth model produces higher amplitudes. Amplitudes are in the frequency domain.

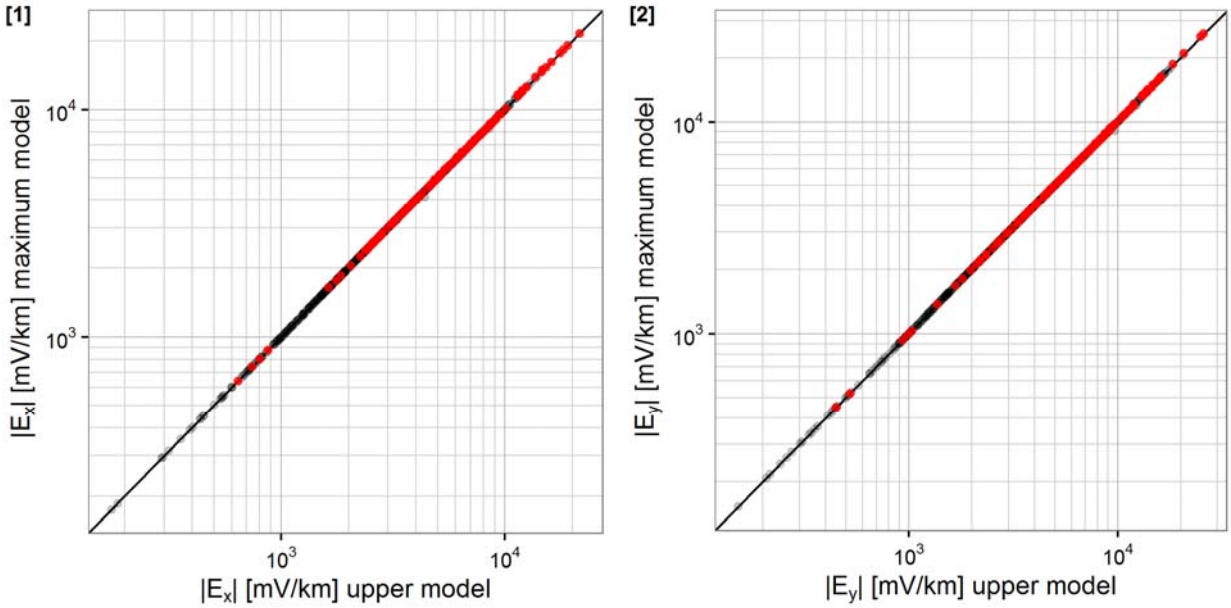

Figure H.3 - Upper Model versus Maximum Model Amplitudes for 2003-10-30
[1] Northward electric field, and [2] Eastward electric field for the upper versus maximum Earth models. Highlighted in red are points for which maximum Earth model produces higher amplitudes and in black for which upper Earth model produces higher amplitudes. Amplitudes are in the frequency domain.

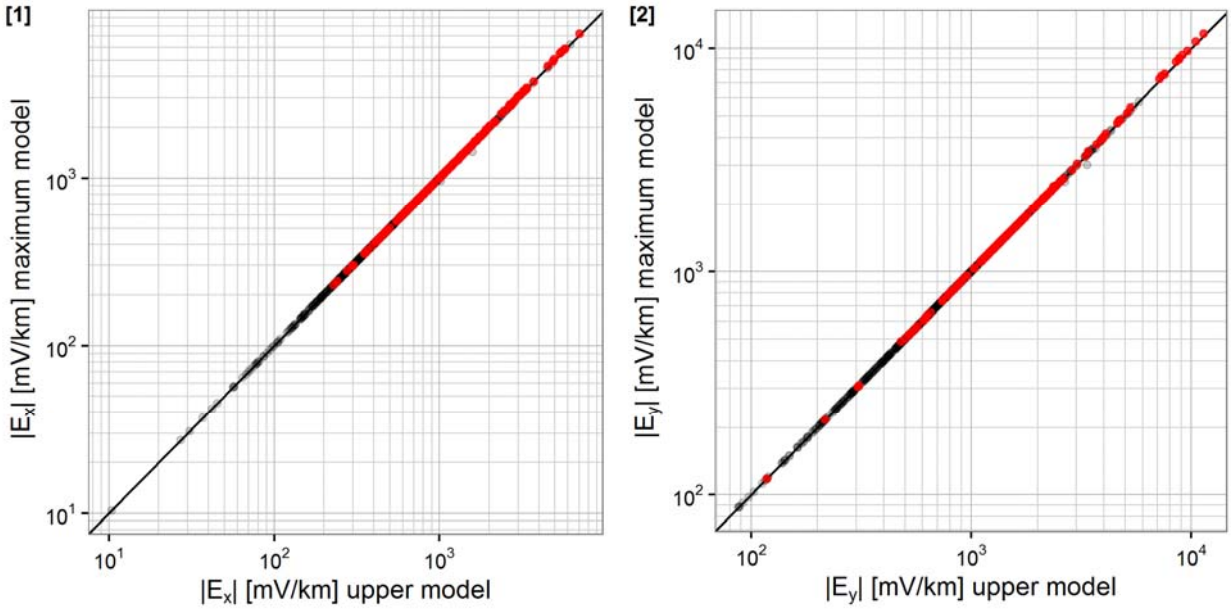

Figure H.4 - Upper Model versus Maximum Model Amplitudes for 2012-03-09
[1] Northward electric field, and [2] Eastward electric field for the upper versus maximum Earth models. Highlighted in red are points for which maximum Earth model produces higher amplitudes and in black for which upper Earth model produces higher amplitudes. Amplitudes are in the frequency domain.

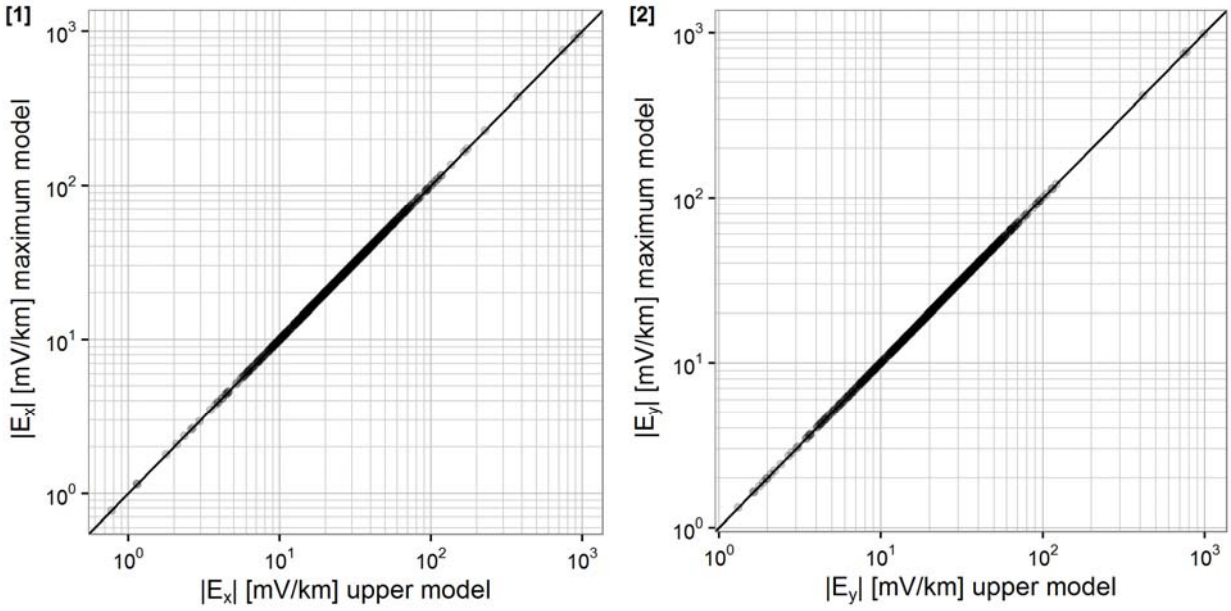

Figure H.5 - Upper Model versus Maximum Model Amplitudes for 2013-10-19
[1] Northward electric field, and [2] Eastward electric field for the upper versus maximum Earth models. Highlighted in red are points for which maximum Earth model produces higher amplitudes and in black for which upper Earth model produces higher amplitudes. Amplitudes are in the frequency domain.

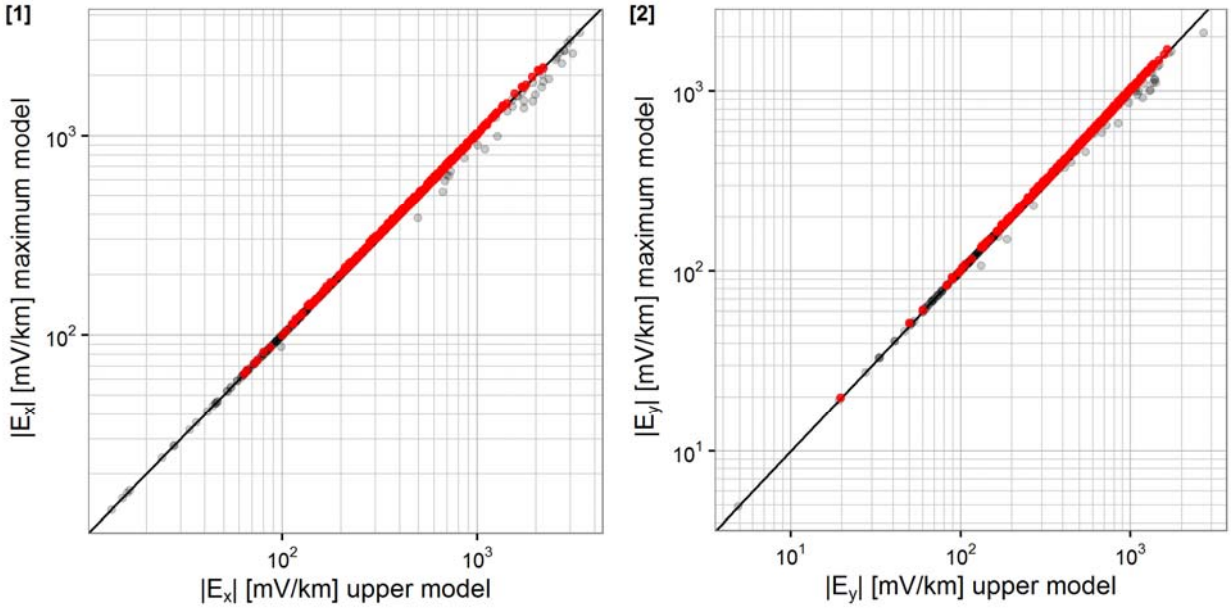

Figure H.6 - Upper Model versus Maximum Model Amplitudes for 2014-06-08
[1] Northward electric field, and [2] Eastward electric field for the upper versus maximum Earth models. Highlighted in red are points for which maximum Earth model produces higher amplitudes and in black for which upper Earth model produces higher amplitudes. Amplitudes are in the frequency domain.